MEMBERS OF THE JURY

Belgium:

Prof. dr. Bert BRONE (Universiteit Hasselt), Promotor

Prof. dr. Annelies BRONCKAERS (Universiteit Hasselt), Co-promotor

Prof. dr. Jean-Michel RIGO (Universiteit Hasselt), Co-promotor

Prof. dr. Ivo LAMBRICHTS (Universiteit Hasselt)

Cuba:

Prof. dr. Liliana Maria Gomèz Luna (Universidad de Oriente, Cuba), Promotor

Prof. dr. Nibaldo Hernández Mesa

Prof. Dr. Lourdes Lourdes Lorigados Pedre

Prof. Dr. Caridad Zayas Vignier

Prof. Dr. Lillian Sierra Calzado

Prof. Dr. Isabel Martínez Motas

Prof. Dr. Juan Francisco Infante Bourzac

Prof. Dr. Diana García del Barco

Prof. Dr. Humberto Morris Quevedo

Prof. Dr. Yohani Pérez Guerra

Prof. Dr. Luis A. Riverón Martínez

Prof. Dr. Osmir Cabrera Blanco

Prof. Dr. Clara Esther Martínez Manrique

Prof. Dr. Julio Cesar Escalona Arranz

To Angela……..

ACKNOWLEDGMENTS

The research work conducted in this doctoral thesis has been financed mainly through the grants awarded by the Belgian government's VlirUos research projects. Also part of the funding was covered by the Special Research Fund Grant 2015, DOCTORAL GRANTS IN THE FRAMEWORK OF THE BILATERAL COOPERATION of the University of Hasselt.

I would like to acknowledge the Biomed Research institute (Biomed) of the University of Hasselt where the *in vitro* models were made for the culmination of this research work and the CNEA for their support in everything related to the development of the *in vivo* model**.**

ABBREVIATIONS LIST

1400 W: N- [3- (Aminomethyl) benzyl] acetamidine (Inhibitor of the iNOS isoform)

2VO: Model of two vessels occlusion

Bapta: 1,2-bis (o-aminophenoxy) ethane-N, N, N ', N'-tetraacetic acid (Ca2 + chelator)

CAM: chicken chorio-allantoic membrane

CENPALAB: National Laboratory Animal Production Center

CNEA: National Center for Applied Electromagnetism

DMEM: Dulbecco's Modified Eagles Medium

DMSO: Dimethyl sulfoxide EC50: Coefficient of effectiveness

eNOS: Endothelial Nitric Oxide

ELFMF: extreme low frequency electromagnetic field

EMF: Electromagnetic field

FBS: Fetal Bovine serum

FGF-2: Fibroblast Growth Factor -2

cGMP: 3 ', 5-cyclic guanosine monophosphate

HMEC-1: human microvasculair endothelial cells (immortalized cell line)

Hsp: Heat shock protein

IC50: Coefficient of inhibition.

iNOS: Induced nitric oxide

L-NAME: N (G) -nitro-L-arginine methyl ester (inhibitors of all NOS isoforms)

L-NMMA: Nw-mono-methyl-L-arginine (inhibitors of all NOS isoforms)

PEMF: Pulsed electromagnetic field

LPS: Lipopolysaccharides

MAPK: Activated mitogenic protein kinase

MTT: 3- (4,5-dimethylthiazolyl-2) -2,5-diphenyltetrazolium bromide

NAK-02: Extremely Low Frequency Magnetic Stimulator

NO: Nitric Oxide

NOS: Nitric oxide synthase

nNOS: Neural nitric oxide

PDGF: platelet- derived growth factor

PBS: Phosphate Buffer Saline α-MEM: modified α-Eagles medium.

TTC: Triphenyl Tetrazolium Chloride

TIA: Transient ischemic attack

VEGF: Vascular endothelial growth factor

VEGFR: Vascular endothelial growth factor receptor 2

TABLE OF CONTENTS

Page

Chapter 1

INTRODUCTION

Stroke also referred to as Cerebrovascular accident (CVDA) can be defined as transient or definitive disturbances in the functioning of one or more areas of the brain which occur as a consequence of a defect in the cerebral blood flow. 95% of cerebrovascular disease (CVD) cases are caused by restriction of blood flow, while 15% are the result of primary cerebral bleedings. Currently, the only approved treatment is thrombolytic use with recombinant tissue plasminogen activator (rt-PA), which has the disadvantage that it can only be applied from 3% to 8.5% of patients, because of its narrow therapeutic window and the possible side-effects. Hence, there is an urgent need to find new therapeutic strategies to counter the post-ischemic physic disability and resulting mortality which makes CVD the third leading cause of death worldwide[1].

In the complex pathophysiology of stroke, numerous biochemical as well as (sub)cellular events are interrelated and coordinated in time and space, which is referred to as the ischemic cascade[2]. The complexity of the signals of this cascade of biochemical reactions not only determines the cellular survival and the neurological deficit post-stroke, but also the mortality after brain damage[3].

At the cellular level, the acute reduction of cerebral blood flow and subsequent depletion of oxygen and glucose causes a shortage in cellular levels of ATP. Next, ATP-dependent membrane ion pumps fail which leads to the ion gradients that run low and results in influx of calcium ions. This ischemic cascade triggers the release of excitatory neurotransmitters particularly glutamate causing excitotoxicity. In addition, the lack of ATP is accompanied by an inflow of water, resulting in rapid swelling of neurons and glia (cytotoxic edema).

The center of the brain region with diminished blood flow (to only 10-25%) following cerebral ischemia is the ischemic core. In this area, the loss of oxygen and glucose results in rapid irreversible necrosis of neurons and the surrounding glial cells within minutes after the insult. The area adjacent to the ischemic core, known as the penumbra area, is a rim of mild to moderately ischemic tissue. In contrast to the tissue in the core area, death of the brain tissue in the penumbra occurs on a longer time scale, i.e. hours after the onset[4]. This zone is able to maintain some physiological functions such as ionic and metabolic homeostasis. If the blood circulation is restored in time, this brain area can potentially be saved[5].

Even though several cellular and molecular mechanisms combine to initiate brain damage, advances in recent years have made it possible to elucidate the different stages in which these events occur, leading to neuronal death[5]. It is now known that there are three endogenous processes involved in neuroregeneration: angiogenesis, neurogenesis and synaptic plasticity, which are activated in the adult brain after different pathological situations[5].

Neuroprotection is the therapeutic strategy for the treatment of CVD aimed to specifically target the neurons and avoiding their death[6]. In this sense, the application of an effective neuroprotector would contribute to increase the therapeutic window and to stimulate restorative processes earlier, in order to reduce the affected area. As stated above, the molecular mechanisms of the early ischemic cascade such as glutamate release, Ca^{2+} influx could be pharmacologically modulated to produce neuroprotection. More than 1000 compounds have been shown to induce neuroprotection after stroke in rodent models[7]. Unfortunately, after nearly 200 clinical trials, all attempts at neuroprotection for ischemic stroke have failed in the clinic.

Among the restorative processes of brain damage, the role of angiogenesis in the formation of new blood vessels to restore collateral circulation is well documented in both laboratory animals as well as humans. Targeting angiogenesis is therefore a useful strategy in the fight against stroke[8]. Myriad angiogenic agents have been described in the literature, among which we can mention the magnetic field, specifically the extremely low frequency magnetic field (ELFMF) with sinusoidal wave forms.

Magnetic fields have been used in multiple clinical applications since the last century[9,10]. Their therapeutic potential for angiogenesis-dependent diseases such as CVD have been extensively explored. Recently, its effect in the repair of tissue in chronic wounds, stimulating the healing processes has been evaluated. These results have allowed a better understanding of the cellular response that induces such stimulus[11].

The putative effect of ELFMFs on the stimulation of angiogenesis, through the increase of tube formation and the proliferation of endothelial cells was shown previously, yet without clarifying the molecular mechanisms of this effect[12–14]. Other sources warn for adverse effect on blood vessel formation, for example on tumor growth[15,16,17]. As within the literature contradictory results are found the need arises to deepen the cellular response and the molecular mechanisms involved in ELFMF induced endothelial cell responses.

In this thesis, we investigate whether ELFMF can be used as a treatment of cerebral ischemia through the stimulation of angiogenesis, in order to determine its possible therapeutic effect in cerebral ischemia, two doses were selected for this study (13.5 mT at 10 Hz and 60 Hz), considering its effectiveness in previous research[18]. In addition, we further unravel the molecular mechanism that mediates the activation

of angiogenesis by ELFMFs in each of the selected doses in *in vitro* (HMEC-1 cells) and *in vivo* (permanent global ischemia).

1.1. Cerebrovascular Disease: From Physiology to Therapy

1.1.1. Definition and epidemiology

CVD includes any transient or permanent disorder resulting from the occlusion or rupture of one or more blood vessels supplying the brain, affecting the functionality of one or more parts of the brain[19].

Hippocrates (460-377 BC) recognized this pathology, which he called "apoplexy". He included it in some of his aphorisms: "*Fulminant stroke is impossible to cure; and even, indeed, it is not easy to cure the less intense, from forty to sixty years is when the individuals are most exposed to stroke"*.

This concept is also known with the Latin term "Ictus" or the Anglo-Saxon "Stroke", which means "blow", demonstrating the sudden and abrupt nature of the process[19].

CVD represents the third leading cause of death in the Western world after coronary heart disease and cancer; as well as the leading cause of physical disability in adults and the second leading cause of dementia, according to data collected in 2003 by the World Health Organization Health (WHO) [20]. Every year, 15 million people in the world suffer at least one stroke, of which five million die. This is equivalent to 32% of deaths from cardiovascular diseases worldwide, according to 2002 statistics; while another five million people are permanently disabled[21]. In this context, it should be noted that for the age range between 65 and 74 years the incidence increases to 25 and 50 respectively per 1000 inhabitants[20]. Because of their magnitude and impact, CVD have been included in the priorities of the health programs of the World and Pan American Health Organization (PAHO and WHO) [20].

In Cuba, as reported in the Statistical Yearbook for Health in 2015[22], the frequency is similar, where about 9256 deaths in that year, and an incidence rate of 82.9 per 100000 inhabitants, being slightly higher for men. In accordance with the data observed worldwide, there is a slight tendency to increase as compared to the previous two years.

1.1.2. Classification

There are many different classifications of CVD depending on the origin of the lesion, etiology, size, morphology, topography, onset and subsequent evolution. In Figure 1.1 a classification according to the clinical cause of CVD is given. (Figure 1.1). 65% of strokes resulting from vascular occlusion present lesions in the territory of the middle cerebral artery, 15% in the brainstem, cerebellum, 9% in the territory of the posterior cerebral arteries, 2% in the territory of the anterior cerebral artery and 9% in borderline or multiple regions[19].

Ischemia occurs in 85% of cases, and is characterized by a decrease in cerebral blood supply, which can simultaneously affect the whole encephalon because of hypotension. Causes may range from cardiac arrest to cardiopulmonary bypass surgery any prolonged shock (global ischemia) or obstruction of one brain artery (focal ischemia).

According to the duration of the focal ischemic event, it may be divided into transient ischemic attack (TIA) or cerebral infarction, depending on whether or not the ischemic deficit reverts within 24 hours[23]. Hemorrhagic ischemia occurs in 15% of cases, characterized by the presence of blood both in the subarachnoid space (subarachnoid hemorrhage) and in the parenchyma or in the interior of the cerebral ventricles (cerebral hemorrhage) [23]. Therefore, cerebral infarction is a prolonged ischemic episode in time, which produces an area of tissue necrosis.

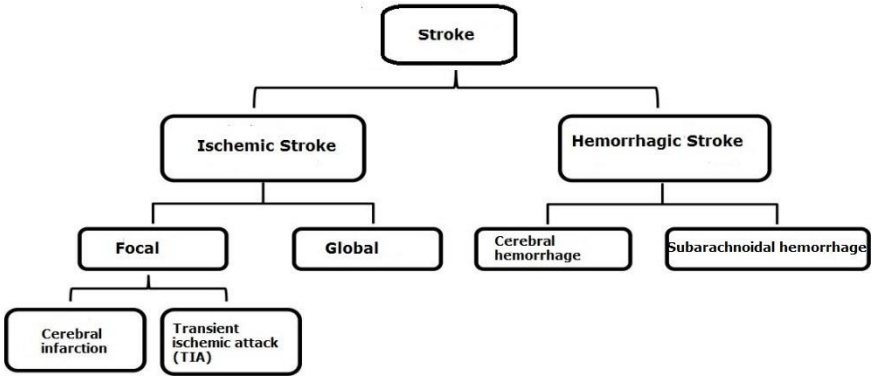

Figure 1.1 Classification of cerebrovascular diseases (CVD) according to their nature, modified from Díez-Tejedor et al., 2001[19].

Three mechanisms of cerebral infarction production have been differentiated: thrombolytic, embolic and hemodynamic. The symptoms will be different depending on the affected arterial territory[24].

1.1.3. Pathophysiology

Brain tissue has a relatively high consumption of glucose and oxygen, depending almost exclusively on oxidative phosphorylation to produce energy. By permanently or transiently occluding any of the arteries that supply the brain, blood flow decreases and thus, the supply of oxygen and glucose in the territory of the affected vessel is impaired[25]. For a short time, and when collateral blood supply is not sufficient to maintain normal blood flow in the territory of the obstructed artery, this reduction can be compensated by physiological mechanisms of flow regulation[1].

On the one hand, a moderate reduction in oxygen supply is balanced by an increase in cerebral blood flow; but a pressure lower than 40 mmHg causes confusion and, below 20 mmHg leads to coma. A situation of hypoxia is not exclusively responsible for acute brain damage; it must be accompanied by ischemia or acidosis. Hypotension increases the effects of hypoxia, as occurs in cardiorespiratory arrest.

If this situation persists, irreversible brain damage is triggered, affecting gray matter, border vascular zones and more distal arterial territories[26,27].

On the other hand, sustained hypoglycemia triggers functional and structural modifications. Glucose concentrations below 20 $mgdL^{-1}$ cause confusion, and below 10 $mgdL^{-1}$ lead to coma[28]. The storage capacity of glucose or glycogen of the brain is reduced, being able to cover the energetic requirements during short periods of time, without neurological sequels. In cases of prolonged fasting, the brain cells derive their energy from the ketone bodies, and structural lesions, consisting of selective cortical neuronal necrosis, with preservation of the glial tissue, accompanied by a decrease in oxygen consumption[29,30].

Under normal physiological conditions, the blood flow of a healthy cerebral parenchyma is greater than 50 mL/100g/min and is independent of variations in perfusion pressure, which is achieved through mechanisms of self-regulation of the cerebral circulation. This is a process that involves biochemical, myogenic and neurogenic factors. In ischemic situations, there is a modification of these self-regulation mechanisms in the affected territory and the perfusion pressure becomes dependent on blood pressure[31](Figure 1.2).

When cerebral blood flow (CBF) drops below 10 mL/100g/min., rapid irreversible cell necrosis occurs in an area referred to as the infarct core. Usually, surrounding the nucleus there is a hypo-perfused zone, whose extension depends on the functioning of the collateral circulation[32]. Within this zone, two regions can be differentiated: a region with CBF <22 mL/100g/min called **ischemic penumbra** in which oxygen consumption is still sufficient to preserve survival but progress to irreversible changes, unless effective treatment is used[1] and another region with CBF> 22 mL/100g/min known as the benign **oligemic zone**, which mostly recovers spontaneously. The penumbra is the most clinically relevant target and is the focus of active research. In this zone, cells shortly after the insult still maintain their

structural integrity. However, functional modifications occur (Figure 1.2 and 1.3): the oxygen supply is insufficient to maintain the correct protein synthesis and oxidative metabolism of glucose, causing lactic acidosis. The ATP content as well as the active transport is only partially maintained, and consequently the synaptic transmission is impaired. If the CBF is not timely restored in the penumbra, the irreversible damage expands into this zone through the despolarization waves (i.e. the penumbra is reverted into core zone)[3].

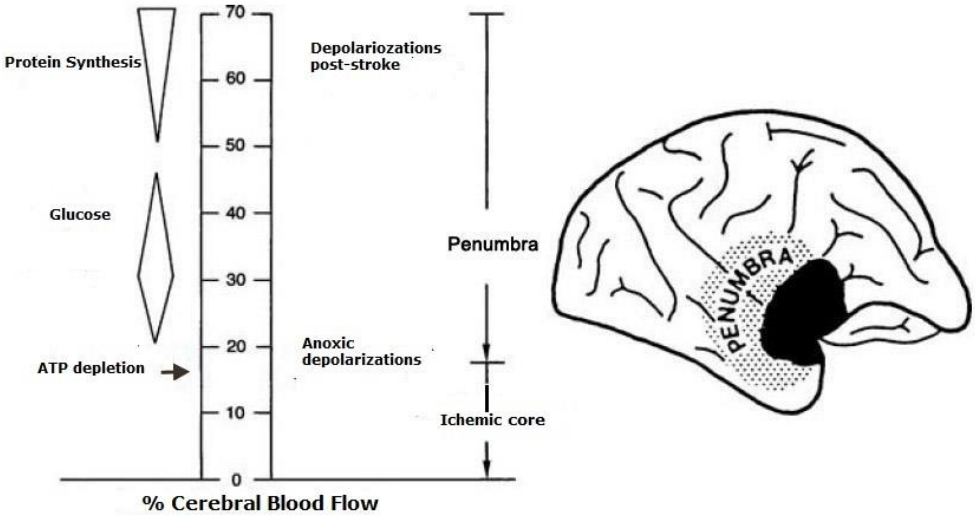

Figure 1.2. Functional and morphological diagram of the ischemic nucleus and the penumbra zone; modified from Hossmann, 2006[33].

Probably the most important part of early recovery after stroke is limited capacity of penumbra/infarct neurones to recover[34–41]. It became clearer in the last years, that penumbra is not just passively dying over time. It is also actively recovering. In penumbra, partially depolarised tissue adjacent to the infarcted core with reduced cerebral blood flow and increased oxygen extraction rate struggle for survival in a very limited time-window. This initial plasticity in majority contributes towards later neurogenesis, angiogenesis and final recovery. Penumbra is a principal target

in acute phase of stroke. Understanding of each of the processes is a major challenge for future therapies in neuroreparation (Figure 1.3).

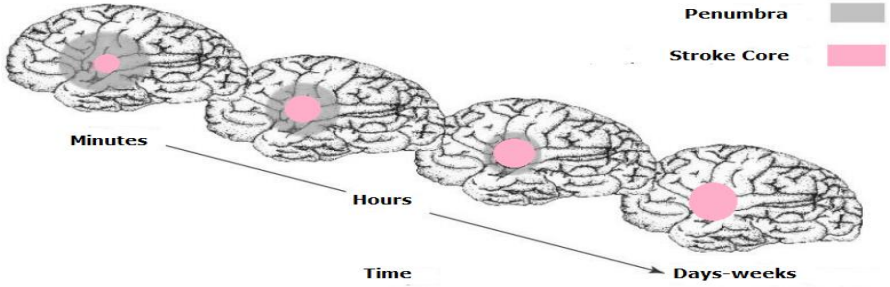

Figure 1.3. Progressive increase of the structural lesion of the penumbra zone; modified from Castillo, 2001[34].

1.2. Components of the ischemic cascade and its biochemical implication

Once the ischemic accident occured, a sequence of biochemical processes known as the ischemic cascade is triggered leading to the destruction of the cerebral parenchyma. These biochemical processes are distinct between neurons, glia and the vascular component (Figure 1.4), contributing to the destabilization of the neurovascular unit. Each of these processes is explained below.

1.2.1. Neural component

Disruption of blood flow causes a decrease in the supply of oxygen and glucose and this prevents the affected brain region from generating the necessary ATP to maintain its energy demand. This lack of metabolic energy results in a failure in the functioning of ATP-dependent Na^+/K^+ pumps, resulting in a rapid depletion of intracellular K^+ and thus a progressive loss of membrane potential[33]. Loss of ionic gradients causes a depolarization of neurons, leading to the opening of voltage dependent Ca^{2+} channels and the unblocking of ligand-gated Ca^{2+} channels[42].

As a consequence, large amounts of Ca^{2+} enter the cells. The concentration of Ca^{2+} increases to approximately twice its physiological value, an increase that occurs in two phases[43]. The first phase is not directly responsible for cell death[44]. As a result of the Ca^{2+} influx, a strong depolarization of the neuronal membrane is maintained, causing an increase in the release of glutamate and other excitatory amino acids causing excitotoxicity [45]. Excitotoxicity is the phenomenon of massive postsynaptic neuronal death, as a consequence of a prolonged and strong activation of the inotropic receptors, mainly the N-methyl-D-aspartate receptor (NMDA) and α-amino-3-hydroxy-5-methyl-4-isoxazolepropionic acid receptor (AMPA), as well as postsynaptic metabotropic receptors[45–47]. Stimulation of the AMPA receptors speeds up the increase of the intracellular Na^{+} concentration, triggers the formation of cellular edema, which in turn is favored by a passive entrance of water, followed by the ionic flow[33,48,49]. On the other hand, the stimulation of the NMDA receptors causes the second phase of the intracellular Ca^{2+} increase, which initiates a calcium dependent cellular injury, apoptosis or necrosis[43]. In cortical cell cultures, sustained activation with NMDA for minutes is sufficient to destroy most neurons[45,50]. In contrast, Ca^{2+} excitotoxicity by AMPA receptor activation occurs more slowly, requiring hours to induce a lethal lesion in the same cell cultures[51,52]. Activation of metabotropic receptors by the release of glutamate causes an increase in Ca^{2+} by the release from its intracellular stores[6,30,52].

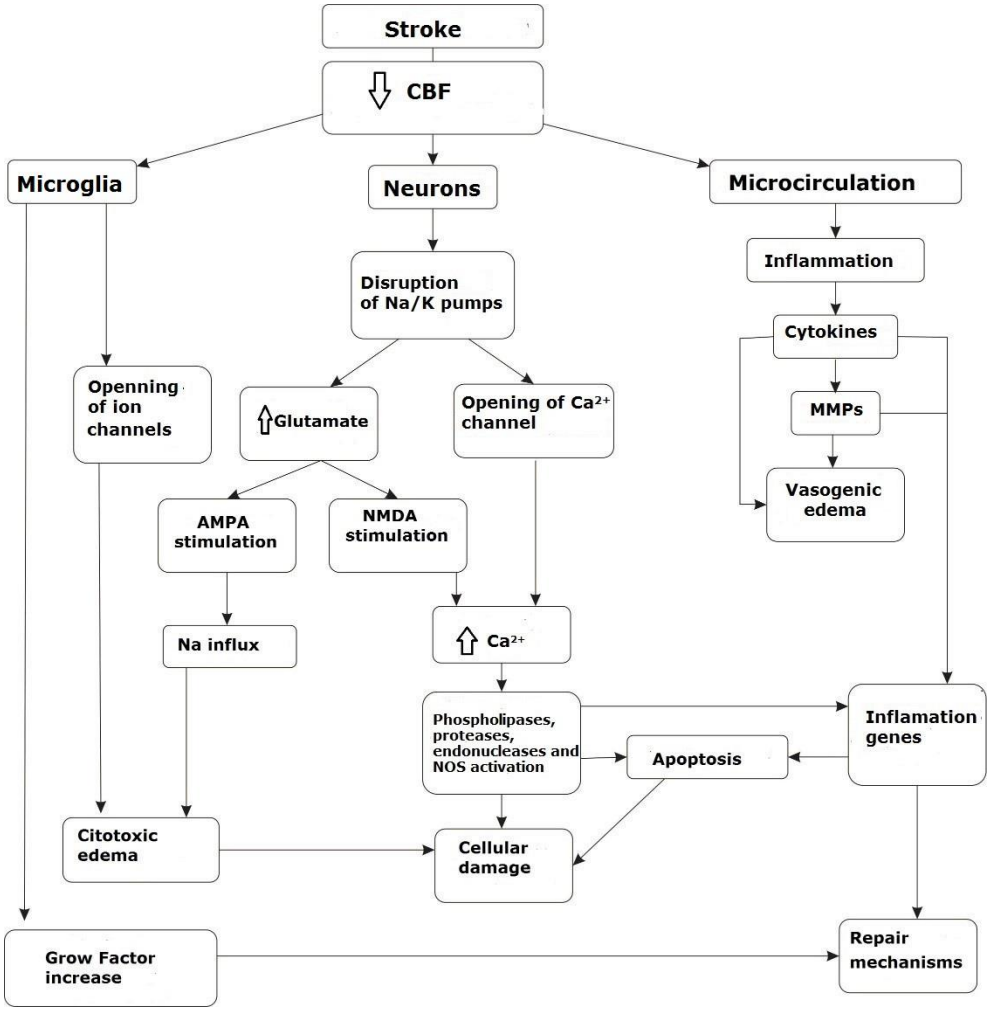

Figure 1.4. Ischemic cascade; modified from Castillo, 2001[34].

This new increase in Ca^{2+} level gives rise to a series of cytoplasmic and nuclear processes leading to tissue damage. At this point, enzymes such as calcium-dependent phospholipases, proteases, nitric oxide synthases (NOS) and endonucleases which degrade cytoskeletal proteins (actin and spectrin 6), extracellular matrix and nucleic acids, are activated[53,54]. In addition, mitochondrial dysfunction occurs due to the opening of the pores, interruption of the respiratory

chain, accumulation of free electrons and the release of NADH and cytochrome C[45,54,55].

Free electrons, which accumulate in the destabilized mitochondria, are able to react with oxygen from reperfusion, producing superoxide anions (O_2^-)[56]. In addition, NMDA activation causes an increase in the expression and activation of cyclooxygenase-2 (COX-2) and phospholipase A_2 in ischemic neurons. COX-2 contributes to the overproduction of superoxides, while phospholipase A_2 leads to the release of arachidonic acid, prostaglandins and thromboxanes. The metabolism of arachidonic acid again produces O_2^-, which stimulates phospholipase A again, forming a detrimental positive feedback pathway[45,57].

The O^- is a reactive oxygen species (ROS) that initiates the cascade of oxidative stress in cerebral ischemia. However, other ROS are formed which increase the deleterious effects, such as the hydroxyl radical (OH^-) and the hydrogen peroxide (H_2O_2) generated by superoxide dismutase (SOD-1) from the superoxide anion. The formation of nitric oxide (NO) by nitric oxide synthase is responsible for the production of other ROS such as peroxynitrite ($ONOO^-$) when it reacts with superoxide[42].The high free radical formation of oxygen causes cellular modifications, due to oxidation of lipids, DNA and proteins.

Simultaneously with glutamate release, anoxia induces the extracellular release of the inhibitory neurotransmitter gamma-aminobutyric acid (GABA). However, this increase is not as significant or persists as much as that of glutamate[30]. GABA exerts its inhibitory effects by binding to two receptors GABA A and GABA B. Stimulation of the ionotropic GABA A receptor is more significant in the gray matter, which causes the entry of Cl^- in the neuron, facilitating its repolarization. On the other hand, the stimulation of the metabotropic receptor GABA B, more active in the white matter, acts together with the G protein and produces a second messenger.

These mechanisms allow a blockade of the entrance of more Ca^{2+} into the axon, reducing its effects[43].

1.2.2. Glial component

In an ischemic accident, not only the neurons are affected, but also the glial cells. Composed of various cell types (astroglia, oligodendroglia and microglia), the neuroglia plays an essential role both in the development of the lesion and in the repair of the tissue[5,58]. Brain injuries and thus also cerebral ischemia trigger an extensive glial response referred to as reactive gliosis. Recent studies show that reactive gliosis exert both beneficial and detrimental effects on restoring brain functions after injury. In the acute phase, glial scar formation is crucial for sealing the lesion site to remodel the tissue, and temporally and spatially controlling the local immune response. The glial barrier seals off the area of damage to prevent further microbial infections and spread of cellular damage, maintain extracellular ion and fluid balance, prevent an overwhelming inflammatory and growth factor responses. This glial scar also stimulates revascularization. However, in the chronic phase, the glial scar is also acts as an impediment to axon regeneration and thus prevents the recovery of CNS.

Astrocytes, under physiological conditions, are responsible for the support of neuronal function and the regulation of metabolic activity, which is highlighted by their active role in controlling the neurotransmitter action of glutamate. When neuronal activity increases, glutamate levels at synapses rises and part of it is subsequently taken up by glutamate transporters[3]. Within itself, glutamate is converted to glutamine, which is transported to and can be used by neurons for the new synthesis of glutamate and GABA[30,45].

The response of astrocytes to infarction is extremely complex and still under investigation. After energetic failure which occurs during ischemia, the consequent

depolarization of the membranes, the opening of the ion channels, and the entry of sodium and water lead to the well-known astrocytic edema. This edema results in decreased physiological recapture of glutamate[33].

Microglia become activated by any insult to the brain in order to protect the cells surrounding the insult. As such they are thought to exert a protective effects of during ischemic attacks[57]. However, other studies show but they might contribute to tissue damage due to the production of cytokines and ROS[59].

In addition, oligodendrocytes, unlike neurons, are less sensitive to mechanisms of excitotoxicity as they do not contain synapses (like all other glial components). The oligodendrocyte progenitor cells are able to traverse the peri-infarct zone to be at the border of that same area, and may, therefore, induce repair mechanisms[5].

1.2.3. Vascular component

The endothelial cells that align the microvasculature of the central nervous system (CNS) differ from the rest of the vascular endothelium by their ability to regulate the passage of molecules or cells to and from the neural parenchyma, constituting the blood brain barrier (BBB)[60]. This selectivity lies in the characteristics of this endothelium, which includes selective transporters and receptors that protect the CNS from a great variety of hydrophobic compounds, as well as in modifications of cellular membranes such as tight junctions limiting the barrier's transcellular permeability[3].

BBB stability is altered in the acute phase of stroke, and is associated with cerebral edema, which is the accumulation of fluid, both inside the cells (cytotoxic edema) as well as in the cellular interstitium (vasogenic edema). Cytotoxic edema is caused by altered permeability of cell membranes and increased intracellular osmolarity associated with increased glutamate concentration and degradation products[61].

Depending on the duration of ischemia, these changes may be reversible or not. If reperfusion occurs, metabolic activity rapidly normalizes. If reperfusion occurs beyond the first six hours after onset of ischemic stroke, edema is aggravated, because increased hydrostatic pressure leads to acceleration of fluid extravasation[62]. Although BBB dysfunction may facilitate inflammation by allowing peripheral immune cells to enter the brain, this migration can in its turn modulate its permeability. However, this process occurs later than seven days after the occurrence of ischemia[3].

In conclusion, control of CBF is modulated through neurons, glia (astrocytes and microglia) and endothelial cells. The increase of glutamate in neuronal synapses causes an internal increase of Ca^{2+}, which entails the activation of different enzymes, including eNOS, capable of producing vasodilation[57,63,64].

1.3. Physiological and molecular aspects of Post-ischemic events

1.3.1. Neurorepair and angiogenesis

After ischemia has occurred, there is an endogenous increase in neurogenesis and angiogenesis in the brain[1,5]. In this process three stages are distinguished: proliferation [where fibroblast and epidermal growth factors (bFGF and EGF, respectively) and brain-derived neurotrophic factor (BDNF) are expressed], migration (involving chemotrophic factors such as integrins, ephrins and reelins) and differentiation and integration (regulated by astrocytes)[27,65,66]. Neurogenesis, especially in its migration stage, may be closely related to angiogenesis and even to vasculogenesis[3]. All of these aspects contribute to the functional improvement of the tissue after a stroke. Endothelial cells begin to proliferate in the areas adjacent to the infarct between 12 and 24 hours after the ischemic event, allowing angiogenesis even three days after the event[4]. In fact, this angiogenesis has been

observed in many cases 3 to 4 days after ischemia; however, revascularization of the damaged regions is achieved weeks after the ischemic attack.

Angiogenesis is the growth of new blood vessels out of pre-existing vessels. A detailed overview on the most important steps of the angiogenic process is described below:

- (i) *Activation of endothelial cells and pericytes*

The earliest morphological changes occurring in the quiescent endothelial cell consist of vascular lumen hypertrophy, nuclear enlargement, prominent nucleolus, and increased numbers of subcellular organelles and the formation of projections from the surface of the membrane. The increase of DNA synthesis by the endothelial cell has been described once the angiogenic mechanism has been initiated. The release of proteases and the plasminogen activator takes place from the new cells in the form of the "endothelial buds"[67].

The pericytes also undergo modifications both in their morphological characteristics and in their topographical relationships. The first changes include the shortening of its protrusions and an increase in the number of cytoplasmic polyribosomes, indicating an active process of protein synthesis[68,69].

- (ii) *Degradation of the basal lamina and extracellular matrix*

This is a necessary step before migration of the endothelial cell can occur. Complete degradation occurs in the area close to the angiogenic stimulus and is colocalized with te site of endothelial cell outgrowth. Similar changes start in the rest of the vascular wall. Therefore, endothelial cell extensions have no basal lamina, but a provisional substrate with altered proteoglycans. Changes in the basal lamina are due to proteolytic enzymes such as collagenase and plasminogen activator synthesized and secreted by activated endothelial cells[67,70].

- (iii) *Migration of endothelial cells from pre-existing vessels*

When the basement membrane of the vascular wall is degraded, endothelial cells protrude through the wall and begin to migrate into the interstitium towards the angiogenic stimulus. Sprouting angiogenesis requires specialization of cells along the migrating projection into “tip,” “stalk,” and “phalanx” cell phenotypes on the basis of the interaction of factors promoting or inhibiting angiogenesis. Tip cells are polarized migratory cells that are at the forefront of the endothelial sprout. These cells branch at the tip of the stalk as they extend philopodia toward the stimulus, yet accomplish this with hardly any proliferation. Stalk cells conversely exhibit a proliferative phenotype responsible for the lengthening of the endothelial sprout. The stalk cells follow the tip cells and all together form strings in the perivascular stroma. The migration of endothelial cells, in response to the extracellular matrix, depends on integrins and cell adhesion receptors (α2β1 and α4β3) [60].

- (iv) *Proliferation of endothelial cells*

According to some authors, during angiogenesis, endothelial DNA synthesis occurs in preexisting vessels before "vascular buds" form in as little as six to eight hours after the angiogenic stimulus is applied[71]. The time-space sequence of the endothelial division remains unclear; consequently, for some authors, the mitosis in the endothelial cells occurs concomitantly to the formation of new buds, while the majority believes that it occurs after the initiation of the migration [69]. It are especially the stalk cells that proliferate while the tip cells do not proliferate. Numerous factors that induce EC proliferation have been described, being some of them the proinflammatory cytokines (IL-1beta, TNF-alfa), nitric oxide (NO), and growth factors like vascular endothelial growth factor (VEGF), platelet- derived growth factor (PDGF) and fibroblast growth factor (FGF- 2).

- (v) *Formation of a new vascular lumen*

During angiogenesis, endothelial cells form tubular channels capable of transporting blood. Two models are considered in the formation of the new vascular lumen: in the first, there is an intracellular vacuolization in the endothelial cytoplasm of adjacent cells, which would lead to an intercellular canalization by connection of the vacuoles. In the second model, an intercellular canalization of the different adjacent endothelial processes takes place. Another controversial aspect is the moment when the new vascular lumen is connected to the initial vascularization, which should be the object of future research but has been proposed to be induced by the increasing blood pressure[27,72,73].

- (vi) Blood vessel maturation

After the formation of a new blood vessels, pericytes are located directly on the capillary wall. These cells share a common basement membrane with ECs and attach by different integrins to extracellular matrix (ECM) proteins[69]. In areas that lack a basement membrane, pericytes and ECs make direct cell-to-cell contacts via junction proteins such as N-cadherin and connexin-43 hemichannels[71], which form gap junctions between the two cell types and allow the transfer of nutrients, metabolites, secondary messengers and ions[3]. Normal function of neuronal circuits and synaptic transmission require an optimal neuronal microenvironment that relies on successful BBB maturation and maintenance. The BBB is formed by continuous EC membrane characterized by the presence of tight junctions and adherens junctions, and acts as a regulated interface between the peripheral blood circulation and the CNS environment[60]. Pericytes play a role in forming and maintaining BBB integrity in both the developing and adult brain[3].

1.3.1.1 The role of nitric oxide in angiogenesis and cerebral ischemia

Since its discovery as an important gaseous molecular messenger in the ‘80s, Nitric oxide (NO) has become the central study object in biomedical sciences. NO is a

unique molecule, with the characteristics of a neurotransmitter and it has vasodilator activity as well. It stimulates vascular smooth muscle synthesis and is involved in the genesis of various diseases such as hypertension, septic shock, inflammation, dementia, and in cerebral ischemia[74–76].

The physiological function of NO includes regulation of vascular flow, increase of blood flow during hypercapnia, participation in cerebral defense mechanisms of microglia, activation of parasympathetic fibers that innervate cerebral vessels, participation in neuronal plasticity processes, learning and memory. In addition, NO participates in other biological processes such as the activation of transcription factors, apoptosis, mitochondrial electron transport, platelet and neutrophil adhesion, stomach contraction, intestine, uterus and heart, penile erection, T cell production, regulation of sleep and blood pressure[63,77–80].

Due to its gaseous nature, NO has different properties than any other neurotransmitter; NO cannot be stored inside vesicles to be subsequently exocytosed[81]. Consequently, when a cell produces NO, it escapes through the cell membrane spreading to the extracellular space[74,82]. The same property of traversing the membranes allows NO to affect other cells without the need for receptors on the surface. It is, therefore, a signal molecule that can be released from any part of the cell and act on the same cell that produces it or on any cell in the vicinity. In mammals, the generation of NO is catalyzed by three different isoforms of enzyme nitric oxide synthase or NOS[83]. For the synthesis of NO, not only the L-arginine and oxygen as substrates are required but also four cofactors: flavin mononucleotide (FMN), flavin adenine dinucleotide (FAD), tetrahydrobiopterin (THB) and nicotinamide adenine dinucleotide phosphate (NADPH). In addition, all NOS subtypes bind calmodulin and contain a heme group[84,85].

To produce one mole of NO, five moles of the guanidine nitrogen of L-arginine, 1.5 moles of NADPH and 2 of the dioxygen are required. The reaction consists of two

separate acts of monoxygenation. The first part consists of the incorporation of an O-atom to the substrate L-arginine, while oxygen is reduced to water, obtaining N-hydroxy-L-arginine (NOH-L-Arg) as an intermediate. The second reaction counts on an electron of the NADPH, another one of the NOH-L-Arg and the O_2^- in form of dioxygen-iron attack the guanidine carbon of the NOH-L-Arg, facilitating the incorporation of O_2^- and a split of C-N bond, releasing a nitrogen atom and giving rise to L-citrulline[86]. In this second reaction, one atom of O_2^- reduces to water and another one joins the nitrogen to form NO. This reaction can be inhibited by structural derivatives of L-arginine, such as N-mono-methyl-L-arginine (L-NMMA) and N-nitro-L-arginine methyl ester (L-NAME)[80,85].

- *Isoforms of nitric oxide synthase*

Due to the characteristics of NO, this molecule cannot be stored. Therefore, the regulation of the enzyme that catalyzes its synthesis is therefore very important; in fact, NO synthase (NOS) is regulated more closely than any other enzyme in the neurotransmitter synthesis pathway[80,87].

So far, three isozymes of NOS have been identified in mammals ; they consist of homodimeric subunits with molecular weights between 125 and 155 kDa[64]. The three isoforms are encoded in three genes located on three different chromosomes[85]. The NOS nomenclature has been liable to confusion. The one that is currently used is accepted by the International Union of Pharmacologists being the three recognized isoforms:

1. Two calcium-dependent constitutive isoforms: the endothelial isoform (eNOS), also known as type III (NOS3) and the neuronal isoform (nNOS), also referred to as type I (NOS1). These isoforms mediate the production of NO in low and physiological quantities[88–90]. nNOS is constitutively expressed by neurons in the brain, but can also be found in spinal cord,

peripheral nerves and skeletal muscle. eNOS is mostly expressed in endothelial cells, but this isozyme can also be found in cardiac myocytes, platelets and certain neurons of the brain.

2. An inducible form (iNOS or NOS2), independent of calcium, which expression can be induced in different cell types, such as macrophages, hepatocytes, neutrophils, smooth muscle and endothelium. This induction occurs in response to different immunological stimuli such as interferon gamma (IFN-γ), tumor necrosis factor alpha (TNF-α) and bacterial lipopolysaccharide (LPS). This isoform catalyzes the production of large amounts of NO, which may be toxic in certain circumstances or for certain cell groups[74,91]. Once expressed, iNOS is constantly active and not regulated by intracellular Ca^{2+} concentrations.

The binding of calmodulin to NOS appears to be the "molecular switch" that allows the flow of electrons from the reductase domain to the heam group, allowing the transformation of O and L-arginine into NO and L-citrulline[64,75].

In cerebral ischemia, NO plays an important but ambiguous role: it can have both protective and harmful effects[74,92], depending on the momentum, the duration of release, the isoform and the cell that synthesizes it. Increase in eNOS activation promotes the vasodilation, angiogenesis and inhibits microvascular adhesion and aggregation, resulting in a neuroprotective role[93–95]. On the other hand, hyperactive nNOS can be stimulated by massive Ca^{2+} influx into neuronal cells and has been implicated in N-methyl-d-aspartate receptor-mediated neuronal death in cerebrovascular stroke[46]. Under those conditions, NO can contribute to excitotoxicity, probably via mitochondrial permeability transition. High levels of NO can also result in energy depletion, due to inhibition of mitochondrial respiration and inhibition of glycolysis. eNOS is activated minutes after the stroke, and maintained for a short period of time, in the brain, eNOS is mainly produced by the

vascular endothelium and the choroid plexus. Although eNOS-NO production is aminor part of total brain NOS activity, this enzyme is critical for the regulation of cerebrovascular hemo- dynamics and for the protection of endothelium integrity from inflammatory, oxidative, and procoagulant stimuli[96]. Therefore, the exogenous manipulation of this molecule has become the target of intensive research[96]. An example of this is the use of selective inhibitors of nNOS, which has resulted in neuroprotection in models of focal ischemia[97]. However, the release of NO by eNOS results in vasodilatation and angiongenesis and is considered to be beneficial after stroke. In accordance, many experimental stroke therapies focus on activation of eNOS.

- *Regulation of eNOS*

Besides Ca^{2+}, many other pathways are involved in the activation of eNOS, such as the association with the protein **Hsp90** (heat shock-associated protein).This protein, is essential and abundant in all eukaryotic cells. Its function is to provide stability and to keep many essential proteins for the cell active, such as those involved in signal transduction or the cell cycle. Hsp90 can form a complex with eNOS hereby acting as an allosteric modulator, inducing a conformational change of eNOS or stabilizing the dimeric form of the isoform, keeping it active[98,99].

Growth factors and shear stress dose-dependently stimulate this association of Hsp90 with eNOS, resulting in increasing NO levels in blood vessels[28]. In addition, also phosphorylation at the Serine 1175 position of eNOS improves the activity of this isoform[98]. This phosphorylation can be regulated by the phosphatidyl inositol kinase 3 (PI3K) / Akt pathway, or Ca^{2+}/calmodulin-dependent protein kinase II (CaMKII), or protein kinase A (PKA)[54](Figure 1.5).

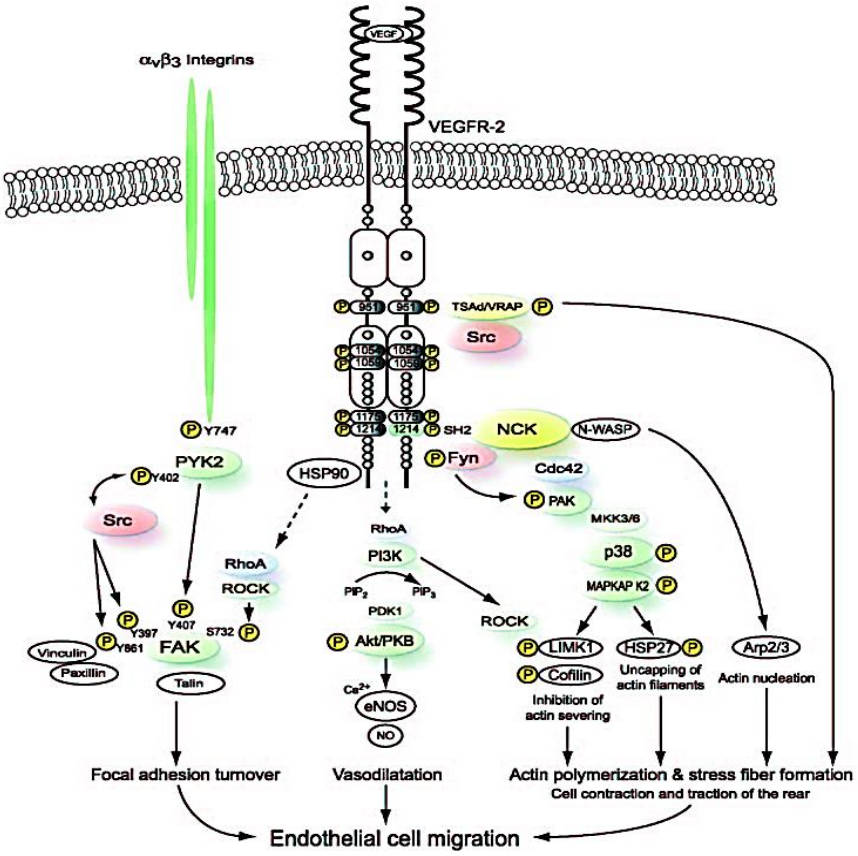

Figure 1.5. VEGFR-2 drives chemotactic endothelial cell migration by contributing to formation of stress fibers. The formation of stress fibers by binding of VEGF to VEGFR-2 requires a cooperative interaction between VEGFR-2 and integrins, especially integrin. The activation of VEGFR-2 initiates its autophosphorylation on Tyr1214. Then, it follows the recruitment of Nck to VEGFR-2 and the sequential activation of Fyn and Cdc42, upstream of the p38 MAP kinase module. Activation of p38 leads to activation of MAPKAP K2 and LIM kinase, which contributes to increase the level of polymerized actin by phosphorylating HSP27 and cofilin, respectively. Of note, Nck can also trigger actin polymerization through activation of the WASP-Arp2/3 pathway. Concomitantly to the activation of p38, the binding of VEGF to VEGFR-2 triggers the recruitment of HSP90 to VEGFR-2, which initiates the activation of RhoA-ROCK and then the phosphorylation of FAK on Ser732. In turn, this changes the configuration of FAK, allowing the phosphorylation of Tyr407 by Pyk, downstream of integrin. This favors the turnover of focal adhesions. Together, the p38-mediated actin polymerization and FAK-mediated turnover of focal adhesions contribute to the formation of stress fibers enabling cell migration by allowing endothelial cell contraction. The activation of PI3K downstream of VEGFR-2 activates Akt/PKB and eNOS. The subsequent production of NO is required for vasodilatation and endothelial cell migration. Figure taken from [60]

The production of NO from eNOS targets the smooth muscle cell that forms the vascular wall. The NO that diffuses through the cell membranes stimulates soluble guanylate cyclase in the smooth muscle cells when it binds to its heme group[85,86]. This binding leads to an allosteric shift of the histidine groups and therewith to a conformational change of the enzyme, which is activated to catalyze the synthesis of cyclic guanosine monophosphate (cGMP) [88,100]. Smooth muscle cells contain a phosphodiesterase specific for cGMP[76].

cGMP activates a protein kinase that carries out the extrusion of Ca^{2+} from the cytoplasm by means of the Ca^{2+}/ Mg^{2+} ATPase pumps causing muscle relaxation and thereby vasodilation, which regulates blood flow and blood pressure[63]. On long term, NO stimulates endothelial proliferation and migration in the angiogenesis process[60,95,101,102]. Therefore, the release of NO by eNOS is considered beneficial after an ischemic attack.

1.4. Neuroprotection in ischemia

Departing from the elements mentioned above, three possible strategies can be derived to minimize the consequences of ischemic stroke: minimize the damage by immediately restoring perfusion (thrombolytic therapies), neuroprotection, and the protection of the neurovascular unit.

Early restoration of perfusion of the affected area has been demonstrated as an effective pharmacological therapy with plasminogen treatment, both in animal models and in clinical trials, and is the only one that has been clinically approved[103].

After a short episode of ischemia, the cells are able to recover ionic homeostasis simultaneously with a (at least partial) recovery of the energy content of the cells[27]. If the ischemia is prolonged, the thrombolytic treatment is not effective, exacerbating the damage by reperfusion. Finally, neuroprotection consists in

preventing or limiting the progression of the ischemic cascade in brain tissue once it has started[104].

As is known, the time factor is crucial to save the largest amount of tissue in ischemic penumbra, hence the concept of therapeutic window implies a period during which the restitution of the regional CBF and other cytoprotective measures can prevent the death of potentially viable cells; as a consequence, if this time window is exceeded any therapeutic measure is considered to be not beneficial[105–107]. In general terms, the earlier treatment is introduced, the greater the benefits. The rapid decrease in CBF followed by a reduction of ATP and energy depletion during stroke triggers the activation of pathogenic processes and a series of complex neurovascular unit responses[44,108,109].

It is well known that as a consequence of cerebral ischemia the integrity of the neurovascular unit is compromised by different mechanisms[5,73]. Therefore, it is necessary to preserve all the structures that compose it, including microvessels (endothelial cells, basal lamina and pericytes), neurons and their axons, astrocytes and other support cells such as oligodendroglia, which is why the concept of neuroprotection should be changed into cerebroprotection, which covers the whole organ[75].

In addition, protection and repair which are activated mechanisms triggered after damage, should be considered as a continuum in the context of the natural cerebral plasticity process. This process is potentiated after injury and includes interrelated processes such as neurogenesis, synaptogenesis, axonal regeneration, oligodendrogenesis, remyelination and angiogenesis which contribute to the repair of the neurovascular unit[5,62,110]. Therefore, from a therapeutic point of view, it is important to find protective and restorative therapies to boost the mechanisms of cerebral plasticity.

According to their primary action mechanism, neuroprotective strategies can be classified into the following groups[36,104,111,112]:

1- Modulators of the excitatory amino acid system.

2- Modulators of the calcium flow.

3- Metabolic activators.

4- Anti-edema agents.

5- Leukocyte adhesion inhibitors.

6- Capturers of ROS.

7- Membrane repair promoters (and inhibitors of its degradation).

8- Compounds with unknown effects.

Due to the redundancy of different metabolic pathways that ultimately lead to cell death, the path to be followed must necessarily go over the use of neuroprotectors capable of interfering at key points in several of these processes.

1.4.1. Strategies related to nitric oxide

Therapeutic modulation of NO production as a treatment in those pathologies in which its involvement has been observed, has generated a growing interest in recent years. Cooke et al. reviewed the potential therapeutic use of NO production modulation in the case of stroke[80].

Neuroprotective strategies have been designed either based on the stimulation of NO in the acute phase by administering the NOS substrate or NO donors, or were oriented to (selective) inhibition of the NOS isoforms[76,96].

In contrast to the deleterious effect of nNOS activation during ischemia, the activation of eNOS plays a protective role by maintaining the regional blood flow. The use of nNOS selective inhibitors has resulted in neuroprotection in focal ischemia models, whereas the use of high doses of non-selective NOS inhibitors,

which also affect eNOS, result in severe alterations of the local CBF and in the subsequent increase in infarct size[90,97]. Evidence in the same sense is provided by the fact that nNOS deficient knockout mice develop less cerebral infarction than wildtype animals, and the cell cultures of these animals are more resistant to damage caused by glutamate and hypoxia/hypoglycemia[113].

There is a great temporal dependence for the effectiveness of pharmacological NOS-targeting strategies in the treatment of ischemia. Nonspecific inhibition of NOS (e.g. with N-ω-nitro-L-arginine methyl ester (LNAME)) during the early stages of ischemic aggression, has been shown to be deleterious causing an increase in infarct size; whereas late nonspecific inhibition 3-6 hours after the onset of the occlusion is beneficial and no longer affects the infarct size[114,115].

The molecular mechanisms involved in the early therapeutic effect of NO are complex. On the one hand, vascular protection is linked to its vasodilatory and antithrombotic properties cGMP-mediated mechanisms which improve blood flow and help maintain perfusion in the area of ischemic penumbra. On the other hand, being a radical, NO can react with ROSs (reactive oxygen species) and free radicals, partially reducing oxidative damage induced by ischemia. It has also been suggested that NO may interact with a specific site of the NMDA receptor or channel, nitrosylating it and decreasing glutamate binding and/or causing a decrease in Ca^{2+} flux[101,116].

Late after ischemia, the endogenous production of NO is caused by the induction of iNOS expression; mainly resulting from reactive astrocytes and the infiltration of neutrophils in the infarcted tissue. This manifestation has been demonstrated in the brain tissue after permanent and transient ischemia in both rodents and humans[92,113,117,118]. This isoform produces large amounts of NO for long periods and is the isoform most likely to be responsible for late damage mechanisms after

cerebral ischemia. It has been observed that NO is able to cause a rapid depletion of neuronal ATP by various mechanism including inhibition of ATP generation by deterring NO and $ONOO^-$ the mitochondrial respiratory chain, a fluctuation on membrane permeability, an inhibition of glycolysis at the level of the enzyme glyceraldehyde-3-phosphate dehydrogenase as well as promoting the consumption of ATP[113,115], resulting in deleterious cellular survival by exacerbating tissue damage.

1.5. ELFMF as a neuroprotective agent

Electromagnetic fields (EMFs) are generally classified according their associated energy. The term electromagnetic spectrum is being used to describe the range of all possible frequencies of electromagnetic radiation.

Depending on the energy, the electromagnetic radiation is categorized as ionizing radiation when it is high enough to separate the electrons from their orbits around the atoms and be able to ionize them. This property is attributed, for example, to X-rays and γ rays [IARC 2013] [119,120]. Long-term exposure to ionizing radiation causes serious health damages.

However, when their energy is not strong enough to ionize molecules, EMFs are called non-ionizing EMFs and are considered, at least conceptually, not as harmful to health[121].

Extremely low frequency magnetic fields (ELFMF) are in the range of 1-300 Hz and in amplitude of 0.2-20 mT and depending on the waveform are classified as sinusoidal ELFMF (ELFMFs) or pulsating (PELFM). These ranges are above the geomagnetic fields, which are in the order of 20-70μT[11].

In general, it has been observed that ELFMF provoke a variety of biological effects[122,123]. Moreover, different mechanisms of interaction have been proposed but so far are not well understood.

Everything in living systems is in motion and changing magnetic field are associated with changing electric field. Endogenous EMF (electromagnetic field) and PEMF (pulsed electromagnetic field) arise from the movement of muscles, tendons, etc. and the actions of the musculoskeletal system itself. Mechanical deformation of dry bone caused piezoelectricity, i.e. bending strain couples to the spatial gradients of permanent dipoles in collagen molecules[124].

At physiological conditions, mechanical stress-generated potentials are formed by different mechanisms including: (a) the streaming potential, which is the electric potential difference between a liquid and a capillary, diaphragm, or porous solid through which it is forced to flow, or (b) the electrokinetic processes, i.e. entrainment of ions because of fluid motion through the bone[125]. In any case, the EMF caused by these reactions are able to penetrate tissue and the MF component can induce electric currents in the bone or muscle tissue by Faraday coupling.

Vibrations of human muscles induce mechanical strains and currents of certain frequencies (5–30 Hz) were found during postural muscle activity (quiet standing) and 10 Hz during walking[126].

In addition we have to keep in mind that ligaments, tendons, fasciae and other connective tissue elements also consist of collagen. This collagen accounts for 30–40% of body protein having piezoelectric properties[127].

On the other hand, the little higher frequencies of brain activity (although still extremely low frequency EMF most of the EEG spectral density is below 100 Hz) are more related to the typical sinusoid waveforms of the EMF. The current densities lie normally in the range from 1 to 10 mA/m^2 (nerve firing around 1–60 Hz),

however, current densities of 1000 mA/m^2 can develop during brief periods of activity (e.g. action potentials) on the surface of nerve or muscle cells[128].

Furthermore, the enzymatic and metabolic activities of cells are mostly processed rhythmically. Thus, every substrate change and every small metabolic cycle has its own up and down often in a sinus wave with a typical frequency[129,130].

There is an interesting correlation between EMF in the natural environment and the endogeneous rhythms of the heart (ECG), brain (EEG) and peripheral nerve activity. It looks as if organisms, including mammalians and humans, have internalized environmental EMF rhythms. These low frequencies are based mostly on metabolic cycles, as seen in experiments with neutrophils and PEMF[131]. Possibly, these dynamics can be disturbed by EMF: magnetic fields at 1 and 60 Hz destabilize rhythmic oscillations in brain hippocampal slices via yet unidentified nitric oxide mechanisms[132]. Conversely, donors of NO and cGMP analogs applied during blockade of NO synthesis lengthen and destabilize intervals between successive rhythmic wave bursts[132]. Rhythmic EEG wave bursts in rat brain hippocampal tissue can also change due to exposure to weak (peak amplitudes 0.08 and 0.8 mT) 1 Hz sinusoidal magnetic fields[132]. Pilla et al. (2013) reports that these field effects depend on synthesis of NO by calmodulin-dependent phosphorylation in the tissue[133,134].

Several studies suggest that the process of angiogenesis influenced by ELFMFs observed *in vitro* and *in vivo* varies considerably depending on dose, frequency, magnetic strength, waveform and exposure times [12,17,122,135].

One of the theories that explain the healing processes induced by ELFMF refers to the activation of the angiogenic cascade facilitating cell migration and proliferation by ELFMF induced transduction cascades[11,136].

In this sense, Pesce et al[11] reviewed extensively an increase in proliferation and migration in *in vitro* and *ex vivo* models through the increase of cGMP, mediated by

the increase of NO at the intensity of 1 mT / 50 Hz. In a review study, published by McKay et al. [137], contradictory results of ELFMF on the effect of ELFMF on the blood flow and vessels of the microvasculature are described, however most studies indicate a positive effect of ELFMF on angiogenesis. These conflicting results found in the literature are fundamentally based on the magnetic field dosage used. In addition, numerous reports indicate the involvement of NO as the primary mechanism[17,137–139]. Gutiérrez-Mercado et al. showed that the ELFMFs at 0.66 mT/120 Hz influence the structure and characteristics of the vascular permeability of the capillaries of the circumventricular organs such as the cerebral parenchyma and the cerebrospinal fluid. Delle et al[12]. observed that exposure to 1 mT / 50Hz of ELFMFs in human umbilical vein endothelial cells (HUVECs), contributed to a significant increase in proliferation, migration and formation of tubes with exposure times of 1-12 h, observing an inhibition of the process at 24 hours[140]. However, in a second experiment, they applied 2 mT / 50 Hz during the same time periods, observing an inhibition on the process[17]. It can therefore be attributed that the phenomenon observed depends in this case on the intensity and time of exposure.

In relation to other variables such as the waveform, Zhou et al.[141] studied that the applied magnetic field (sinusoidal, triangular, square or saw tooth) exerts an effect on the proliferation and migration of rat osteoblasts; recognizing that differences depended on the form of variation of the applied field. These results suggest that it is necessary to take this parameter into account when studying magnetic field application.

Research aim:

In the present study the effect of ELFMF is investigated on a global ischemia model. This is carried out through an evaluation at molecular, cellular, tissue and behavioral level, by exploring its effects on the angiogenic process in detail, thereby

contributing to the clarification of possible mechanisms of action. This approach creates new opportunities for the development of a therapy for cerebral ischemia.

CHAPTER 2

MATERIALS AND METHODS

This research was developed using *in vitro* and *in vivo* models to demonstrate angiogenic effect of ELFMFs. *In vivo* studies were carried out at the National Center for Applied Electromagnetism (CNEA, Universidad de Oriente), with the collaboration of the National Center for Laboratory Animal Production (CENPALAB) and the Center for Toxicology and Biomedicine (TOXIMED). *In vitro* studies were carried out at the 'Biomedisch Onderzoeksinstituut' (Centro de Biomedicina-BIOMED) at the Hasselt University, Belgium.

2.1. General Logic of Research

The experimental design of the research was carried out in order to contribute to the clarification of cellular and molecular mechanisms of ELFMFs (at doses: 13.5 mT/ 10 Hz and 60 Hz) as a potential neuroprotective treatment in cerebral ischemic disease. Figure 2.1 presents the general logic followed in this research.

In vitro and *in vivo* studies were performed to evaluate the possible mechanisms involved in angiogenesis. Endothelial cells are used as as models (HMEC-1) for *in vitro* studies. The model of chronic hypoperfusion by permanent occlusion of both carotid arteries in Wistar rats for *in vivo* studies is used.

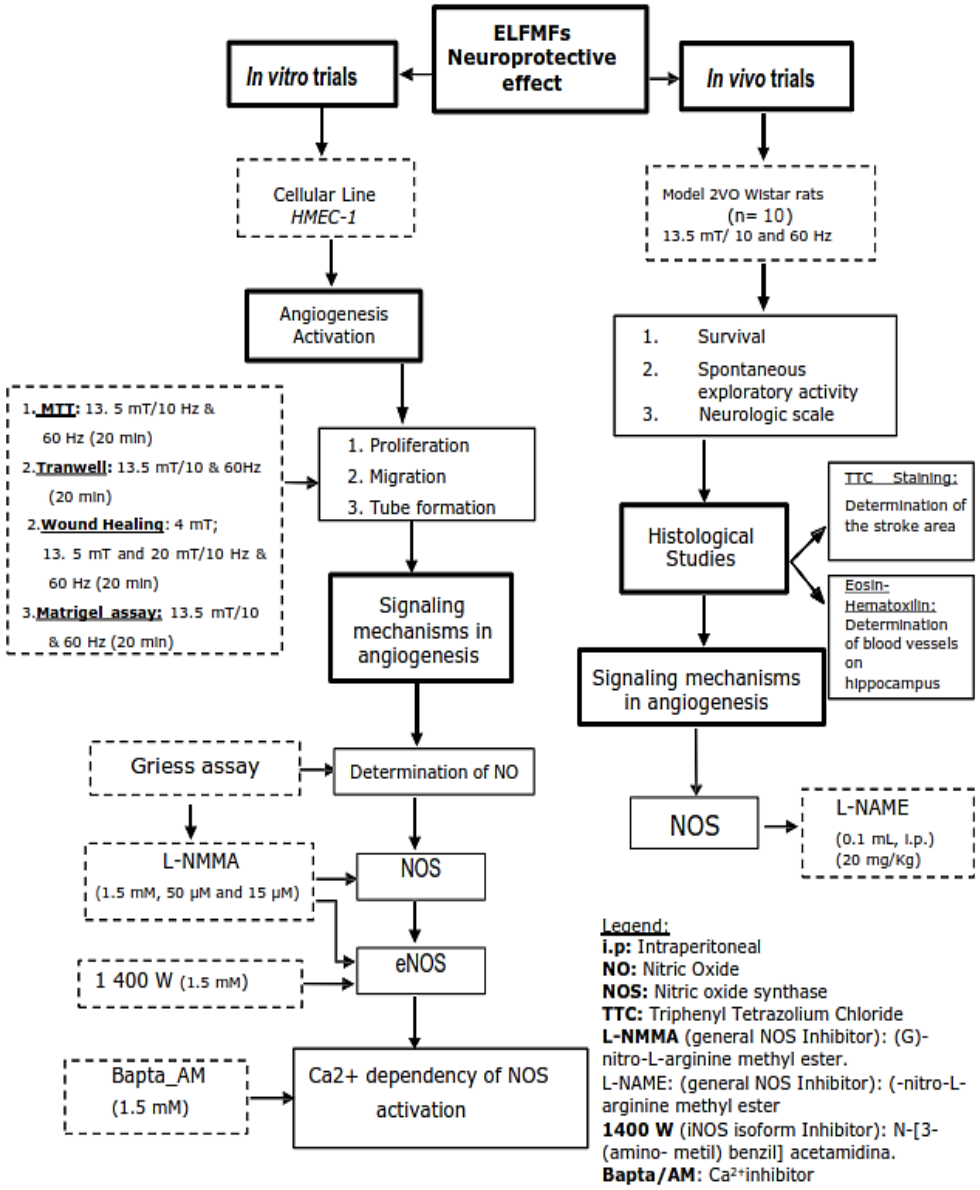

Figure. 2.1. Flow diagram of the experimental logic used.

2.2. Characterization of ELFMFs for experimental development

The intensity and frequency values selected for this study are based on recommendations from Marañon et al., which evaluated different intensities and frequencies in the PUIg model (Permanent Unilateral Ischemia in the Gerbil of Mongolia), obtaining the best results for 13.5 mT / 10 Hz And 60 Hz[18].

To generate the 60 Hz signal, the magnetic stimulator NAK®-02 was designed and built by the National Center for Applied Electromagnetism (*Centro Nacional de Electromagnetismo Aplicado*: CNEA). This equipment has the technical certification, granted by the *Centro de Estudios de Tropicalización* and with two registrations granted by the Center of State Control of Medical Equipment (*Centro de Control Estatal de Equipos Médicos*: CCEEM).

A function generator (IT-112/1, Russia) coupled to a high-fidelity amplifier (10 Hz to 20 kHz bandwidth and 60 W output power) was used to generate the 10 Hz signal. Both devices generate a sinusoidal waveform hence the acronyms chosen to make reference to the ELFMFs.

The magnetic field generated (Figure 2.2) was certified by the CNEA Magnetic Characterization Laboratory, highlighting its non-homogeneous distribution; thus, the value reported in this research work is the maximum value on the surface of the inductor. The coils (inductors) used to apply the treatment were solenoids with iron core 40 mm in diameter (working surface area).

The intensity of the generated field was controlled with a micrometric positioning system, using a surface Gaussimeter, model 5180 F.W. Bell (Pacific Scientific, OECO, USA).

For each experiment, the minimum, maximum and mean values of the magnetic field strength in relation to the working volume (Bmin, Bmax and Bmed, respectively) were calculated by means of 3D finite element simulation (Table 1).

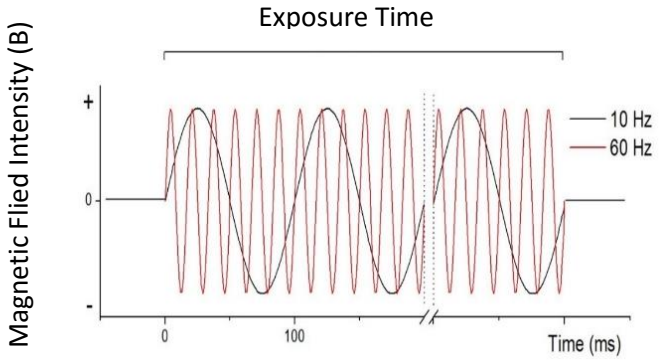

Figure 2.2 Diagram with the waveform used (continuous sinusoidal at 10 and 60 Hz).

Table 1. Induction levels of the ELFMFs (minimum, medium and maximum) in each volume of work employed.

	Work Volume			
B(mT)	Rat Encephalon	96-wells Plate	24-wells Plate	Petri dish
$B_{mín}$ ± DE	2.12 ± 0.45	2.12 ± 1.25	2.12 ± 0.85	2.11 ± 0.41
B_{med} ± DE	3.25 ± 0.69	3.25 ± 1.91	3.24 ± 1.30	3.24 ± 0.62
$B_{máx}$ ± DE	4.38 ± 0.92	4.38 ± 2.58	4.37 ± 1.75	4.38 ± 0.34

Note: The mean values (med), minimum (min) and maximum (max) and standard deviation (SD)

2.2.1. Methodology for the application of in vitro ELFMFs

For the *in vitro* studies three experimental groups were formed:

1. Control without application of ELFMFs (Group 1)
2. Exposure to ELFMFs: 13.5 mT 60 Hz for 20 min. (Group 2)
3. Exposure to ELFMFs: 13.5 mT 10 Hz for 20 min. (Group 3)

In the case of the *in vitro* wound healing test, other inductions of the ELFMFs are included: 4 mT and 20 mT at 10 Hz and 60 Hz during the same exposure time, in order to determine the optimum intensity of endothelial cell migration.

2.2.2. Methodology for the in vivo application of ELFMFs

The experiment was designed to last for seven days. The surgery was performed on day 0. After three hours the first ELFMFs dose was applied and continued for three days, with a duration of 20 minutes for each exposure. The animals were randomly distributed into five groups:

1. Sham operated: operated following the procedure described, but without carotid occlusion (n = 5);
2. Sham exposed: after induction of ischemia, the inductors are placed on the cranial cavity for the time established for the treatment, but with the equipment turned off (n = 5);
3. Control: which was caused by ischemia without treatment (n = 13);
4. Exposure to ELFMFs: 13.5 mT / 60 Hz (n = 13);
5. Exposure to ELFMFs: 13.5 mT / 10 Hz (n = 13).

2.3. In vitro trials

2.3.1. Selection of the cell line

The HMEC-1 cell line (immortalized endothelial cells of the human microvasculature) was chosen as the experimental model for this study. The selection criterion was based on previous experiments to evaluate angiogenesis[142,143]. The cell line was supplied by the Centers for Disease Control and Prevention (Atlanta, GA), which were kept in freezing at -80 °C until further cultivation.

2.3.2. Cell culture

Cultivation of HMEC-1 cells was performed in T-25 flasks containing 5 mL of the MCDB 131 culture medium (Invitrogen, Carlsbad, CA) enriched with 10% fetal bovine serum (Biochrom AG, Berlin, TO THE.); 10 mM L-glutamine (Gibco, Paisley, UK); 10ng.mL^{-1} human epidermal growth factor (hEGF, Gibco, Paisley, UK); 1 mg.mL^{-1} hydrocortisone (Sigma, St. Louis, MO); 100 U / mL penicillin and 100 mg/ mL streptomycin (Sigma, St. Louis, MO) following the methodology used by Bronckaers et al[143]. Cells were incubated at 37 °C in a humidified atmosphere, 5% CO_2.

2.3.3. Study of angiogenic effect of ELFMFs on HMEC-1 cells

2.3.3.1. Evaluation of cell proliferation

To determine the effect of ELFMFs on HMEC-1 endothelial cell growth the number of cells proliferated was determined with 3-(4,5-dimethylthiazolyl-2)-2,5-diphenyltetrazolium bromide (MTT) (Sigma, St-Louis, MO)[143,144].

The cell density was determined as described in section 2.3.2. Cells were seeded at a density of 1 ×10^6 cel.cm^{-2}in a 96-wells microplates in 200 µL of modified α-Eagle

culture medium (α-MEM). After 24h of incubation, supernatant was removed and the cells are washed with PBS (1x). In this study two controls were established; for them, the culture medium was replaced with 200 µL of modified Eagle's medium (α-MEM) (Sigma, St-Louis, MO) enriched with FBS (Biochrom AG, AL.) at 10% for the positive control, and 0.1% for negative control. Cells were exposure to ELFMFs for one, 2 or 4 days. In each experiment, every condition was performed in triplicate (n=5).

At the end of the treatment the culture medium was replaced by a solution of 10 µM MTT (5 mg mL^{-1}) in 90 µL of α-MEM with 10% of FBS. The mixture was incubated for 4 hours. After this time, the supernatant was removed and 175 µL of 0.1 M DMSO-glycine solution (Sigma) was added to each well. The optical density, which is a measure of the cell density and thus growth, was quantified with a microplate reader (Benchmarka, Biorad Laboratories, AL) at a wavelength of 540/550 nm.

2.3.3.2. Evaluation of cellular migration

For the quantification of the cell migration after the ELFMFs application, according to each experimental group, two methods were used in order to guarantee the accuracy of the results and their subsequent interpretation: pore tranwell migration assay and the wound healing test.

a) Transwell assay

The Modified Boyden Chamber assay was used to assess transwell migration. These chambers have polycarbonate filters with 8 µm pores (Thincert™ Inserts, Greiner BIOone, Kreimsmünster, Aus)[145], which were placed in 24-well microplates: resulting in two compartments separated by the membrane. HMEC-1 cells were added to the upper compartment with an initial density of 10^6 cel.cm^{-2} in 300 µL of α-MEM culture medium with 0.1% FBS. In this study, two controls were established;

500 µl of α-MEM with 0.1% FBS (negative control) or 10% (positive control) were added to the lower compartment.

The plates were incubated for three hours; ELFMFs were then applied in the two selected doses (13.5 mT / 10 Hz and 60 Hz for 20 min). After 24 h the cells were fixed with 4% paraformaldehyde and stained with 0.1% crystal violet for quantification. Cells that did not migrate were removed from the top face of the insert membrane with a cotton swab. The cells that have transmigrated through the membrane are photographed with a Jenoptik ProgRes C3 (Jenoptik, Jena, AL) camera coupled to an inverted microscope (Nikon eclipse TS100, JP) with a 100 x magnification. The surface occupied by migrated cells was quantified with Carl Zeiss Axiovision 4.6 software. For this study, five replications (n=5) were performed, evaluating exposure to single-dose ELFMFs with a single stimulation for 20 min.

b) Wound Healing test

This test allows to observe v the directional migration of the cells towards an empty the area at a pre-established time; [146]. For the comparisons, snapshots were used, monitoring for 24 hours.

Five replicates were performed for each group in this trial (n=5), evaluating exposure to ELFMFs in six doses. A control group, without application of the ELFMF was also included. The doses of ELFMFs used, were:

1. 4mT / 10Hz
2. 4mT / 60 Hz
3. 13.5mT / 10Hz
4. 13.5mT / 60Hz
5. 20 mT / 10Hz
6. 20 mT / 60 Hz

These doses were included to make a dose response curve. This trial is relevant to demonstrate the potential of ELFMFs to increase the migration velocity of cells to the empty space between the cells.

For the procedure, special silicone inserts (Ibidi, Planegg / Martinsried, Germany) were used which consist of a transverse partition separating the cell suspension into two compartments, leaving an empty area in the center of the cells, which simulates a scar[146].

The inserts are adhered to a Petri dish containing 5 mL of MCDB-131 medium (Invitrogen, Carlsbad, CA). Cells were added at an initial density of 11,600 cm^{-2} cells in each compartment of the insert. The plates are then incubated for 24 hours. Next, inserts were removed with sterile forceps leaving an empty space between two areas filled with cells. After 4h, ELFMFs were applied, placing the inductor in such a way that the scar was exactly above the center of the inductor. 24h later, cells were fixed and stained with 0.1% of crystal violet.

The samples were allowed to dry and then pictures were taken using a Nikon eclipse TS100 (Jenoptik, Jena, Al) inverted microscope camera with a 10 x 40 magnification. The Carl Zeiss Axiovision 4.6 Software was used to determine the area occupied in the wound by migrated cells. The values are presented in relative units that represent the times the treated groups are contained in the control group.

We calculated the coefficient of effectiveness (EC_{50}) that is expressed through the concentration of the agonist that causes a response on the midline between the upper limit and the lower limit of the curve.

c) Tube formation assay

The wells of an Angiogenesis µ-slide (Ibidi) were coated with growth factor reduced, phenol red-free Matrigel Basement Membrane Matrix (Corning, Bedford, MA, USA). After the matrix had solidified, 10,000 HMEC-1 were seeded per well. 1 hour

later, ELFMFs (10 and 60Hz) was applied for 20 minutes. After 6 hours two representative images were taken at a 4x magnification level with an inverted Nikon eclipse TS100 microscope equipped with a relay lens (Nikon Microscope DXM Relay Lens MQD42070) and a Jenoptik ProgRes C3 camera. The Angiogenesis Analyzer plugin in Image J was used to determine the number of nodes and total branching length[147].

2.3.4. Molecular analysis

2.3.4.1. Determination of nitric oxide by the Griess method

Nitric oxide (NO) is formed by various isoforms of the enzyme nitric oxide synthase (NOS), undergoing rapid oxidation to nitrite (NO_2^-) and / or nitrate (ON_3^-). The concentration of nitrites in the medium was determined as an indicator of the production of NO by the Griess reaction (Colorimetric method) (Corp. Promega, Madison, USA)[148].

The maintenance and quantification of HMEC-1 cells was similar to that described in section 2.3. Cells were seeded in in 24-well microplate (300 µl) and incubated for 4 h under previously described conditions. Subsequently, ELFMFs (13.5 mT / 10 Hz and 60 Hz) were applied in a single dose for 20 min. The samples were kept in incubation under the same controlled environment conditions, and the NO quantification was performed 24 h and 48 hours after ELFMFs application. After waiting for the selected time period, 50 µL of supernatant was taken and added in triplicate in 96-well microplates. The experiment was performed 5 independent times (n =5).

a) Preparation of the calibration curve

Three columns were designated for the preparation of the reference curve and 50 µL of the MCDB-131 medium was dispensed. 1 mL was prepared with 100 µM of

the standard nitrite solution provided by the Griess kit, diluting 1: 1000 in MCDB-131 culture medium. Next, 100 µL of the nitrite solution (100 µM) was added to the first three columns (1-3) of row A, on the microplate. Six serial dilutions (50 µL per well) were immediately performed to obtain a nitrite concentration range of 1.56 to 100 µM.

b) Spectrophotometric determination of nitrites

For the spectrophotometric determination, 50 µL of 1% Sulfanilamide were taken and added to each wells; After 5-10 minutes of incubation, 50 µL of N-1-naphthyllethylenediamine (0.1% NED solution) [1: 1] was added, allowing to stand again for 5 to 10 min. Next, Absorbance was measured within 30 min in a microplate reader at 540 nm (Benchmark, Biorad Laboratories). To determine the concentration of nitrites (µM), the mean absorbance was taken after subtraction of the blancs and the nitrite concentration was calculated by extrapolation of the values of the standard curve.

2.3.4.2. Indirect determination of the enzyme nitric oxide synthase

To determine the participation of the enzymes nitric oxide synthase, the NO concentration in the culture of endothelial cells HMEC-1 was evaluated by adding a specific inhibitor for NOS: L-NMMA. Different concentrations of the inhibitor (1.5 mM, 50 µM and 15 µM) were used to evaluate the dose-dependent response[87,149,150].

The cell suspension (300 µL) was added in 24-well microplates with an initial density of 1 x 10^6 cells per well. Cells were incubated for 4 hours under previously described conditions.

Subsequently, the cells were preincubated for 15 min. with the inhibitor at the corresponding concentration; then stimulated with ELFMFs at 13.5 mT / 10 Hz and

60 Hz for 20 min. Samples were maintained in incubation under the same controlled environment conditions for 24 h. The supernatant was added in 96-well plates and the concentration of nitrites was determined as described previously in section 2.3.4.1. Once the NO concentration values were obtained, a dose-response curve was constructed and the inhibition coefficient (IC50) was calculated. IC50 represents the concentration of the inhibitor that is required for 50% inhibition. Five repetitions were performed with three replicates each (n=5).

2.3.4.2.1. Determination of the isoforms of nitric oxide synthase

Two inhibitors were used for this study: the 1 400 W, selective inhibitor of iNOS and the inhibitor L-NMMA inhibiting all NOS isoforms.

The cell suspension (300 µL) was added in 24-well microplates; then the cells were incubated for 4 h. Subsequently, the cells were preincubated for 15 min. with 1.5 mM of 1 400 W or 1.5 mM of L-NMMA[86,90,151]. The stimulation was then performed with ELFMFs at 13.5 mT / 10 Hz and 60 Hz for 20 min. Samples were maintained in incubation under the same controlled environment conditions for 24 h. Determination of nitrite concentration was performed as described previously in section 2.3.4.1. In this study, five independent studies were performed (n= 5).

2.3.4.2.2. Determination of Ca^{2+}-dependent isoforms

In order to elucidate the role of Ca^{2+} in the production of NO in response to ELFMFs, BAPTA / AM (Tocris Bioscience, UK) was used as an intracellular Ca^{2+} chelator, according to YoungHee et al. [152] methodology. In this study, seven groups were formed:

1. Control
2. Cells + BAPTA / AM (10 µM)
3. Cells + BAPTA / AM (100 µM)

4. Cells + BAPTA / AM (1 mM)

5. 13.5 mT / 60Hz + BAPTA / AM (10 µM)

6. 13.5 mT / 60Hz + BAPTA / AM (100 µM

7. 13.5 mT / 60Hz + BAPTA / AM (1 mM)

HMEC-1 cells were added in 96-well microplates with an initial density of 1 x 10^6 cells per well; then, they were incubated for 4 h.

Later, different concentrations of the BAPTA / AM inhibitor (1 mM, 100 µM, 10 µM) dissolved in DMSO (10 µM) 163,164 were added to both groups. Subsequently, the samples are preincubated for 30 min, after stimulation with the ELFMFs at 13.5 mT / 10 Hz and 60 Hz, during 20 min. They are, then, allowed to stand for 24 h in incubation, under the same previously described controlled environment conditions. The toxicity of DMSO was verified by adding 10 µL to the HMEC-1 cell culture, establishing a control.

The spectrophotometric determination of the nitrite concentration was performed as previously described in section 2.3.4.1. Five replicates were performed with three replicates (n = 15).

2.3.5. Determination of the influence of nitric oxide synthase on cell migration: participation of isoforms

Cell migration was determined by the pore migration trial as described in section 2.3.3.2. Endothelial cells HMEC-1 were preincubated for 15 min. with the inhibitor L-NMMA (NOS inhibitor) at a concentration of 1.5 mM[95]. For this study, four groups were formed:

1. Control

2. Cells + L-NMMA

3. Cells + 13.5 mT / 60 Hz

4. Cells + 13.5 mT / 60 Hz + L-NMMA

All groups were stimulated for 20 min, with corresponding doses. Five repetitions were performed with three replicates (n = 15).

For the determination of NOS isoforms, the procedure described above is used. The determination of the nONS isoform was ruled out, and two inhibitors were used: 1 400W to inhibit the formation of iONS and L-NMMA to inhibit the formation of eNOS. Both inhibitors were added at a concentration of 1.5 mM (in the upper compartment)[153], 15 min. before applying the ELFMFs. Six groups were considered in the trial:

1. Control

2. Cells + 13.5 mT / 60 Hz

3. Cells + 13.5 mT / 60 Hz + L-NMMA

4. Cells + 13.5 mT / 60 Hz + 1 400 W

5. Cells + LPS (1 ng mL-1)

6. Cells + LPS (1 ng mL-1) + 1 400 W

A group to which E. coli lipopolysaccharide (LPS) was added as a positive control was used to stimulate the production of ions. All groups were stimulated with a dose of ELFMFs as appropriate for 20 minutes.

2.4. In vivo experiments

2.4.1. Selection of the experimental model

The experimental biomodel used in this study was the Wistar rat (Rattus norvegicus). The animals were supplied by the *Centro Nacional para la Producción de Animales de Laboratorio* (National Center for the Production of Laboratory

Animals), with their corresponding health certificate, according to the quality standards adopted by that institution. The care and management of the animals is performed according to the guidelines established by the Canadian Council for the Care of Laboratory Animals[50], keeping them under controlled environmental conditions, with a temperature between 19 and 25 ° C, relative humidity between 50 and 65% and photoperiod 12 hours light / dark. Water and food were supplied *ad libitum*[154].

The protocols used to work with this biomodel were previously evaluated and approved by the Ethics Committee and the Scientific Council of the CNEA, in accordance with the international standards of protection and management GE^{-1}: 1994, ISO 10993-11 and ISO 10993 -12 and the good laboratory practice regulations approved by CECMED. The design and development of each experiment was carried out in compliance with the 3R rule (reduction, reproducibility and repetitiveness) that govern good methodological practices.

2.4.2. Obtaining the model of permanent bilateral ischemia by occlusion of both carotid arteries (2VO)

For this study, 49 male rats were used, with an average weight of 250-350 g. The model of permanent bilateral ischemia was developed by occlusion of both carotid arteries (2VO) [154].

The surgical procedure was performed under general anesthesia with monosodium thiopental (Corden Farma SA, IT) (40-50 $mg.Kg^{-1}$) inoculated intraperitoneal. The animals were placed in the supine position. The surgical area was shaved and disinfected with alcohol to 70%.

A 3-cm V-shaped incision was made in the pharyngeal region. Then the skin, the subcutaneous tissue and the fascia of the cervical region and the cutaneous muscle were removed until the submaxillary salivary glands were visualized. To visualize

the carotid arteries and the vagus nerve, sternohyoid muscles and sternomastoids were separated. Once the carotids are located, they are bound to interrupt blood flow[2,154]. Finally, the animals were placed in the boxes corresponding to their experimental group and were maintained with a thermal blanket, at a stable temperature of 37 ° C, until their recovery. The study was double-blinded to avoid bias in the results.

2.4.3. Description of the euthanasia technique

At the end of the experiments, animals were euthanized by intracardiac perfusion. The animals were anesthetized and subjected to food restriction 12 hours before the infusion, to facilitate the anesthetic effect. The superficial and deep reflexes were checked before starting the surgical procedure.

Once the sedation was achieved, the animals were placed in a supine position. A V-shaped incision was made in the sternal keel using scissors to access the thoracic cavity, leaving the heart open which allowed perfusion of 0.9% saline solution and 10% paraformaldehyde into the circulatory system through a left ventricle puncture and aortic advancement, all in order to be able to fix the brain for histological analysis findings.

For the extraction, cutting and preparation of the sample for the histological analysis, the brain tissue was removed from the cranial cavity by performing coronal cuts of approximately 2 mm of thickness.

In the experiments where the staining with 2, 3, 5-triphenyltetrazolium chloride (TTC) was performed, the animals were previously anesthetized, and then killed by decapitation for the extraction of brain tissue.

2.4.4. Methodology to evaluate the effectiveness of ELFMFs as neuroprotecting agent

Motor activity was assessed through the open field test 24 h prior to ischemia, and seven days later. The neurological scale was applied 24 h and 7 days after surgery. In the case of survival, it was monitored daily. On the seventh day, euthanasia was performed and the brain tissue was removed for subsequent histological studies (Figure 2.3).

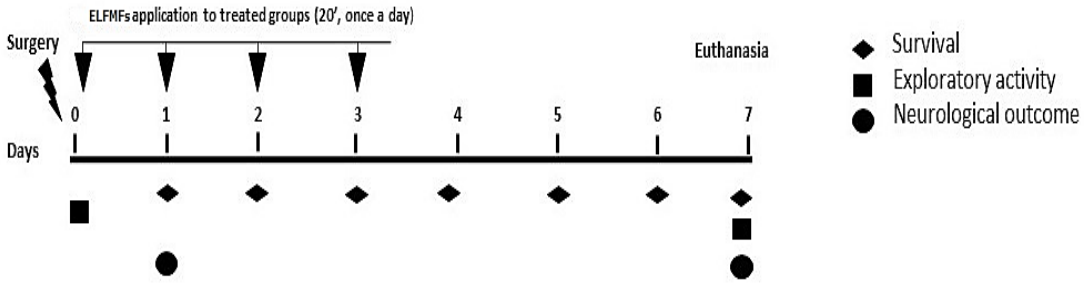

Figure 2.3. Experimental design of *in vivo* experiments

2.4.4.1. Monitoring Survival

Survival was monitored daily during the seven days of the experiment. The number of live animals in each experimental group was calculated. For this analysis only animals with a satisfactory recovery of anesthesia were taken into account, animals that had complications during the surgical procedure such as bleeding and / or death before 24 h were excluded.

To evaluate spontaneous exploratory activity, the open field test was performed to evaluate the effect of ELFMFs, on locomotor recovery after ischemia. In this test were quantified the times the animals raise on their hind legs, and the times that

crossed the fourth quadrant of the field. The behavior was evaluated one day before the surgery and seven days after the surgery. The animals were placed in the center of the field (sides with dimensions 72 x 72 cm, acrylic). The exploratory activity of each animal was recorded with a Panasonic camera (SDR-S26, IT) for further analysis.

2.4.4.3. Assessment of neurological status

For the evaluation of the neurological affection, the criteria of Lawner et al[155]. were used to establish a quantitative scale that allows the classification of animals according to the degree of damage (Annex 1). This permits to quantify through the observation of clinical parameters on a scale of 0 to 9 points, the degree of neurological deterioration (0 being the absence of neurological damage).

This test was performed for each animal, at 24 hours and seven days after ischemia, in order to evaluate brain damage and recovery after treatment. At the end of the experiment euthanasia was performed.

2.4.4.4. Evaluation of the effectiveness of ELFMFs on the reduction of ischemic area in vivo

For this study nine animals were used, distributed in three groups:

1. Control
2. Exposure to ELFMF at: 13.5 mT / 60 Hz
3. Exposure to ELFMF at: 13.5 mT / 10 Hz.

The area of cerebral infarction was determined using the 2,3,5-triphenyltetrazolium chloride (TTC; Sigma-Aldrich) staining method[62,156,157]. For the extraction of brain tissue, the animals were killed by decapitation. Coronal sections

of 2 mm were then performed and incubated for half an hour in the 2% TTC solution, dissolved PBS.

This compound is a substrate for the redox chains of the mitochondria: those that have not been affected by the ischemia react with the TTC, giving a reddish coloration to the tissue[62]. The affected region does not get any color, displaying white regions. Immediately, sections were photographed using a 13-megapixel camera (Samsung Inc., UK). The images were analyzed using Imagj Software (NIH, Bethesda, MD), which quantifies the pixels distributing them in colors and calculates the area in cm^2.

2.4.4.5 Quantification of blood vessels in the hippocampus region

The formation of blood vessels after ELFMFs application was quantified through histological analysis using the eosin-hematoxylin staining method. For this study 15 animals were used, distributed in three experimental groups (n = 5):

1. Control
2. 13.5 mT / 60 Hz
1. 13.5 mT / 10 Hz

Euthanasia and brain extraction were performed as described in section 2.4.3. Sections of brain tissue were set in paraffin; then, with the help of a microtome (Microtome, Leitz 1400, Al), 1.9 mm of the Bregma caudal region were cut to obtain sheets of 8 µm of thickness[97]. The obtained films were stained by the traditional eosin-hematoxylin staining method, locating the region corresponding to the hippocampus in them, in which the number of blood vessels was quantified.

For this endeavor, an Optical Microscope (Carl Zeiss, Jena, Al) was used, with a 10 x 10 magnification. The study was performed in a double-blind fashion, to avoid bias in the results.

2.4.4.6. Enzyme nitric oxide synthase Inhibition Trials

Permanent occlusion of both carotids was performed on 40 Wistar rats used for this study, as described in section 2.4.2. Then, 0.1 mL of L-NAME (20 mg Kg^{-1})[158] was administered intraperitoneally (i.p), 15 min, before applying ELFMFs and during the four days of treatment with ELFMFs. The animals were randomly assigned to four experimental groups (n = 40):

1. Control (ischemic animals)
2. 13.5 mT / 60 Hz
3. 13.5 mT / 60 Hz + L-NMMA
4. Ischemic + L-NMMA

2.4.4.6.1 Survival evaluation

Survival was monitored daily during the seven days of the experiment. Only the animals with a satisfactory recovery of anesthesia were taken into account for this analysis. Those animals that had complications during the surgical procedure such as major bleeding and/or death before 24 hours were excluded. The results are expressed as a percentage.

2.4.4.6.2 Determination of the ischemic area

For the histopathological determination of the ischemic area, the TTC staining method was used. For this study, 16 rats (n = 4) distributed in each experimental group were used. They were euthanized after 7 days by the decapitation method. Brain extraction and TTC staining were performed as described in sections 2.4.3 and 2.4.4.4, respectively. Brain sections were immediately photographed using a 13-megapixel camera (Samsung Inc., UK). The images were analyzed with the free

imaging software (NIH, Bethesda, MD), calculating the infarct area as described in section 2.4.4.4.

2.5. Statistical analysis

The regularity of the samples was verified through the D'Agostino and Pearson test. To compare the results of the neurological scale between 24h and 7 days and the BABTA / AM inhibitor trial, the ANOVA repeated analysis was performed; followed by the Bonferroni multiple comparison post hoc tests. The remaining data were compared using a one-way ANOVA by means of the Kruskall Wallis test; followed by the Dunnes *post hoc* test for comparison between groups. The results are presented as means ± standard error (EE). Statistical differences were performed with a statistical significance of 95% ($p < 0.05$). The Kaplan-Meyer statistical test was used for survival analysis. All data were processed and calculated using GraphPad Prism 5 version 5.01 (GraphPad Software, Inc., © 2013, San Diego, California, USA).

CHAPTER 3. RESULTS

3.1. ELFMFs stimulates angiogenic characteristics of HMEC-1 cells *in vitro*

3.1.1 ELFMFs stimulates cell proliferation

One of the first steps in angiogenesis is activation of endothelial cell propagation. For all in vitro experiments, the ELFMF treatment of 13.5 mT at 10 Hz and 60 Hz was evaluated because at these doses a neuroprotective effect has been observed in our previous results in gerbil model of focal ischemia[19]. An MTT assay was performed to measure the effect of ELFMF on endothelial cell metabolic activity which gives an indication on cell viability and proliferation. Figure 3.1 presents the relative amount of cells after 4 subsequent days of 20 min ELFMFs exposure at dose of 13.5 mT, 10 and 60 Hz compared to untreated control conditions. The highest number of cells and thus highest proliferation rate was observed in the group treated with 13.5 mT / 10 Hz. Statistical analysis revealed that the 10Hz treatment significantly induced cell proliferation in comparison with control group (139.1 ± 25.5% vs 100 ± 19.1%, * $p \leq 0.05$). The cell proliferation between untreated cells and the group receiving 60Hz was not found to be statistically different. There was also no significant differences between the 10 and 60 Hz ELFMFs (139.1 ± 25.5% for 10 Hz vs 127% ± 8.5% for 60 Hz, respectively).

The effect of other ELFMF application protocols on cell proliferation was tested. Cells that received ELFMF application during 2 days did not proliferate more than untreated cells. In addition, when the cell proliferation was measured 2 days after 4 subsequent days of EMFMF treatment, also no significant increase in the number of cells between EMFMF treatment and control group could be demonstrated.

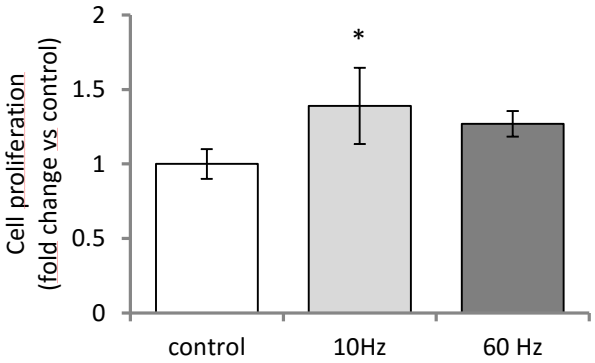

Figure 3.1 ELFMFs stimulates proliferation of HMEC-1 cells. HMEC-1 were seeded, the next day they were stimulated with 13.5 mT ELFMF at 10 or 60Hz, 20 minutes per day during 4 subsequent days. Proliferation was assessed with the MTT assay on the fourth day and the resulting absorbance was compared to unstimulated cells**.** Values are expressed as mean ± STDEV, *p≤0.05, as calculated with one-way ANOVA with a Bonferroni Multiple Comparison Test) (n= 4).

3.1.2 ELFMFs stimulates cell migration

3.1.2.1 Transwell assay

Endothelial cells migration represents an essential step in the angiogenic cascade, and therefore it was examined whether ELFMF application is capable of stimulating this process in a transwell migration assay (Figure 3.2). HMEC-1 were seeded onto an insert with 8 µm pores on a lower compartment containing medium with either 0 or 10% serum. After 4 hours, HMEC-1 received ELFMF treatment and again 24 hours later, the cells that have transmigrated towards the lower surface of the insert were visualized (Figure 3.2 A). An increase in cell density was observed in the groups that were stimulated with a single exposure of 20 min 13.5 mT at 10 Hz and

60 Hz, when the lower compartment contained medium enriched with 10% FCS. Migration of HMEC-1 was significantly increased by 3.0-fold and 2.4-fold when submitted to 10Hz and 60Hz stimulation respectively (* p≤0.05) (Figure 3.2 B). On the contrary, no cells were observed when the inserts where placed in wells containing culture medium without serum (0%), probably due to the absence of a chemotactic agent.

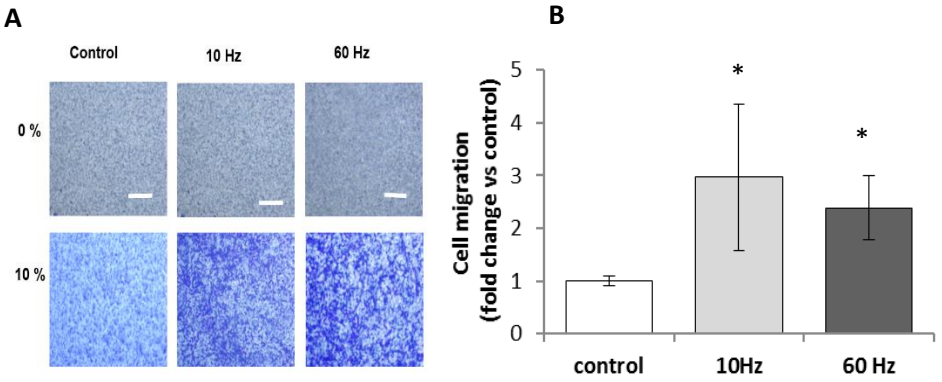

Figure 3.2. ELFMF stimulates Transwell migration of HMEC-1. To assess migration, HMEC-1 cells were seeded onto 8µm insert, with in the lower compartment 500 µl of either a-MEM + 0% FBS or 10% FBS. 4 hours later ELFMF was applied. A) After 24 h, the cells migrated towards the lower surface were stained with crystal violet (Scale bars=200 mm), B) The area on the lower surface of the insert occupied by cells was quantified. Values are expressed as mean ± STDEV, *p≤0.05, as calculated with one-way ANOVA with a Bonferroni Multiple Comparison Test). (n= 5)

3.1.2.2 Wound Healing assay

The effect of ELFMF on HMEC-1 migration was verified by means of a complementary model, i.e. the wound healing assay. In this model cells are allowed to migrate into an empty space (wound) between 2 monolayers of cells. In our study, cells were exposed to different magnetic flux intensities (Figure 3.3). Application of 2.5 mT and 5 mT (both 10 Hz and 60 Hz) failed to increase the amount

of cells in the scar area compared to the control group (Figure 3.4A). However, increasing the induction to 13.5 mT and 20 mT (at 10 and 60 Hz) leads to an increase in HMEC-1 covering the empty areas of the wounds (Figure 3.3).

For each intensity, the area occupied by the cells 24h after ELFMFs treatment was normalized to the area occupied by unstimulated cells and this 'fold change vs control' was taken as a measure for migration (Figure 3.4B). Graph 3.4B shows that for lower intensities, the increase cell migration is proportional to the increase in magnetic flux. However, maximum migration was obtained for 13.5 mT with both frequencies, showing significant differences with respect to the control group (* $p \leq 0.05$ vs control). Half maximal effective concentration (EC50) was ± 5.58 mT for both applied frequencies. Application of 13.5 mT stimulus was shown to lead to a significant induction of cell migration, while the 20 mT stimulus did not result in a significant difference compared to the control group. A slight reduction in covered wound area was observed in the 20mT compared to the 13.5 mT, but this was also not statistically different.

In conclusion, in both the transwell assay as well as in wound healing model, ELFMFs at 13.5 mT at 10 Hz and 60 Hz have a positive effect on the migration of endothelial cells. The amount of cellular migration depends on the doses of ELFMFs applied to the cell culture, with a saturation of cell motility observed after 13.5 mT.

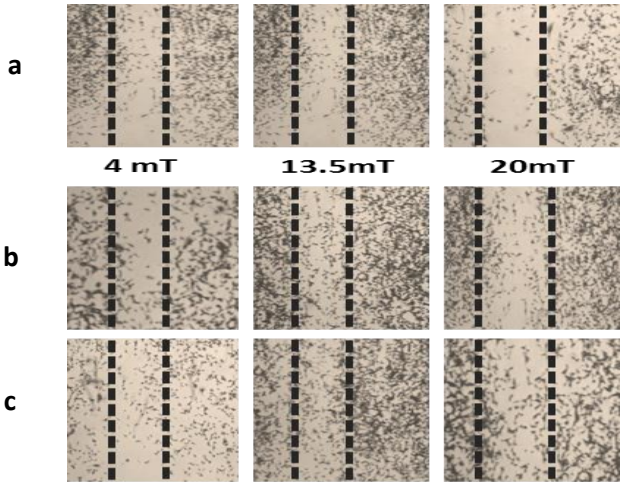

Figure 3.3. ELFMF stimulates cell migration in the wound healing model. Cells were seeded in an insert and the next day the insert was removed, leaving an empty space or wound. Next, cells were subjected for 20 minutes to different magnetic flux intensities (4, 13.5 and 20 mT) at various frequencies: a) 0Hz/control, b) 10 Hz and c) 60 Hz. After 24 hours the amount of cells migrated into the empty space was determined. The dashed lines delimit the original area of the wound formed by the insert before the start of the experiment.

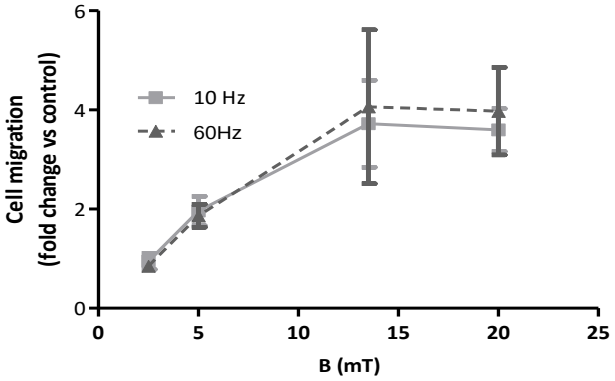

Figure 3.4. Quantification of cell migration in wound healing model. Analyses in wound healing model *in vitro* after stimulation with various magnetic flux intensities: 2.5 mT, 5 mT, 13, 5mT and 20 mT at both 10 and 60 Hz. Values are expressed as mean ± STDEV, *p≤0.05, as calculated with one-way ANOVA with a Bonferroni Multiple Comparison Test) (n=4).

3.1.3 ELFMFs stimulates tube formation of HMEC-1 cells

Finally, the capacity of ELFMFs to induce tubulogenesis was investigated using a Matrigel tube formation assay. Application of 20 minutes of ELFMFs at 60Hz 1 hour after seeding the HMEC-1 cells onto the gel significantly induced formation of tubes (Fig 3.5). The total number of nodes was increased 2.32 times while the total branching length was increased 2.9-fold. 10 Hz showed a tendency to increase tube formation but this was not statistically different.

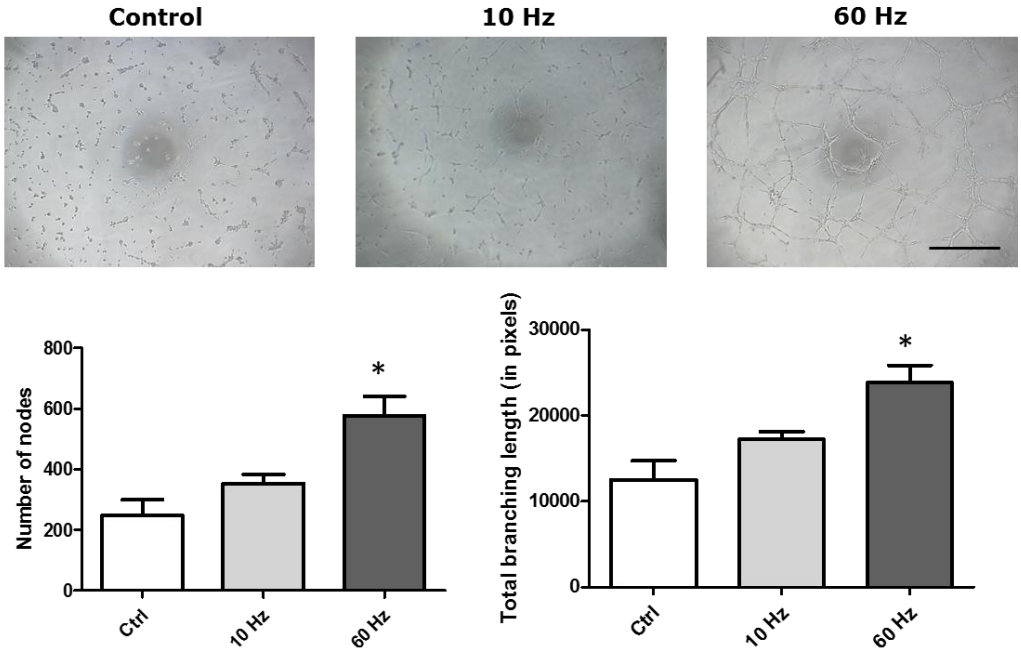

Figure 3.5 ELFMFs induces tube formation. HMEC-1 were seeded into a matrigel and 1 hour later ELFMFs was applied. 6 hours later, the number of formed nodes and the total branching length was assessed. Values are expressed as mean ± STDEV, *p≤0.05, as calculated with one-way ANOVA with a Bonferroni Multiple Comparison Test) (n=5). Data obtained by Kemps, H & Bronckaers, A.

3.2. ELFMFs stimulated the production of Nitric Oxide and Nitric Oxide synthase

3.2.1 Production of nitric oxide (NO)

The results mentioned above show the effect of ELFMFs on endothelial cell proliferation, migration and tube formation. In order to elucidate the possible biochemical mechanisms through which ELFMFs affect these processes, the production of NO which is a key signaling molecule during angiogenesis was investigated. HMEC-1 were exposed to 20 min ELFMF (13.5 mT / 10 Hz and 60 Hz). After 1 h and 24 h, NO concentration in the medium was measured by means of a Griess assay.

The effect of ELFMFs begins to be apparent after 1h of treatment, showing an increase in the concentration of extracellular NO for both frequencies compared to the control group, however this increase was not statistically different (Figure 3.5). The highest values were reached after 24 hours of application of the stimulus, being 3.9 times higher for the group treated with 60 Hz and 2.8 times higher for the 10 Hz treated group (2.8 ± 1.3 μM). Only the 60 Hz treatment at 24 h was found to significantly increase the NO concentration compared to the control group (3.9 ± 1.3 μM vs control group, * $p \leq 0.05$).

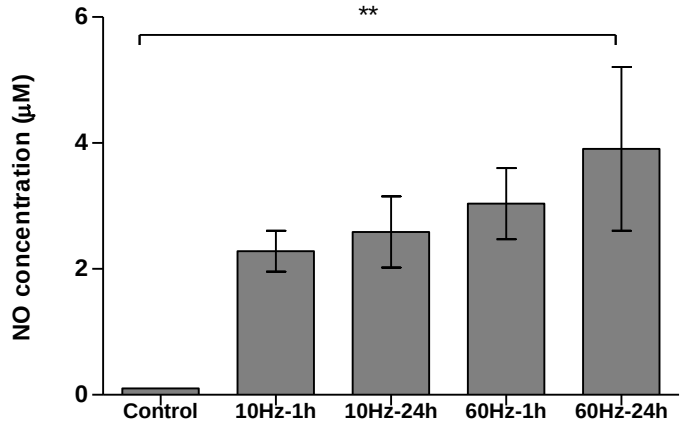

Figure 3.6 ELFMF increases NO production of HMEC-1. NO concentration induced by ELFMFs was measured by Griess assay, 1h or 24 h after treatment of 13.5 mT ELFMFs for 20 min at 10 or 60 Hz. Values are expressed as mean ± STDEV, n=4,*p≤0.05, as calculated with one-way ANOVA with a Dunn's Multiple Comparison Test.

3.2.2. Activation of the enzyme nitric oxide synthase

One of the most frequent routes for the synthesis of NO is through the activation of the NOS enzyme. In order to determine if NOS catalyzes the synthesis of NO after ELFMFs was applied, different concentrations of the general NOS inhibitor L-NMMA were added to the HMEC-1 cells. The dose-response curve obtained (Figure 3.7) shows that as the concentration of the inhibitor increases, the NO concentration decreases in a dose-dependent manner. The estimated value of the IC_{50} reached after 1h and 24h after ELFMFs application was found to be 85.53 µM/ 1h and 59.88µM / 24h for 10 Hz; while for 60 Hz it was only 7.3 µM / 1 h and 2.7 µM / 24 h.

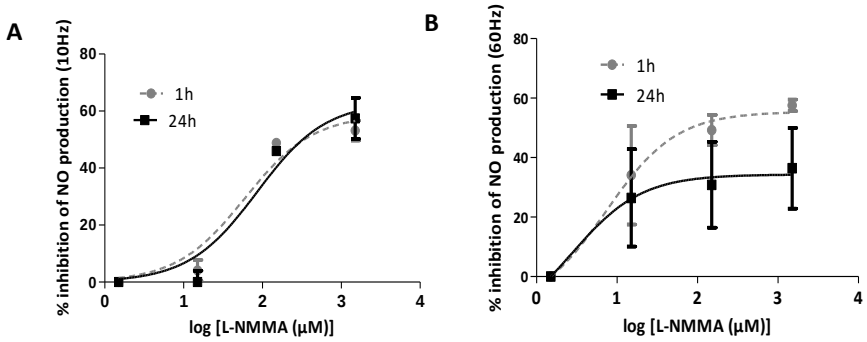

Figure 3.7 Inhibitory effect of L-NMMA (1.5mM, 150µM, 15µM, 1.5µM), a NOS inhibitor on the NO production of HMEC-1 subjected to 20 min of 13.5 mT ELFMF at (a) 10 Hz and (b) 60 Hz. NO production was measured 1h or 24h after treatment. Values are expressed as mean ± STDEV, n=4,*p≤0.05, as calculated with one-way ANOVA with a Dunn's Multiple Comparison Test, n=4.

3.2.3. Identification of nitric oxide synthase isoforms activated by ELFMFs

There are three isoforms of the NOS enzyme: endothelial (eNOS), neuronal (nNOS), and inducible (iNOS). Endothelial cells constitutively only express eNOS, and under certain conditions iNOS. nNOS is not found in endothelial cells. Two inhibitors are therefore used to determine which isoform is activated by ELFMFs: 1400W as a specific inhibitor of iNOS and L-NMMA which is an inhibitor of all NOS isoforms. To our knowledge, there is no specific eNOS inhibitor synthesized yet. To elucidate which isozyme is activated by ELFMFs, HMEC-1 cells were incubated with various NO inhibitors and the NO production 24h after ELFMF treatment (13.5 mT, 60 Hz, 20 min) was measured (Figure 3.8). As described in Figure 3.6 above, our results show that exposure to ELFMFs of 13.5 mT at 60Hz significantly increases the NO concentration in the HMEC-1 compared to the control (6.29 ± 1.71 vs 1.51 ± 0.33, *** p≤0.001). When an inhibitor for the iNOS isoform (1400 W) was added, it was observed that it failed to decrease ELFMF-induced NO concentrations significantly,

leading to the conclusion that the NO synthesis was not dependent on this iNOS isoform. However, with the addition of L-NMMA, an inhibitor of all NOS isoforms, the NO concentration decreased significantly compared to the treated group (1.65 ± 2.2 vs 6.29 ± 1.71; * p≤0.05). In conclusion, these data suggest that the eNOS isozyme contributed most to the ELFMF-induced NO production (Figure 3.8).

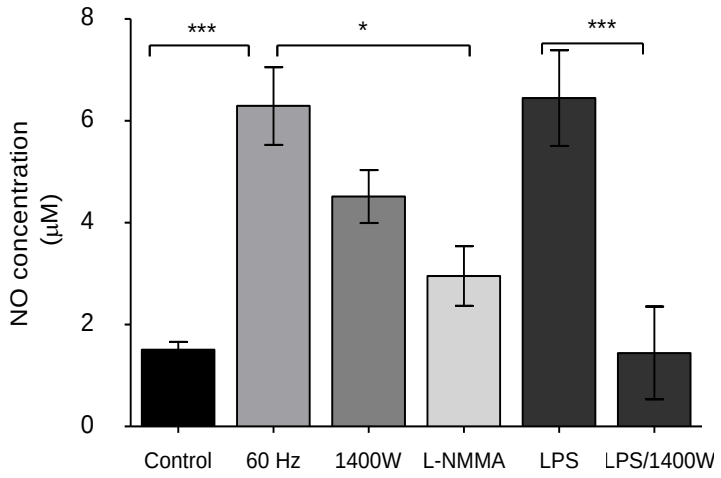

Figure 3.8 The effect of various NOS inhibitors on the NO production induced by ELFMFs. HMEC-1 were treated with 13.5 mT / 60Hz for 20 minutes in presence or absence of various inhibitors of NOS, 24h later NO production was measured. Legend: L-NMMA: Nw-mono-methyl-L- arginine (NOS isoform inhibitor); LPS: Lipopolysaccharide; 1400 W: N- [3-(aminomethyl) benzyl] acetamidine (Inhibitor of the iNOS isoform). Values are expressed as mean ± STDEV, n=4,*p≤0.05, *** p≤0.001 as calculated with one-way ANOVA with a Dunn's Multiple Comparison Test, n=5.

In this study, LPS was added to the culture of endothelial cells as a positive control group, with the purpose of inducing the activation of the iNOS isoform. When the iNOS inhibitor (1400W) is added in presence of LPS, a significant decrease of the NO concentration is observed compared to the condition where only LPS is given. This is evidence that the 1400 W at the tested concentration is able to inhibit iNOS-derived NO. Nevertheless, incubation of the same concentration of 1400W fails to

inhibit ELFMF-induced NO production, strongly indicating that ELFMF activates another isozyme of NOS than iNOS.

3.2.4. Ca^{2+} as mediator in the formation of NO in HMEC-1 exposed to ELFMFs

Ca^{2+} acts as a second messenger modulating the activity of many mediators and also NOS, in particular eNOS and nNOS[174]. In order to determine the involvement of Ca^{2+} in the ELFMF-provoked NO production, HMEC-1 were stimulated with 13.5 mT, 60 Hz ELFMF and incubated with different concentrations of BAPTA-AM, which is a cell permeable and thus intracellular Ca^{2+} chelator.

NO levels of HMEC-1 which were only incubated with the BAPTA-AM, were similar to NO levels of cells that did not receive any treatment, proving that the applied BAPTA-AM concentrations are not toxic (Figure 3.9). When this chelator was added to the samples stimulated with 60 Hz, a dose-dependent decrease in NO concentration was observed. As the concentration of BAPTA-AM increases, the NO concentration decreased proportionally. In presence of 10µM BAPTA-AM, the ELFMF-induced NO production slightly decreased (0.55 times compared to the group treated with 60 Hz alone). Addition of 100 µM and 1 mM BAPTA-AM resulted in a significantly decrease of ELFMF-induced NO production (*** $p \leq 0.001$ vs 60 Hz). These results suggest that the increase in NO by ELFMFs (13.5 mT / 60 Hz) is Ca^{2+} ion dependent.

BAPTA-AM needs to be solved in DMSO, a substance that may be toxic to cells. In order to verify that the change in NO concentration is due to the action of the chelator and not due to DMSO, a group treated with DMSO alone was included. The results showed that the NO values obtained are similar to those of the untreated cells, verifying that the change of NO levels is caused by the chelating action of BAPTA-AM and not it's solvent DMSO.

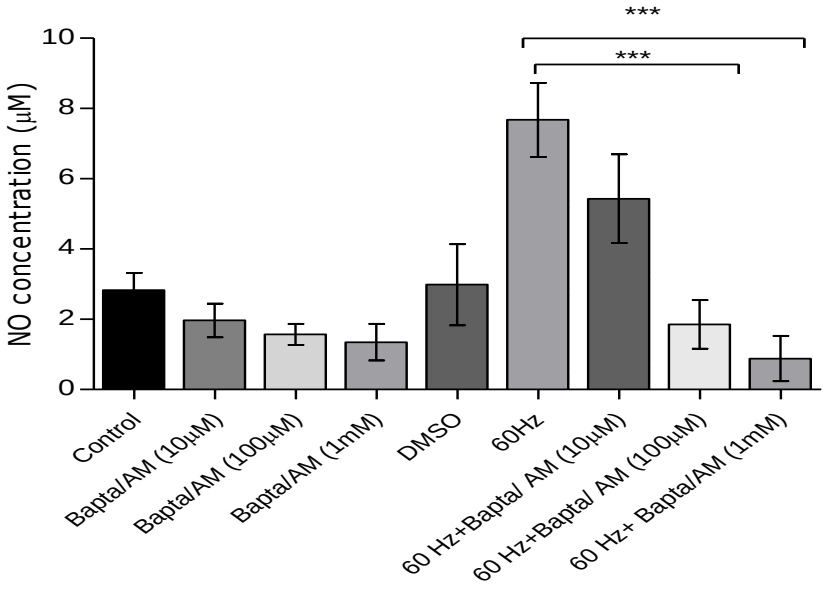

Figure 3.9. Effect of the Ca^{2+} chelator BAPTA-AM on the NO-levels of HMEC-1 in presence or absence of ELFMFs. HMEC-1 were treated with 13.5 mT, 60Hz ELFMF in combination with various concentrations of BAPTA-AM. 24h later, NO production was assessed with the Griess assay. Legend: BAPTA/AM: 1,2-bis (o-aminophenox) ethane- N, N, N ', N' - DMSO: Dimethyl sulfoxide. Values are expressed as mean ± STDEV, n=4, ***p≤0.001, as calculated with one-way ANOVA with a Dunnet's Multiple Comparison Test, n=4.

3.3. NO and NOS isozyme involvement of ELFMF provoked HMEC-1 migration

A combined analysis of the results obtained in this thesis so far, shows the capacity of ELFMFs to stimulate the proliferation and migration of endothelial cells. In addition, ELFMFs also increase NO levels, which is mediated by the activation of Ca^{2+}-dependent eNOS. However, it is very important to link the cellular response with the molecular mechanisms observed *in vitro* and thus to demonstrate the interrelation between them. Therefore, we analyzed the effect of NOS inhibitors on the ELFMF-induced endothelial migration in the transwell assay.

In accordance with the results previously obtained, ELFMFs at 13.5 mT / 60 Hz significantly stimulated the migration of HMEC-1. Addition of the NOS inhibitor (L-NMMA, 1.5 mM) to the ELF-MF-treated endothelial cells shows a significant decrease in migration compared to the group that only received ELFMFs (27.69% ± 6.52 vs 60.01% ± 15.41 respectively, **p≤0.01) (Figure 3.10). The percentages of cell migration of HMEC-1 treated with both L-NMMA and ELMF decreased to the values obtained by the group that did not receive any treatment. This result indicates that the increase in cell migration by the action of ELFMFs is mediated by a NOS enzyme.

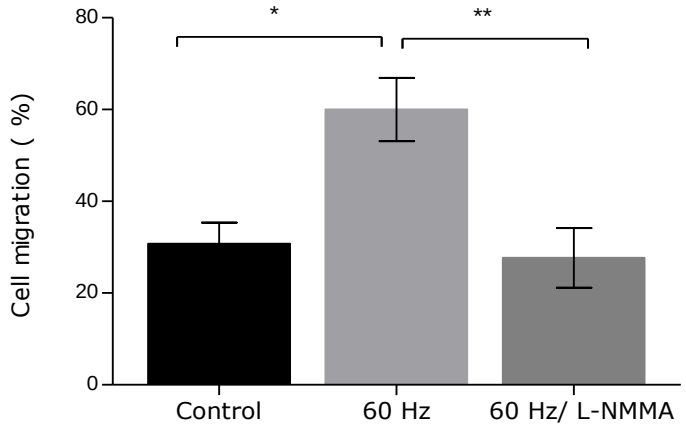

Figure 3.10. Effect of NOS inhibitor L-NMMA on ELFMF-induced HMEC-1 transwell migration. HMEC-1 were seeded onto transwell inserts and treated with 1.5 mM L-NMMA and/or ELFMF (13.5mT, 60 Hz). 24 hours after induction, the number of migrated cells was assessed by staining cells with crystal violet and calculating the area occupied by the purple migrated cells (in%). Values are expressed as mean ± STDEV, n=4, *p≤0.05, **p≤0.01, as calculated with one-way ANOVA with a Dunnett's post hoc test.

Figure 3.11 shows the effect on HMEC-1 cell migration in combination with various NOS inhibitors to determine which NOS isoform is involved. The increase in cell density after ELFMF stimulation was already macroscopically evident, as can be

observed as an increase in area occupied with purple stained endothelial cells. In contrast, empty, white regions were observed for the group that was not stimulated (control). When the inhibitor of the iNOS (1400 W) was added to HMEC-1 treated with ELFMFs, no decrease in migration was observed. In contrast, when L-NMMA which inhibits all NOS isoforms, was added to ELFMF-stimulated cells, the number of colored cells decreased to the levels of unstimulated control HMEC-1 cells. Statistical analysis showed that in the group treated with 60 Hz and L-NMMA, the migration significantly decreased 2.1-fold compared to the group treated with 13.5 mT / 60 Hz alone (23.8% ± 6, 03 vs 51.07% ± 10.70 respectively, * p≤0.05).

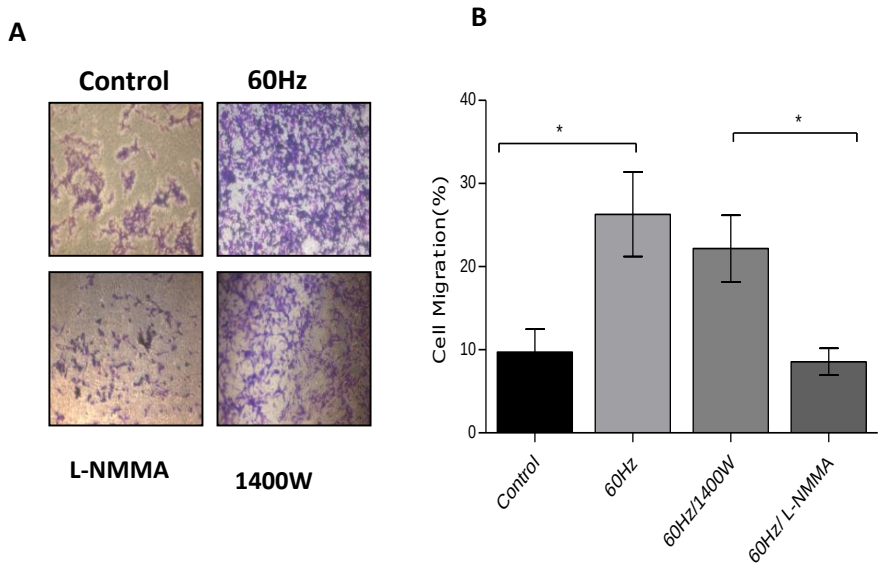

Figure 3.11. Effect of various NOS inhibitors on the HMEC-1 induced cell migration. A) HMEC-1 were transferred on transwell inserts and treated with NOS inhibitors and/or ELFMF (13.5mT, 60 Hz). B) 24 hours after induction, the number of migrated cells was assessed. Legend: L-NMMA: Nw-mono-methyl-L-arginine (Inhibitor of the isoform NOS); LPS: Lipopolysaccharide; 1400 W: N- [3- (aminomethyl) benzyl] acetamidine (Inhibitor of the iNOS isoform). Values are expressed as mean ± STDEV, n=5, * p≤0.05, as calculated with one-way ANOVA with a Dunnett's post hoc test.

However, in cells treated with ELFMFs and the iNOS inhibitor no significant decrease in migration was found compared to the group treated with ELFMFs alone

(Figure 3.11). Since the unspecific NOS inhibitor but not the specific iNOS inhibitor is able to prevent ELFMF-induced endothelial migration, our results strongly suggest that this effect is mediated by the increase of eNOS-dependent NO.

3.4 ELFMFs exhibits neuroprotective properties in *rat 2VO* model

In this part of the thesis, we describe the effect of ELFMF in a cerebro-vascular ischemic stroke model. Cerebro-vascular ischemia was induced in rats by occlusion of the two common carotid vessels, i.e. the 2VO model. These animals where either untreated or received ELFMF treatment (10 or 60 Hz both 13.5 mT) for 20 minutes on 4 subsequent days, with the first treatment 3 h post-surgery.

3.4.1 ELFMFs increased Survival

Figure 3.12 depicts the survival rate of the rats 7 days after surgery. This model is a severe ischemia model, with only 40% of rats surviving after 7 days. Rats treated with ELFMFs showed a considerable increase in survival rate. The highest survival was obtained for the group treated with 13.5 mT / 60 Hz with 80%; twice as much as in the control group. In the case of the group treated with 13.5 mT / 10 Hz, 60% of survival was obtained, being 1.5 times higher than in the control group.

It was also observed that 100% survival was obtained in the sham operated group, showing that the mortality in the animals submitted to the surgical procedure was only caused by the ischemic process and not attributed to any other damages that occurred during the manipulation.

To rule out any effect of the treatment procedure, i.e. anaesthesing and restraining the animals for 20 minutes during 4 subsequent days, we included a sham exposed group. This is a group of animals which underwent 2VO surgery and placed in a restrainer just like the 10 and 60 Hz ELFMF group but without switching on the

magnetic flux. In this sham exposed group, no difference in survival was found compared to the ischemic group (39.2% and 38.46%, respectively) (Figure 3.12b).

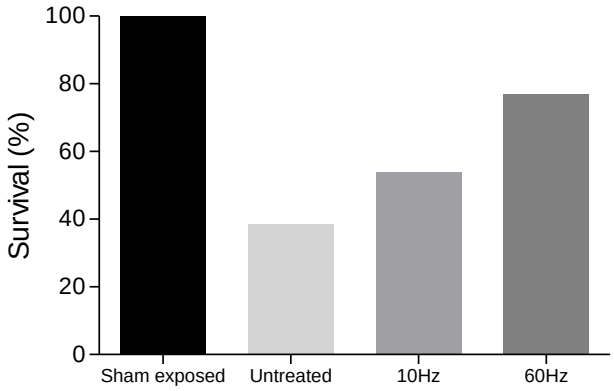

Figure 3.12. ELFMF treatment increase survival in the rat 2VO model. Common carotid arteries were concomitantly occluded in rats and they were treated with 20 minute sessions of 13.5 mT NP-SEMF of 10 or 60 Hz for 4 days. The effect on survival was assessed after 7 days, n = 10 per group.

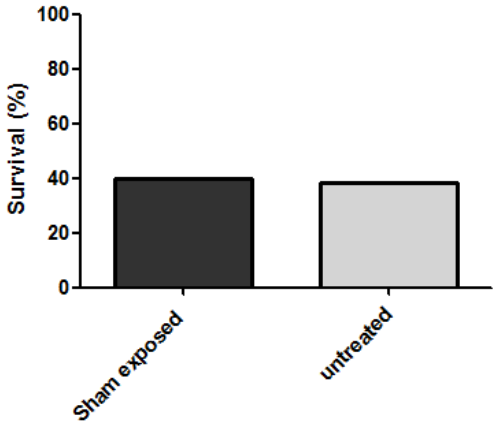

Figure 3.12b. Comparison of survival between sham exposed animals and untreated animals in the rat 2VO model. Common carotid arteries were concomitantly occluded in rats. Rats were either untreated or they were placed in the ELF-MF equipment for 20 minutes sessions but with the magnetic flux switched off. The effect on survival was assessed after 7 days. No statistical differences were found.

3.4.2. Spontaneous exploratory activity

The spontaneous exploratory activity of the surviving rats was assessed 7 days after surgery, by using the open field test. The number of times animals raise on their hind legs was quantified (i.e. number of rears (Figure 3.13A).

Animals submitted to ELFMF treatment showed an improvement of locomotion after 7 days post injury as can be observed by the increase in the number of rears. The results were significantly higher for the ischemic group treated with 13.5 mT / 60 Hz compared to the untreated group (51.70 ± 13.07 vs. 29.60 ± 8.53; * p≤0, 05). The group treated with 13.5 mT / 10 Hz showed no significant difference from the control (43.29 ± 10.67) (Figure 3.13).

We analyzed the number of times the animals crossed the fourth quadrant of the open field, which is a measure for the functional recovery of locomotor activity (Figure 3.13B). It was observed that the groups treated with 13.5 mT / 10 Hz and 13.5 mT / 60 Hz showed significant increase in number of crossings in comparison with to the untreated ischemic group (Control) (10 Hz: 40.29 ± 3.34 and 60 Hz: 42.50 ± 9.44 vs Ischemic: 12.20 ± 3.34; * p≤0.05). In both cases it took less time to reach the fourth quadrant than in the ischemic group without treatment, which favored the increase in the number of times they crossed the fourth quadrant (Figure 3.12). Surprisingly, the number of the rears and crossings of both treatment groups reached the levels of the sham operated group, leading to the conclusion that ELFMF induced recovery of the animals to normal levels.

There were also no significant differences between the sham exposed group and the untreated (ischemic) group. In conclusion, these data show that ELFMFs cause substantial improvements in the recovery of the motor activity of the animals after provoked ischemia.

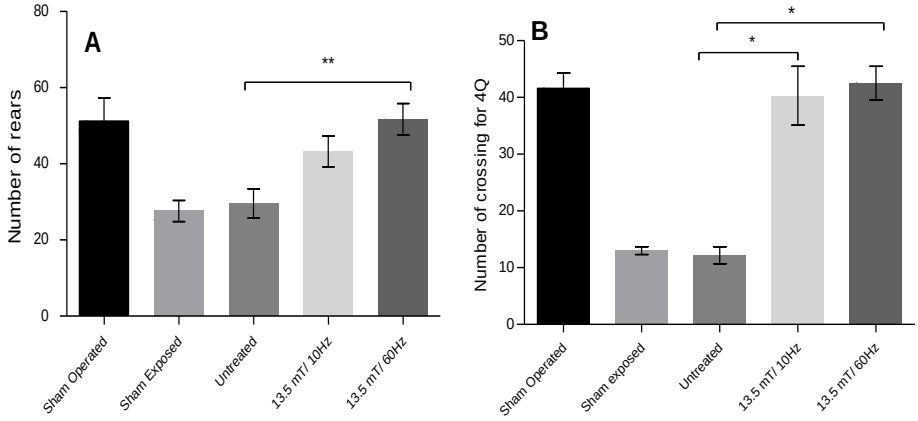

Figure 3.13. ELFMFs induce motor recovery in the rat 2VO model as assessed with the open field behavioral test. A. Effect in the number of rears; B. Effect on the frequency to cross the fourth quadrants. n=10, * p≤0.05 vs control, as analyzed with a Kruskal-Wallis test with a Dunnett's post hoc test.

3.4.3 Neurological Outcomes

Neurological deficit in the rat 2VO model was assessed with the neurological scale 24h and 7 days after surgery. The higher the scale, the higher the number of neurological deficits. It was observed that all groups that underwent full 2VO surgery achieved an average score of 8.79 ± 1.41 (mean ± SE) at 24 h after the operation. The sham operated group had a low average score of 0.40 ± 0.5 (Mean ± SE), meaning they had almost no neurological deficits (Figure 3.14).

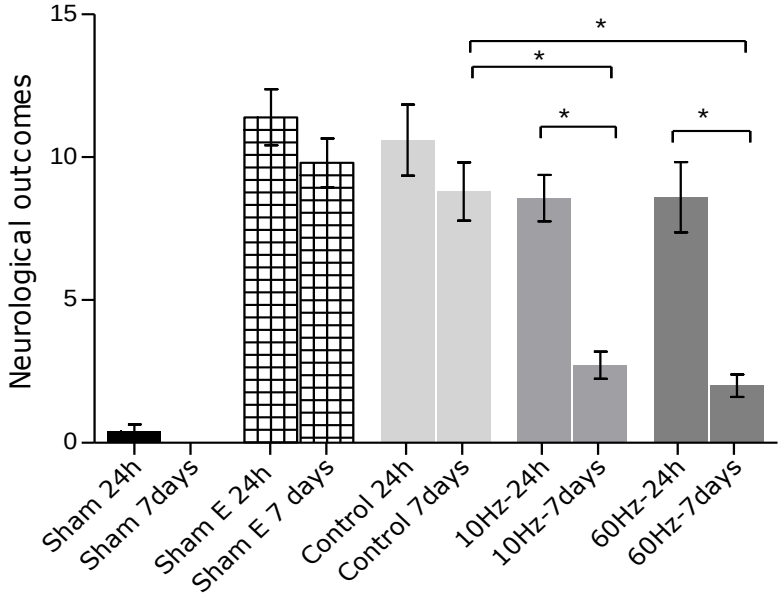

Figure 3.14 Neurological scale was determined 24h and 7 days after surgery in the rat 2VO model (n=5/sham group and n=13/untreated and treated groups); *p≤0.05 vs control as calculated with a Repeated Measurement ANOVA.

At 7 days post-surgery, the ELFMF-treated rats showed significant improvement compared with the ischemic control group, significantly decreasing the values of the neurological scale (2.714 ± 1.259 for 10 Hz and 2.0 ± 1.247 for 60 Hz vs 8.80 ± 2.28 for the ischemic control group, In addition, no substantial functional recovery was observed in the untreated and sham exposed groups, and the neurological scale of these animals remained high with respect to the groups treated with ELFMFs.

3.4.4 ELFMFs reduced ischemic area

To verify if there is reduction in infarcted area after applying ELFMFs, fresh brains were analyzed with TTC staining. As shown in Figure 3.15A both cerebral hemispheres are severely damaged in the untreated ischemic group.

Unstained (white) regions show that the extent of damage affected the regions of the cortex (red arrow), the striatum (yellow arrow) and the hippocampus (white arrow). However, both treatment protocols resulted in a decrease in the affected regions showing mostly red colored regions corresponding to healthy tissue.

To quantify the area of ischemic tissue, the total mean pixel intensity was calculated as the average of mean intensities of all brain sections (Figure 3.15 B). This mean pixel intensity was significantly reduced from 155.4 ± 5.8 in untreated animals to 59.8 ±3.3 for 60Hz indicating a reduction in total white necrotic area in the 60 Hz condition. The 10 Hz application did lead to a slight reduction in lesion size, although this difference was not statistically significant. (Figure 3.15).

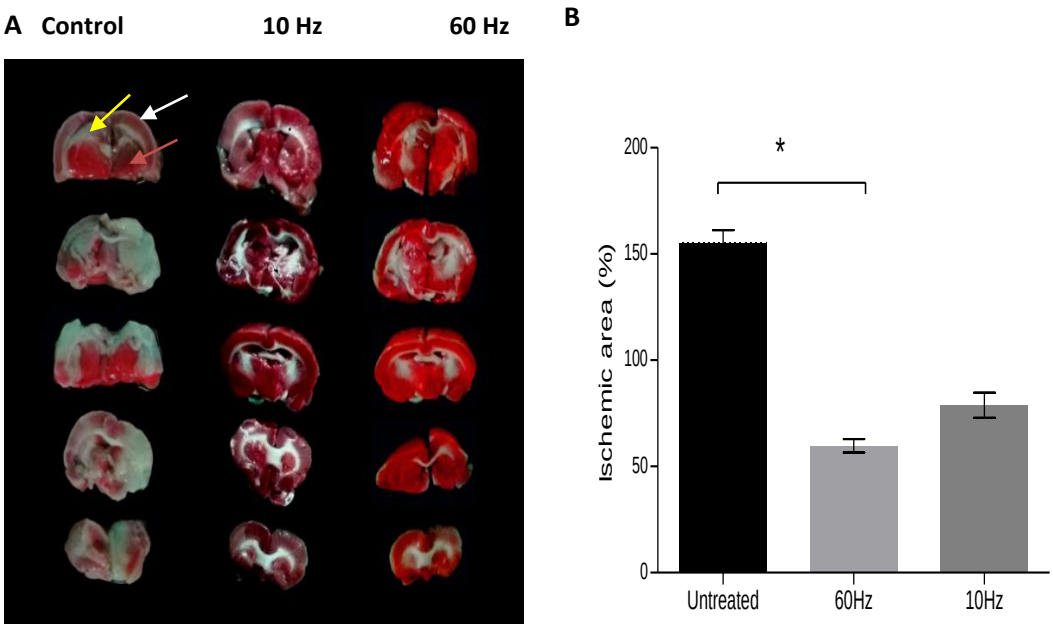

Figure 3.15. **ELFMF reduce ischemic brain area**. (A) Brain slices of 2VO occluded animals 7 days after surgery, without treatment and with 10 Hz or 60Hz ELFMF, TTC staining were used. The arrows indicate the cortex (red arrow), the *striatum* (yellow arrow) and the hippocampus (white arrow).B). To assess the amount of ischemic tissue, the total mean pixel intensity was calculated as the average of mean intensities of all brain sections,*p≤0.05, as analyzed with Imagej software, n=5.

3.4.5. Quantification of blood vessels in the hippocampus region

To analyze the effect of ELFMFs on the cerebral tissue of ischemic rats and to validate the angiogenic effect obtained in the *in vitro* tests, we assessed the number of blood vessels in hippocampus. In the 2VO model, the hippocampus is considered to be the primary zone for histological studies[59]. Brain tissues obtained 7 days after surgery and the abovementioned ELFMF treatments were processed for H&E staining and the number of blood vessels in the hippocampus were counted.

An increase in the number of vessels in this region for both treatment groups was observed (Figure 3.16). The number of blood vessels was 2.3 times more for the group treated at 60 Hz (19.4 ± 4.7) and 1.5 times more for the group treated at 10 Hz (12.9 ± 6.4) compared to the ischemic untreated group (8.50 ± 4.12). Statistical analysis of the blood vessel counts showed that only for the group treated with 60 Hz ELFMF, the number of capillaries was significantly higher than in the group that did not receive any treatment (* $p \leq 0.05$). In contrast, there were no significant differences between the 10 Hz application and untreated conditions (Figure 3.16).

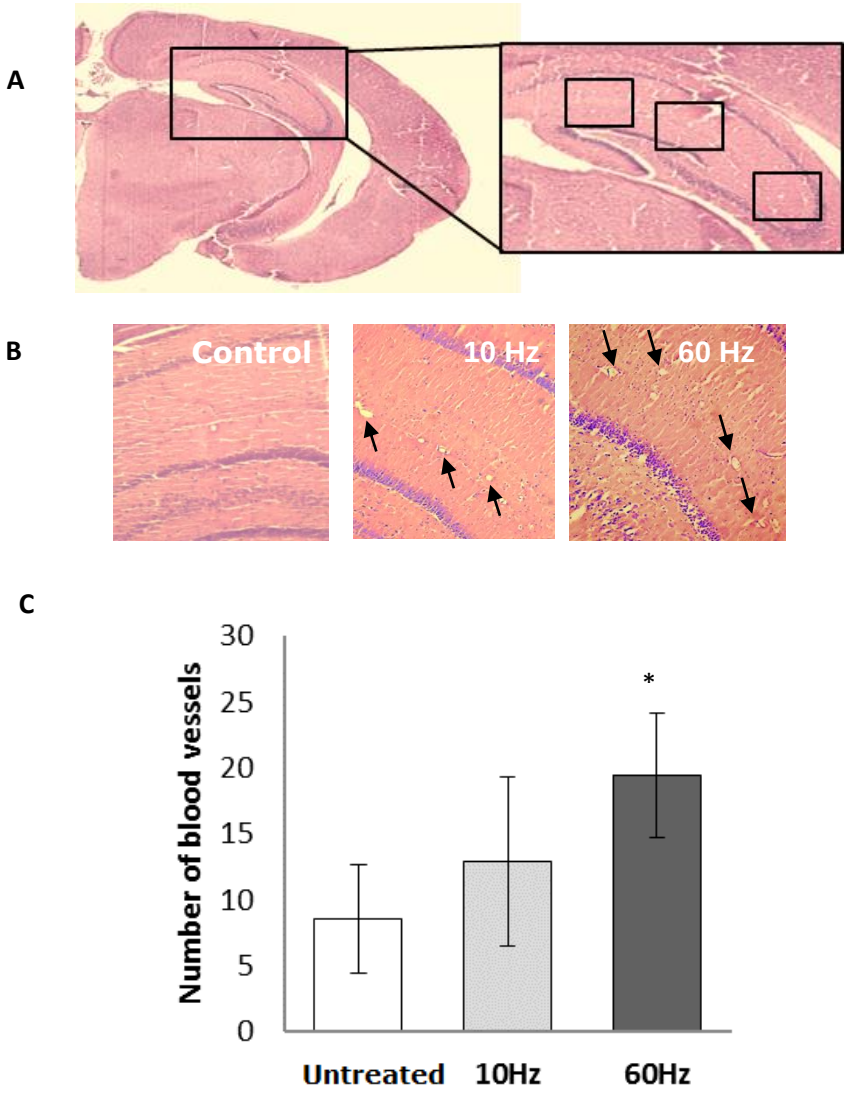

Figure 3.16. The number of blood vessels counted in the brain sections of the 2VO rat model. A) Pictures show hematoxyline eosine section of brains of 2VO rats, A. Images of brain sections analyzed: hippocampal regions C1, C2 and C3; B) H& E sections (a) untreated (b) ELFMFs at 13.5 mT / 10 Hz (b), 13.5 mT / 60 Hz (c); Several blood capillaries are depicted with red arrows. Pictures were taken at 100x magnification. Scale of the bar 200 µm; C) Variation of VS number in the hippocampus region, graph representing the number of blood vessels (BV) counted, *p≤0.05 vs control, according a one-way ANOVA with a Bonferroni Multiple Comparison Test.

3.5. Nitric oxide inhibition tests in rat 2VO model after ELFMFs treatment

In order to study the involvement of NO in the beneficial effects of ELFMFs after stroke, an *in vivo* study with the non-specific NOS inhibitor L-NAME was conducted. Rats underwent 2VO surgery and ELFMF treatment schedule as mentioned above but one group was additionally injected with L-NAME 15 min before each ELFMF application. ELFMF treatment of 13.5 mT / 60 Hz was chosen for this study since it showed the best results in the reduction of the ischemic area and in the increase in the number of the blood vessels. 2VO surgery was performed and rats were divided in four different groups: untreated, injections of L-NAME, 60 Hz ELFMF alone, combination of L-NAME and 60Hz ELFMF

3.3.1 Inhibition of Nitric Oxide affect survival

In the untreated ischemic the mortality rate 7 days after surgery was very high, with only 40% of survivors. Rats receiving L-NAME injections had a comparable survival rate. As already shown previously, application of 60Hz ELFMF had a dramatic effect on the survival, increasing it to 80%. The beneficial effect of ELFMF on survival after 2VO-induced ischemic stroke disappeared when NO-synthesis was blocked: the survival rate of the group receiving both L-NAME and ELFMF was comparable to that of untreated animals. In general, in the group treated with 60Hz, the administration of the NOS inhibitor (L-NAME) dramatically reduced the survival from 80% to 30% (Figure 3.17 A).

3.5.2. Inhibition of Nitric Oxide increases the ischemic area

As already mentioned above, 2VO dramatically affects the viability of the brain tissue, resulting in a big amount of white ischemic tissue in TTC stained brain slices. 60 Hz treatment is able to reverse this damage, as shown by the significant decrease in ischemic area. Administration of the L-NAME inhibitor 15 min. before the

treatment with 60 Hz, significantly increased the infarct area compared to group receiving ELFMF treatment alone (136.1 ± 16.25 for 60 Hz + L-NAME vs 61.45 ± 10.59 for 60 Hz) (* $p \leq 0.05$). The affected ischemic area of rats treated with L-NAME alone was comparable with that of the untreated animals. (Figure 3.16 B). In conclusion, NOS inhibitor administration (ip) reverses the effect of ELFMFs on ischemic area recovery, confirming NOS activation as the possible mechanism of action of ELFMFs.

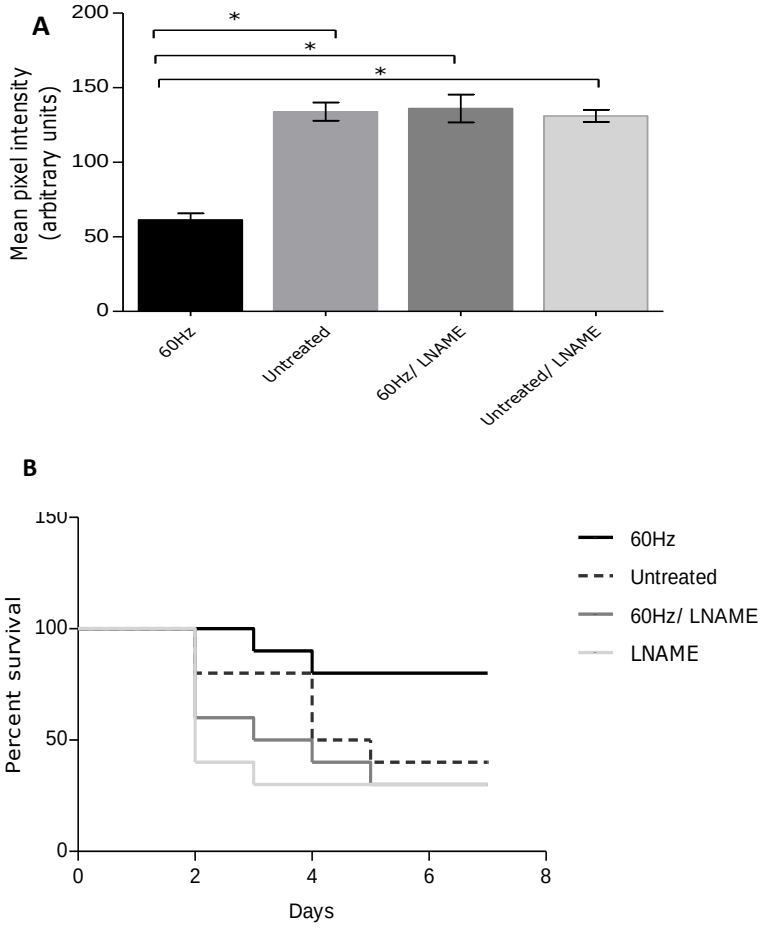

Figure 3.17. **The effect of the NOS inhibitor L-NAME on the beneficial effects of 60Hz ELFMF in 2VO stroke model**. A Kaplan-Meier graph shows that the survival rates 7 days after surgery, n=10 B. The ischemic area in the brain of the surviving rats was measured by TTC staining 7 days after surgery. To assess the amount of ischemic tissue, the total mean pixel intensity was calculated as the average of mean intensities of all brain sections. (n=8/group, *p≤0.05 vs untreated group, according to a Kruskal-Wallis ANOVA test with a Dunnett's post hoc test).

CHAPTER 4. DISCUSSION

ELFMF is known to have a therapeutic effect in a wide variety of pathologies such as non-union bone fractures, failed joint fusions, and congenital pseudarthroses[159] However, the molecular mechanisms that underlie these macro-effects remain to be elucidated. In this context, the contributions of Martin L. Pall and Gartzke & Lange, showing that ELFMF rapidly activates voltage-dependent channels resulting in a rapid Ca^{2+} influx, should be highlighted. These investigations included ELFMF at 50 and 60 Hz, radiofrequency, static magnetic field (SMF), static electric field and pulsating magnetic field (nanopulse); was observed that static magnetic fields ranging from 27 to 37 mT and time varying magnetic fields with frequencies between 7 and 72 Hz and amplitudes between 13 and 114 mT (peak) directly interact with the Ca^{2+} [160,161].Another relevant contribution related to the present thesis is that of McKay et al. [137], who emphasized that the effects of ELFMF on blood flow, microcirculation and microvasculature is related to NO activation.

The data mentioned above provided the foundations for the research topic of this thesis: Exploring the potential of ELFMFs as neuroprotective therapy for cerebral ischemia in its acute phase.

The current research paradigm within the field of ischemic stroke is that complex cascade of events associated with the secondary damage is triggered as a consequence of the initial damage (cessation of blood flow)[162]. In this perspective, all new pharmacological and non-pharmacological therapies are directed to save the greatest amount of viable tissue and thus prevent the extension of cerebral ischemia: this implies that to be effective, these therapies must be initiated within the first 3 h after ischemia[163].

Up to now, the only treatment approved in the clinic is recombinant tissue plasminogen activator (rt-PA); however only a small subset of patients can receive it because of its narrow therapeutic window, multiple contraindications and numerous side-effects. This strongly indicates that it is highly necessary to search for new therapies to treat the disease in its acute phase in order to guarantee higher patient survival and restoration of brain functions.

The increasing interest in the application of pro-angiogenic therapies as treatment against ischemic stroke is based on the observed relationship between reduced cerebral blood flow, decreased vascular regeneration and reduced functional recovery of the brain after cerebral ischemia[8]. ELFMF has been used for the treatment of diseases whose improvement depends on the increase of angiogenesis, such as venous ulcers in the lower limbs[11], heart failure[182], cerebrovascular diseases[164] and neurodegenerative diseases such as Huntington's disease[165]. These applications all confirm its positive effects on the increase in vascular permeability and blood vessel formation[122,166]; hence providing the base to test its potential in the treatment of cerebral ischemia. Even in the chronic phase, it could benefit ischemic patients who show reduced blood flow in areas that have not been affected by ischemia. Additionally, we hypothesize that this therapy is also effective in aged patients over 60 years of age, who tend to have a decrease in the ability to form new vessels, resulting to a lower functional recovery capacity[73,167].

The angiogenic effect of ELFMF has been studied in different models and diseases[10,135,140,168,169]; however, the evidence related to the pro-angiogenic effect in cerebral ischemia is insufficient and the molecular mechanisms involved are not clarified. In addition, the potential translation of ELFMF treatment towards the medical practice is difficult because of contradictory results regarding its angiogenic effect, often reported as stimulant and other times as an inhibitor[17]. This paradox

can be explained by differences in a wide variety of variables such as exposure time, frequency, level of induction and waveform used [170–172], as well as the selected experimental model[12,173–175]: therefore, the results in the literature are difficult to compare and interpret. This striking lack of a systemic approach or a universal application method means that very good results in one pathology might be harmful or resulting in side-effects for other disorders[12,17,176]. This is important given the strong correlation between angiogenesis and carcinogenesis[177].

This thesis examined at cellular and molecular levels the dose-effect relationship, which is necessary for its application in the clinical phase. The fundamental objective was focused on demonstrating the beneficial role of ELFMFs at 13.5 mT/ 10 and 60 Hz in ischemic brain disease through the stimulation of angiogenesis. All results obtained in this research have the aim to contribute to the understanding and elucidation of the cellular and molecular mechanisms that are triggered after the application of ELFMFs (13.5 mT at 10 Hz and 60 Hz) *in vitro* and *in vivo* models. It is also the ambition to lay the foundations of a future clinical therapy for cerebral ischemia. In addition, technical details such as the resulting field strength on the inductor surface, the field distribution and the mean, maximum and minimum magnetic flux densities values are calculated for each work volume used (Table 1): This contributes to the reproducibility of the study and will enhance the understanding of the mechanisms that are triggered by ELFMF.

4.1 Effect of ELFMFs on HMEC-1 behavior *in vitro*

Although the angiogenic effect of ELFMF *in vitro* has been previously studied[12], given the great heterogeneity found in the literature, a methodological strategy was designed to verify the angiogenic effect of the proposed doses (13.5 mT / 10 and 60 Hz) in a *in vivo* model, in this case with the chorioallantois membrane (CAM) of fertilized chicken embryos (Annex 2). The optimal exposure times and doses

(13.5 mT, 10 and 60 Hz, 20 min) obtained from that study, founded the basis on further unraveling the angiogenic mechanism of ELFMF in different experimental models *in vitro*.

To investigate which cellular actions contribute to the angiogenic effect of the selected ELFMFs, their effect on the proliferation, migration and tube formation in human microvasculature immortalized endothelial cells (HMEC-1) was evaluated *in vitro (*Figure 3.1 and 3.2)[143,145]. Four applications of 20 min ELFMFs at 13.5 mT/ 10Hz favored the growth of cells of the *in vitro* model, indicating a direct activation of one of the first steps in the angiogenic cascade. Nevertheless; the same effect is was not observed at 13.5 mT / 60 Hz and 2 applications of ELFMF was also not enough to induce cell proliferation.

With regard to proliferation, we can mention the work of Katsir et al.[178], who report an increase in embryo fibroblasts of chickens exposed to ELFMF (0.7 mT/ 100 Hz) for 24 h. On the other hand, Monache et al.[12] reported an increase in expression of vascular endothelial growth factor receptor 2 (VEGFR2) after applying 1 mT / 50 Hz for 24 h in human umbilical vein endothelial cells. Mc Kay et al. described the activation of endothelial cell proliferation and changes in human microvasculature in the range of 0.5 mT to 20 mT with frequencies from 1 Hz to 72 Hz[137]. It was not indicated if the specified doses are measured on the inductor or in the work volume, and sometimes the wave type used and the time of the application are omitted, making an accurate comparison impossible. In the studies cited above, there were no dose-response curves provided but all studies concurred in stating that ELFMFs induced endothelial cell proliferation[179].

Here we presented a significant increase in HMEC-1 migration as observed in the transwell migration assays with a single application of ELFMFs for 20 min, for both tested doses (13.5 mT / 10 and 60 Hz). Accordingly, stimulus with 13.5 mT / 10 Hz

and 60 Hz, significantly increases the migration in the 'wound healing' test. In case of this type of migration assessment, also other doses were applied to define the best effect and to assess a dose-dependent correlation. In comparison with other tested intensities, the 13.5 mT induced the strongest endothelial response. It was even observed that with increasing intensity up to 20 mT, there is a discrete decrease in migration compared to the 13.5 mT.

The matrigel tube formation assay indicated that ELFMF 13.5 mT induces tube formation at 60 Hz. This trend could also be observed by 10 Hz, but this was not statistically different. Previous studies, reported that a ELFMF of 1 mT intensity for 1, 6 and 12 h, promoted HUVECs proliferation, motility and tubule formation and that VEGFR2 (KDR/Flk-1) was involved in the angiogenic response of HUVECs to ELFMF[12], whereas the same author using 2 mT whit same experimental conditions found a contrary effect. This apparent controversy is not surprising because it has been extensively demonstrated that amplitude, frequency and exposure pattern windows of EMFs can influence significantly their biological effects.

According to some authors, the proliferation of endothelial cells occurs concomitantly to the formation of new buds, while the majority believes that it occurs after the initiation of the migration[69]. In conclusion, our results document that the angiogenic potential of ELFMFs (13.5 mT / 10 and 60 Hz) is mediated by the stimulation of the proliferation, migration and tube formation steps in this cascade. Induction of proliferation needed 4 sessions of ELFM, while tube formation and migration only required 1 dose, indicating that the migration and tubulogenesis process is more sensitive to magnetic stimulation.

4.2. Effect of ELFMFs on the Nitric Oxide and Nictric oxide synthase

4.2.1 Production of NO in vitro and identification of the nitric oxide synthase isozyme involved

NO plays an important role in the activation of angiogenesis. A recent study by Wang et al. indicate the significant role of endogenous NO in regulating the formation of blood vessels and capillaries in the cerebral cortex, improving memory retention in Sprague-Dawley rats [79].

Previous studies demonstrate that MF exerts a vasodilating effect, increasing blood flow and blood pressure affecting microcirculation and microvasculature[137], cutaneous tissue[180] and circumventricular organs[181]. McKay et al. suggest this effect is mediated by the increase of NO[137]. Also, Mirko et al[11,14] show that NO is the signal molecule involved in the healing of chronic wounds by the action of ELFMF.

Given the role that NO plays in the activation of angiogenesis, it could be the key signaling molecule involved in the neurological recovery after ELFMF. Therefore we first measured the NO production in HMEC-1 with the Griess assay, demonstrating that ELFMFs at 13.5 mT / 10 Hz and 60 Hz cause an increase in NO concentration. The maximum NO concentration was obtained 24 h after the application of ELFMFs for both groups. 13.5 mT at 60 Hz was the most effective treatment mode resulting in an NO concentration three times higher than the control unstimulated cells (13.5 mT / 60 Hz).

NO mediates different physiological functions of the nervous system. In pathological conditions, an accumulation of NO results in harmful effects which produce neurotoxicity, thereby worsening the ischemic cascade[57]. In contrast, NO induces vasodilatation and angiogenesis which are processes that reduce

penumbra size and increase functional recovery after stroke. The role of NO as either a protective or harmful signal molecule is associated with the isoenzyme that synthesizes it and the cell where it is produced[89] It has been observed that the NO produced by the eNOS isoform in endothelial cells has a neuroprotective effect, promoting angiogenesis. Likewise, it has been verified that eNOS deficiency cause alterations in blood flow recovery and reserve capacity in cerebral ischemia[63]. In addition, it has been observed that the angiogenic effect mediated by the eNOS enzyme improves proliferation and neuronal migration, which directly stimulates the functional recovery after ischemia was provoked in mice[182]. NO generated by nNOS and iNOS in neurons and immune cells respectively, is considered to contribute to neuronal damage[113]. Therefore, the determination of the isoforms that are activated after the application of ELFMFs has great value from the physiological and therapeutic point-of-view.

Next, we demonstrated that this ELFMF-induced synthesis of NO in the endothelial cells depends on the eNOS enzyme, as this could be inhibited by the general NOS inhibitor L-NAME but not by the iNOS inhibitor 1400W, excluding iNOS isoform in the mechanism. nNOS is not expressed by endothelial cells, hence its participation in the EMF-MF induced endothelial cell actions is excluded. However, in other cell types or models, it might be possible that the ELFMF activates nNOS and this has to be subject of further investigations using NOS-knockout animals to dissect out the NOS isoform of interest. Also others report the activation of NO/NOS by ELFMF. Jeong et al.[202] reported that ELFMF at 60 Hz may produce hyperalgesia in mice by modulating NO synthesis via Ca^{2+}-dependent NOS which is modulated by NOS-dependent NO synthesis, while Sung et al. confirm the increase of NO levels in the brain of healthy Wistar rats, right after treatment with ELFMF (2 mT/ 60 Hz).

We thus showed the role of ELFMF in the modulation of enzyme activity of endothelial NOS[183]; nevertheless; the mechanism behind this specific interaction with NOS has not yet been clarified. One of the hypotheses that could explain the interaction phenomenon of the ELFMFs with the NOS enzyme is through its prosthetic group; through the ferromagnetic effect[184] this group contains in its configuration the iron ion (Fe^{2+} and Fe^{3+}) (Figure 4.1). Several studies demonstrate the interaction of ELFMF with ferromagnetic biological materials such as magnetite (Fe_3O_4)[184,185], and the heme group[10,186]. This interaction would modulate the activity of NOS enzyme influencing the rate of NO formation, which would imply possible conformational changes in favor of the stimulus of the enzymatic activity that would operate independent of the involved isoform and its cellular location.

It has to be mentioned that eNOS activation is tightly controlled by a complex regulatory mechanism including various co- and post-translational lipid modifications, phosphorylation on multiple residues and regulated protein-protein interactions. Association with post-translational proteins such as calmodulin (CaM) and heat shock protein 90 favors activation of this enzyme. Phosphorylation of eNOS at Ser-1177 (in the reductase domain) is also key and can be achieved by various kinases such as Akt, protein kinase A (PKA), and AMP-activated protein kinase (AMPK). One of the most studied activation proteins of eNOS activation is the Ca^{2+}-dependent CaM. Increase in cytoplasmic calcium levels activates CaM, which binds to eNOS to promote the alignment of the oxygenase and reductase domains of eNOS, leading to more efficient NO synthesis. In addition, CaM can activate CaM kinase II, which phosphorylate eNOS on Ser1177. Another layer of regulation is provided by the subcellular distribution of eNOS: it has myristoylation and palmitoylation sites capable of binding to a fatty acid[84,98]. This allows it to be associated with the lipid membrane of the cells, which differentiates it from the other two isoforms (nNOS and iNOS) which are water soluble and are free in the

cytoplasm. It is possible that this association to the membrane facilitates the synthesized NO to be closer to the cellular exterior and to be able to diffuse quickly to the blood or adjacent smooth muscle cells. Furthermore, it has been proven that eNOS can be found in the Golgi apparatus and in the cytosol; although in this latter location eNOS activity is reduced and thus less NO concentration is synthesized[187,188]. In summary, this implies that ELFMF can stimulate eNOS by a multitude of mechanisms and that extensive studies are needed to fully characterize the molecular interaction between ELFMF and eNOS.

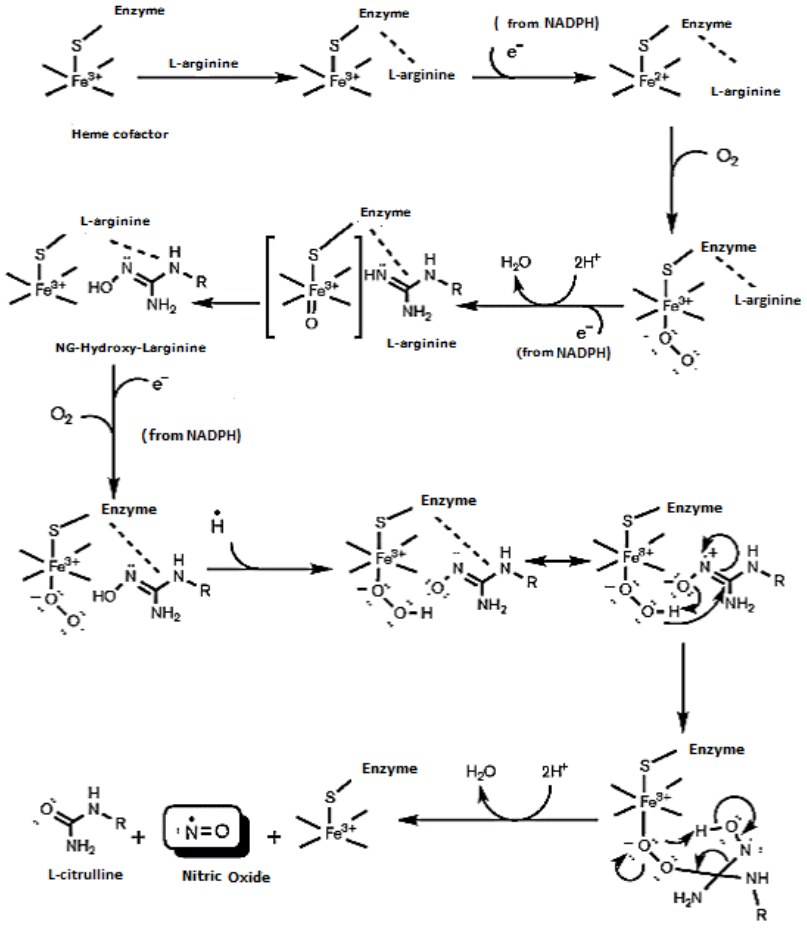

Figure 4.1 Chemical mechanism of the NOS enzyme and possible targets of ELFMFs. Adapted from Boga et al.[86]

From our results, it is inferred that stimulation of NO synthesis is the molecular mechanism that mediates the angiogenic effect of the ELFMFs (13.5 mT / 60Hz). At present, preclinical therapies for brain ischemia with NO donors (i.e. systemic applied synthetic drugs) are being evaluated with promising results. However, their effectiveness is based on application of the doses and for a specific period of time[78] and resulting in many side effects. This suggest the potential advantage of ELFMFs as an enhancer of early angiogenesis through local NO synthesis specifically in the brain or at the site of damage because ELFMF could be locally applied on the skull.

4.2.2. Ca^{2+} as a messenger of NO synthesis

Calcium is serves as a second messenger in neural function in which the concentration of calcium inside the cell regulates a series of enzymatic events caused by kinases. Thus, any exogenous agent that affects the flow of calcium ions either into or out of the cell could potentially have a major impact on biologic function.

We first explored the possibility whether Ca^{2+} is a mediator in the ELFMF-induced NO production. Both nNOS and eNOS isozymes can be activated by CaM, which activity depends on Ca^{2+}. Our results shown that the addition of the Ca^{2+} chelator BAPTA-AM dose-dependently inhibited ELFMFs-induced NO secretion in HMEC-1 cells. The interaction of Ca^{2+} with ELFMFs has been the object of previous studies. In this sense, Blackman et al.[189] demonstrated that ELFMFs (1-120Hz) changes the infflux and exflux (from intracellular stores) of Ca^{2+} ions in brain tissue *in vitro*. Also, Santoro et al.[174] showed in lymphoid cells that exposure to an ELFMF of 2 mT/ 50 Hz changes the plasma membrane and induces reorganization of the cytoskeleton. It is generally accepted that the plasma membrane surface is the site of interaction with EMFs and that some of the effects are dependent on Ca^{2+} regulation.

In this study it was hypothesized that the observed effects could be related to the effect of oscillation of the ions during the vibration force by the induction gradients of the ELFMF. According to a hypothetical biophysical model, this would exert a mechanical pressure on the plasma membrane, altering the electrochemical balance by conformational changes of the protein channels, causing its opening and mechanical closure, which stimulates the influx of Ca^{2+} towards the cellular interior[190].

4.2.3. Relationship of the NO / eNOS pathway with angiogenesis in vitro

In order connect the angiogenic processes to the molecular mechanisms in vitro, a migration study was carried out, inhibiting the formation of NOS in HMEC-1 cells, exposed to a ELFMFs of 13.5 mT / 60 Hz and investigating this effect on the ELFMF-induced migration of endothelial cells. Addition of the iNOS inhibitor 1400 W did not inhibit the migratory effect of ELFMF while the general inhibitor L-NMMA reduced EC motility. These experiments clearly indicate that ELFMF induces EC migration by activating NO production of eNOS. Further studies are needed to investigate the role of CaM, Ca^{2+} or other signaling molecules in ELFMF induced endothelial cell migration.

4.3. Neuroprotective effect of ELFMFs in a model of chronic hypoperfusion

The most recent findings explaining the pathophysiology of ischemia are basically based on experimental models. While *in vitro* models allow the examination of processes at the molecular level, animal models are designed to evaluate medical interventions[191,192].

Marañón et al. have demonstrated the neuroprotective effect of ELFMFs in a model of focal ischemia in the Mongolian gerbils, where different doses were used to evaluate variables such as survival, motor and neurological recovery, defining the

best treatment with 13.5 mT / 10 and 60 Hz. This study served as a reference to elucidate the cellular and molecular mechanisms that are activated when using the same doses and times of exposure[18].

The model of focal ischemia in experimental animals is the one commonly used to reproduce cerebral ischemia or stroke. However, in this study a model of chronic hypoperfusion was chosen to evaluate the angiogenic effect of ELFMFs in the restoration of blood circulation through the formation of new vessels in the hypoperfused regions [59,193].

Further, it is widely known that 2VO induces neuronal damage with varying degrees of severity in different mammal species. Two species frequently employed for carotid occlusion studies are the rat and the gerbil[154]. These two models create distinct ischemic conditions in the brain. Because of the lack of communicating arteries between the carotid and vertebral systems, carotid occlusion in the gerbil leads to severe forebrain ischemia. In contrast, the complete circle of Willis in the rat affords compensatory flow from the vertebral arteries therefore causes cerebral hypoperfusion rather than stroke[59]. In this perspective, this model is more appropriate for our study's specific objective: investigation of angiogenesis after ischemic stroke of the brain.

The current research also applies the global ischemia model in Wistar rats, in order to evaluate the neuroprotective effect of ELFMFs by evaluating the following indicators: survival, motor activity and neurological activity.

Considering that the survival value reported for this experimental model is 30%[59], the increase of this variable constitutes a fundamental parameter to evaluate the neuroprotective effect of the ELFMFs. We could demonstrate that ELFMF (13.5 mT, 60 Hz) manages to significantly reduce the mortality of the animals, resulting in a survival of 80%. In addition, an increase in functional outcome was observed for

both frequencies and a reduction in affected (dead) brain tissue was observed. To our knowledge we are the first to report an increase in survival in global ischemia models induced by ELFMF. The results indicate that treatment with both doses of ELFMFs promotes motor recovery and clinical signs, which is related to improvements in the neurological state of the experimental model, with a marked effect for 13.5 mT / 60 Hz. Our results are consistent with the studies by Râus et al.[194] and Marañón et al.[195], who report changes in motor behavior in the ischemia model in the Mongolian Gerbil after applying ELFMFs.

To establish the angiogenic effect of ELFMF on brain tissue after ischemic stroke, the blood vessels were counted in the hippocampus 7 days after surgery. This area of the brain was selected based on previous reports describing that particularly in the 2VO model this area is mostly affected[59,154].

ELFMFs at doses of 13.5 mT / 10 Hz slightly increased the number of blood vessels in the hippocampus region, while in the 13.5 mT / 60 Hz the amount of blood vessels was significantly elevated. Similar results have been reported by Yang et al.[42], who observed that ELFMF improves circulation in a model of traumatic brain injury in Sprague-Dawley rats[186]. Although, other doses and a different animal model were used, this study has the same conclusion as ours indicating that ELFMF induces angiogenesis in vivo. Yet, a confirmation of NO being a key molecule in the mechanism of action was lacking.

In the 2VO model, the effect of inhibition of the NOS enzyme with L-NAME on the beneficial effect of ELFMF was investigated. Animals treated with 13.5 mT / 60 Hz and injected with the inhibitor, displayed increased mortality and the ischemic area was significantly increased compared to the group treated with the same dose ELFMF without the inhibitor. These observations confirm that NOS and NO play a crucial role in the therapeutic role of ELFMF after stroke. Additional studies using

eNOS KO mice or with inhibitors of other NOS isozymes are needed to fully confirm the contribution of eNOS in vivo. In previous studies, it has been observed that the inhibition of eNOS enzyme in genetically modified animal models showed a decrease in the formation of new blood vessels, which negatively affects the circulation [46]. In this perspective, preclinical therapies for brain ischemia with NO donors are being evaluated obtaining with good results; however, its effectiveness is based on application of the correct systemic amount and various sides effects are observed[78]. Local application of ELFMFs as an enhancer of early angiogenesis through local NO synthesis embraces the potential advantage of avoiding side effects.

Angiogenesis is a highly active process that can last several weeks after cerebral ischemia, particularly in the penumbra area. This region has a high recovery capacity. However, the depolarizing waves of the infarct nucleus stimulate the extraction of oxygen from the area, which means that the survival of the cells in this region has a limited time window[3]. Any therapy that is designed to act on the penumbra, is thus considered to be given as soon as possible after the onset of the ischemic stroke.

In this thesis, the *in vitro* and *in vivo* results are coherently linked to demonstrate the angiogenic effect of ELFMFs as a possible treatment of cerebral ischemia. Analyzing the overall results it is possible to state that the best results were obtained at the dose with 13.5 mT / 60Hz, showing its neuroprotective potential effect on brain tissue in ischemic Wistar rats. Our data suggest that this dose activates angiogenesis in vitro and in vivo by the Ca^{2+}/eNOS /NO pathway, which may be the basis for the further development of this new neuroprotective therapy.

Although the treatment with ELFMFs promotes improvements in the experimental model *in vivo*, a marked divergence in the cellular response between both doses is

observed, which is verified through the increase of the number of vessels and the reduction of the area of infarction in the cerebral tissue in an experimental model. In vitro, good responses are seen for both 10 and 60 Hz, while for the increase of blood vessels in vivo, only the 60 Hz is effective. There are differences in proliferation and *in vitro* migration of endothelial cells between both doses, suggesting that different intracellular cascades might be involved. It is described that the Ras/Raf/MEK/MAPK pathway [57], the kinase signaling (Akt)[216] or the stress protein (Hsp90) are activated[196], all being mechanisms that induce a rapid proliferation. Taken together it is tempting to suggest that the frequency of ELFMF is determinant for the resulting effect [197,198].

Stimulating angiogenesis not only restores blood flow, but would favor the process of neurogenesis, as well as rescuing neurons and astrocytes from cell death. The junction between neurons, astrocytes and endothelial cells (neurovascular unit), participate in the main functions of the brain such as metabolism and maintenance of blood flow[79]. In this order, the formation of new vessels by the action of ELFMFs, possibly stimulate the union of the astrocytes to the vascular wall by means of close joints, stabilizing the blood-brain barrier[199].

According to the vascular niche hypothesis, adult neurogenesis occurs via regeneration and repair of damaged tissue and it is only produced in an angiogenic environment, based on the complex interaction between the vasculature of the brain and neuronal function as a structural and functional unit[110]. In future experiments, it would be nice to investigate whether EMFLF also restores the number of neurons and astrocytes in vivo, particularly in the penumbra area. This is difficult to investigate in the 2VO model as here no local core and penumbra is observed.

It is important to emphasize that the failure of neuroprotective strategies in the clinical phase is suggested to be caused by the fact that these have been directed to independent targets of the ischemic cascade, without taking into account the complex cascade molecular events that are triggered immediately after decrease of the CBF[3,74].

In this sense, the angiogenic effect of ELFMFs, with the consequent reestablishment of CBF in the penumbra zone, constitutes a potentially promising strategy for the treatment of cerebral ischemia in the acute phase, which would be oriented to the protection of the neurovascular unit as a whole.

4.4. General Discussion

The importance of restoring blood flow in the area of ischemic penumbra is crucial to stop the massive neuronal necrosis and apoptosis by restoring the energy supply of neurons and thus reducing the area of the ischemic nucleus, a fact that is directly related to the improvement of post-ischemic disability.

CBF normalization only promotes complete recovery when it occurs very early after the onset of stroke and it may contribute to prevent the spread of infarction within the first few hours after ischemia[7]. Otherwise, the ischemic cascade is not manageable and it is even enhanced by reperfusion, which in itself is responsible for other collateral damage. In practice, the time from establishing the symptoms of ischemia to its treatment is a critical factor that determines the efficacy of neuroprotection. In this research, the therapeutic window is taken into account within the first three hours of ischemia, hence providing evidence that will contribute to timely and effective intervention through the stimulation of angiogenesis in the acute phase of the disease. In contrast, it is generally considered that in vivo, the angiogenic process needs 7 days, while we show that our

angiogenic therapy is only effective when given within the 3 first hours after onset of the disease. This might have two explanations: first of all, it remains possible the ELFMF induces besides angiogenesis other mechanisms such as vasodilatation or inhibition of apoptosis. In that perspective, it should be noted that NO is a very imported key molecule in vasodilatation. Secondly, the 2VO model is a very invasive model, resulting in a rapid high mortality rate which is so high that it can never be reversed by any therapy when given not within 3 hours. Therefore, another ELFMF should be tested in a less severe model of ischemic stroke such as the distal middle artery occlusion model. In that model, different application times after surgery should be further explored. This animal model is also more representative for the clinical situation, as in patients ischemic stroke is evoked by occlusion of one blood vessel.

It is worth noting that during treatment with ELFMFs at the doses used with acute and chronic exposures, no signs of toxicity were detected (results not shown), this fact can be further verified, with increased survival in the *in vivo* model, obtaining the best results (80%) for the group treated with ELFMFs at 13.5 mT / 60 Hz.

Advances in the analysis of the cellular and molecular mechanisms of ischemic cascade alongside with increased research on the use of ELFMFs as a modulatory therapy for angiogenesis provide the basis for establishing recommendations for short-term therapeutic use.

This study shows that treatment with 13.5 mT / 60 Hz stimulates important steps of the angiogenic cascade (Annex 3). The results allow us to propose a combination therapy using two frequencies: 13.5 mT / 10 and 60 Hz, to immediately stimulate angiogenesis in the acute phase of ischemia. This result, together with the significant increase of the blood vessels, demonstrated the angiogenic effect at the

preclinical level, which is the basis for the application of this neuroprotective therapy in the clinic.

The therapeutic value of the treatment is given by the role of angiogenesis after cerebral ischemia, as a defense mechanism, in order to restore the supply of oxygen and glucose in the affected cerebral area[8]. The new vessels formed in the process, would provide neurotrophic support to neurons[200]. Taking into consideration the interrelation between angiogenesis and neurogenesis, it might constitute a new therapeutic route in the treatment of patients who have suffered from cerebral ischemia, not only reperfusing the zone of penumbra, but protecting the neurovascular unit as a whole[3,201].

Although the preclinical evidence shows great heterogeneity in the results, it has been shown that the amplitude, frequency and time of exposure influence the biological response, activating different molecular pathways depending on the dose[12]. This research confirms that the frequency has a determinant role of the induced biological effect; at 13.5 mT / 60 Hz the molecular pathway that activates angiogenesis *in vitro* and *in vivo* is the synthesis of NO/ eNOS dependent Ca^{2+}, whereas this route is not stimulated at 13.5 mT / 10Hz (Annex 3). This thesis confirms the beneficial effects of ELFMFs on brain tissue, increasing the blood vessels formation of the microvasculature, altering blood flow according to the varying metabolic requirements of the tissues and to stabilize blood flow and pressure by making local regulatory adjustments.

The hypotheses that are most promising to explain the angiogenic effect of ELFMFs considering the results obtained in this study would be on the one hand the stimulus of the enzymatic processes through the interaction of the ELFMFs with the prosthetic hemo group of the NOS enzyme (ferromagnetic theory) [184,202], and on the other hand, increase of intracellular Ca^{2+} concentration[198]. Both processes

would favor the increase of NO, through NOS and/or Ca^{2+} mechanism. More research is needed to elucidate which of those two possible mechanisms is key for the ELFMF-induced angiogenic effects.

On the other hand, the functional improvements were promoted by the neuroprotective effect of the ELFMFs through the increase of the blood vessels, a fact that was demonstrated through the reduction of the ischemic area in the slices of cerebral tissue. In this case, the best results were recorded with the ELFMFs at 13.5 mT / 60 Hz.

When considering the angiogenic effect *in vitro* and *in vivo,* results demonstrated that treatment with ELFMFs specifically with 13.5 mT / 60 Hz promotes angiogenesis mediated by the action of eNOS (Annex 3). We assume activation of eNOS because of the fact that iNOS and nNOS inhibitors have no effect and because iNOS and nNOS are not expressed by endothelial cells. Nevertheless, other experiments e.g. with eNOS siRNA are needed. Also the Ca^{2+} dependency of the ELFMF needs to be verified as eNOS is a Ca^{2+}-dependent enzyme.

In conclusion, future clinical trials should thus be based on 13.5 mT/ 60 Hz. This treatment could favor the mechanisms of restoration and neuroplasticity in ischemic animals, favoring the neurovascular unit conditioned by an angiogenic environment. This would open new therapeutic possibilities to stimulate neurogenesis and recovery of brain areas using a safe and non-invasive method.

As a summary, this study presents clear evidence of the activation of important angiogenic cascade steps by the ELFMFs, being illustrated by the increase in the number of blood vessels and thereby reducing the ischemic area. Results that are closely related to high survival values in the treated groups, as well as in neurological recovery and improvements in motor coordination. The dose that

allows the best neuroprotective effect in CVD according to the *in vitro* and *in vivo* tests is that of 13.5 mT / 60Hz which may be the basis for the development of a new neuroprotective therapy.

CONCLUSIONS

1. ELFMFs at the doses tested (13.5 mT / 10 and 60 Hz) induces angiogenesis in vitro, as demonstrated in the proliferation, migration and tube formation assay.

2. It is demonstrated that the molecular mechanism that mediates the *in vitro* angiogenic effect of ELFMFs at the dose 13.5 mT / 60Hz is the stimulation of NO synthesis by the eNOS enzyme; however, this route is only slightly activated at 13.5 mT / 10 Hz, illustrating that this effect is dose dependent.

3. The neuroprotective potential of ELFMFs *in vivo* in a severe stroke model is clearly verified. Significant improvements in survival, motor activity and neurological recovery were demonstrated for both doses (13.5 mT / 10 and 60 Hz).Hz.

4. The in vivo angiogenic effect of ELFMFs (13.5 mT / 10 and 60 Hz) is demonstrated by decreasing the ischemic area and increasing blood vessel formation in the hippocampal region in Wistar rats, being more effective the dose 13.5 mT / 60Hz, which is related to the stimulation of NOS activity for this specific dose.

5. The ELFMFs induce biological and physiological effects in the systems tested related to angiogenesis in cerebral ischemia, which provides a foundation for its use as neuroprotective therapy, with the most effective dose being 13.5/ 60 Hz;

RECOMMENDATIONS

1. To deepen the mechanisms involved in the increase of proliferation to 13.5 mT/ 10Hz through the study of pro-angiogenic mediators.

2. Dilute whether the nNOS isoform is stimulated by ELFMFs using specific inhibitors such as N-4-2-3-chlorophenylmethylamino ethylphenyl thiophenecarboximidamide dihydrochloride (ARL 17477).

REFERENCES

1. Donnan, G. A., Fisher, M., Macleod, M., Davis, S. M. & Donnan GA, Fisher M, Macleod M, D. Sm. Stroke. *Lancet* **371,** 1612–1623 (2008).
2. Chen, Y.-C. *et al.* Stroke, angiogenesis and phytochemicals. *Frontiers in bioscience (Scholar edition)* **4,** 599–610 (2012).
3. Casals, J. B. *et al.* The use of animal models for stroke research: a review. *Comp Med* **61,** 305–13 (2011).
4. Liu, J. *et al.* Progress in Neurobiology Vascular remodeling after ischemic stroke : Mechanisms and therapeutic potentials. *Prog Neurobiol* **115,** 138–156 (2014).
5. Tobin, M. K. *et al.* Neurogenesis and inflammation after ischemic stroke: what is known and where we go from here. *J Cereb blood flow Metab* **34,** 165–170 (2014).
6. Font, M. A., Arboix, A. & Krupinski, J. Angiogenesis, neurogenesis and neuroplasticity in ischemic stroke. *Curr Cardiol Rev* **6,** 238–44 (2010).
7. Weita, T., Zhang, S. & Tian, Y. Progress in Neurobiology Excitotoxicity and stroke : Identifying novel targets for neuroprotection. *Prog Neurobiol* **115,** 157–188 (2014).
8. Karsy, M. *et al.* Neuroprotective strategies and the underlying molecular basis of cerebrovascular stroke. *Neurosurg Focus* **42,** E3 (2017).
9. Ergul, A., Alhusban, A. & Fagan, S. C. Angiogenesis: A harmonized target for recovery after stroke. *Stroke* **43,** 2270–2274 (2012).
10. Akpolat, V., Celik, M. S., Celik, Y., Akdeniz, N. & Ozerdem, M. S. Treatment of osteoporosis by long-term magnetic field with extremely low frequency in rats. *Gynecol Endocrinol* **25,** 524–529 (2009).
11. Funk, R., Monsees, T. & Özkucur, N. Electromagnetic effects - From cell biology to medicine. *Prog Histochem Cytochem* **43,** 177–264 (2009).

12. Pesce, M., Patruno, A., Speranza, L. & Reale, M. Extremely low frequency electromagnetic field and wound healing: Implication of cytokines as biological mediators. *Eur Cytokine Netw* **24,** 1–10 (2013).

13. Delle Monache, S., Alessandro, R., Iorio, R., Gualtieri, G. & Colonna, R. Extremely low frequency electromagnetic fields (ELF-EMFs) induce in vitro angiogenesis process in human endothelial cells. *Bioelectromagnetics* **29,** 640–648 (2008).

14. Saliev, T., Mustapova, Z., Kulsharova, G., Bulanin, D. & Mikhalovsky, S. *Therapeutic potential of electromagnetic fields for tissue engineering and wound healing*. *Cell Proliferation* **47,** 485–493 (2014).

15. Patruno, A. *et al.* Effects of extremely low frequency electromagnetic field (ELF-EMF) on catalase, cytochrome P450 and nitric oxide synthase in erythro-leukemic cells. *Life Sci* **121,** 117–123 (2015).

16. Williams, C. D., Markov, M. S., Hardman, W. E. & Cameron, I. L. Therapeutic electromagnetic field effects on angiogenesis and tumor growth. *Anticancer Res* **21,** 235–245 (2013).

17. Qinlong, M. *et al.* Extremely low-frequency electromagnetic fields affect transcript levels of neuronal differentiation-related genes in embryonic neural stem cells. *PLoS One* **9,** 900–41 (2014).

18. Delle Monache, S. *et al.* Inhibition of angiogenesis mediated by extremely low-frequency magnetic fields (ELF-MFs). *PLoS One* **8,** e79309 (2013).

19. Cardonne, M. M. *et al.* Efecto Neuroprotector de los Campos Magnéticos de Frecuencia Extremadamente Baja en Biomodelos de Isquemia Cerebral Miriam. in *CLAIB* 3–6 (2007).

20. Díez-Tejedor E, del BO, Alvarez SJ, Munoz M, A. G. Classification of the cerebrovascular diseases. Iberoamerican Cerebrovascular diseases Society. *Rev Neurol* 455–464 (2001).

21. Salud., O. M. *The Atlas of disease cardiovascular and stroke.* (2003).

22. Álvarez-Sabin, J. Stroke secondary prevention: still a lot to do. *Med Clin* 340–342. (2011).

23. MINSAP(Ministerio de salud publica). *Anuario Estadístico de Salud 2014*. (Ministerio de Salud Pública. Cuba, 2015).

24. Barker-Collo, S. *et al.* Sex Differences in Stroke Incidence, Prevalence, Mortality and Disability-Adjusted Life Years: Results from the Global Burden of Disease Study 2013. *Neuroepidemiology* **45,** 203–214 (2015).

25. Revisi, C. Tratamiento actual del ataque cerebrovascular isquémico (ACV) agudo. *Neurology* **49,** 467–498 (2008).

26. Hall, A. A. *et al.* Delayed treatments for stroke influence neuronal death in rat organotypic slice cultures subjected to oxygen glucose deprivation. *Neuroscience* **164,** 470–7 (2009).

27. Niño-de Mejía, M. C. Protección cerebral. *Rev Mex Anestesiol* **33,** 189–195 (2010).

28. Silvestre, J. S., Smadja, D. M. & Levy, B. I. Postischemic Revascularization: From Cellular and Molecular Mechanisms to Clinical Applications. *Physiol Rev* **93,** 1743–1802 (2013).

29. Gubern Mérida, M. C. & Carme, M. Nuevos determinantes moleculares en la respuesta a isquemia cerebral. *TDX (Tesis Doctorals en Xarxa)* (Universitat de Girona, 2015).

30. Di Carlo, A. Human and economic burden of stroke. *Age Ageing* **38,** 4–5 (2008).

31. Hugon, J., Vallat, J. M. & Dumas, M. Role of glutamate and excitotoxicity in neurologic diseases. *Rev Neurol (Paris)* **152,** 239–248 (1996).

32. Farrell, R. M. & Falcone, T. Blood pressure in acute stroke : which questions remain ? **38,** 385–89 (2015).

33. Hossmann, K.-A. Cerebral ischemia: Models, methods and outcomes. *Neuropharmacology* **55,** 257–270 (2008).

34. Hossmann, K. A. Pathophysiology and therapy of experimental Stroke. *Cell Mol Neurobiol* **26,** 1055–1081 (2006).

35. José Castillo. LUCES Y SOMBRAS DE LA NEUROPROTECCIÓN EN LA ISQUEMIA CEREBRAL. *Rev Neuro-Psiquiatría del Perú* **64,** 100–110 (2001).

36. Borsello, T. *Neuroprotection Methods and Protocols*. *Methods in Molecular Biology* **399,** (Humana Press, 2007).

37. Burridge, S. Neurodegenerative diseases: Novel route to neuroprotection. *Nat Rev Drug Discov* **11,** 906–907 (2012).

38. Ginsberg, M. D. Adventures in the Pathophysiology of Brain Ischemia: Penumbra, Gene Expression, Neuroprotection: The 2002 Thomas Willis Lecture. *Stroke* **34,** 214–223 (2003).

39. Sutherland, B. A. *et al.* Neuroprotection for ischaemic stroke: Translation from the bench to the bedside. *Int J Stroke* **7,** 407–418 (2012).

40. Arrich, J., Holzer, M., Havel, C., Müllner, M. & Herkner, H. in *Cochrane Database of Systematic Reviews* (ed. Arrich, J.) **9,** CD004128 (John Wiley & Sons, Ltd, 2012).

41. Montaner, J. Fisiopatología de la isquemia cerebral. *Avances en patología neurovascular* **1,** 202 (2007).

42. Schaller, B. J., Bahr, M. & Buchfelder, M. Pathophysiology of brain ischemia: Penumbra, gene expression, and future therapeutic options. *Eur Neurol* **54,** 179–180 (2005).

43. Tomita, M. Pathophysiology of brain edema. *Cerebrovasc Dis* 33–46 (2005).

44. Szydlow & ska, Kinga; Tymiansk, M. Calcium , ischemia and excitotoxicity. *Cell Calcium* **47,** 122–129 (2010).

45. Hankey & Graeme. *Stroke. Your questions answered.* (Elsevier, 2007).

46. Lai, T. W., Zhang, S. & Wang, Y. T. *Excitotoxicity and stroke: Identifying novel targets for neuroprotection*. *Progress in Neurobiology* **115,** 157–188 (2014).

47. David, T., Jo, D.-G., Arumugam, T. V, Nagy, Z. & Nardai, S. Emerging Roles of

Sirtuins in Ischemic Stroke. *Brain Res Bull* **36,** 112–125 (2017).

48. Chen, J. *et al.* A non-ionotropic activity of NMDA receptors contributes to glycine-induced neuroprotection in cerebral ischemia-reperfusion injury. *Sci Rep* **7,** 3575 (2017).
49. Hossmann, K. A. Viability thresholds and the penumbra of focal ischemia. *Ann Neurol* **36,** 557–565 (1994).
50. Donkin, J. J. & Vink, R. Mechanisms of cerebral edema in traumatic brain injury: therapeutic developments. *Curr Opin Neurol* **23,** 293–299 (2010).
51. Cho, T. *et al.* Long-term potentiation promotes proliferation/survival and neuronal differentiation of neural stem/progenitor cells. *PLoS One* **8,** e76860 (2013).
52. Mao, X., Gu, X. & Lu, W. GSG1L regulates the strength of AMPA receptor-mediated synaptic transmission but not AMPA receptor kinetics in hippocampal dentate granule neurons. *J Neurophysiol* **117,** 28–35 (2017).
53. Chen, J. *et al.* Deletion of TRPC6 Attenuates NMDA Receptor-Mediated Ca2+ Entry and Ca2+-Induced Neurotoxicity Following Cerebral Ischemia and Oxygen-Glucose Deprivation. *Front Neurosci* **11,** 138 (2017).
54. Terpolilli, N. A. *et al.* Nitric oxide inhalation reduces brain damage, prevents mortality, and improves neurological outcome after subarachnoid hemorrhage by resolving early pial microvasospasms. *J Cereb blood flow Metab* **32,** 132–148 (2015).
55. Davis, S. M. & Pennypacker, K. R. Targeting antioxidant enzyme expression as a therapeutic strategy for ischemic stroke. *Neurochem Int* **107,** 23–32 (2017).
56. Karachitos, A., Jordan, J. & Kmita, H. VDAC-targeted drugs affecting cytoprotection and mitochondrial physiology in cerebrovascular and cardiovascular diseases.. *Curr Med Chem* **45,** 325–359 (2017).
57. Rastogi, R., Geng, X., Li, F. & Ding, Y. NOX Activation by Subunit Interaction

and Underlying Mechanisms in Disease. *Front Cell Neurosci* **10,** 301 (2016).

58. Pacher, P., Beckman, J. S. & Liaudet, L. Nitric Oxide and Peroxynitrite in Health and Disease. *Physiol Rev Publ* **87,** 315–424 (2007).

59. Bodega, G., Forcada, I., Suárez, I. & Fernández, B. Acute and chronic effects of exposure to a 1-mT magnetic field on the cytoskeleton, stress proteins, and proliferation of astroglial cells in culture. *Environ Res* **98,** 355–362 (2005).

60. Farkas, E., Luiten, P. G. M. & Bari, F. Permanent , bilateral common carotid artery occlusion in the rat : A model for chronic cerebral hypoperfusion-related neurodegenerative diseases. *Brain Res Rev* **54,** 162–180 (2007).

61. Lamalice, L., Le Boeuf, F. & Huot, J. Endothelial Cell Migration During Angiogenesis. *Circ Res* **100,** 782–794 (2007).

62. Simard, J. M., Kent, T. A., Chen, M. K., Tarasov, K. V & Gerzanich, V. Brain oedema in focal ischaemia: molecular pathophysiology and theoretical implications. *Lancet Neurol* **6,** 258–268 (2007).

63. Poinsatte, K. *et al.* Quantification of neurovascular protection following repetitive hypoxic preconditioning and transient middle cerebral artery occlusion in mice. *J Vis Exp* **99,** e52675 (2015).

64. MacLauchlan, S. *et al.* Endothelial nitric oxide synthase controls the expression of the angiogenesis inhibitor thrombospondin 2. *Proc Natl Acad Sci U S A* **108,** E1137-45 (2011).

65. Habib, S. & Ali, A. Biochemistry of nitric oxide. *Indian Journal of Clinical Biochemistry* **26,** 3–17 (2011).

66. Yen-Patton, G. P. A., Patton, W. F., Beer, D. M. & Jacobson, B. S. Endothelial cell response to pulsed electromagnetic fields: stimulation of growth rate and angiogenesis in vitro. *J Cell Physiol* **134,** 37–46 (1988).

67. Wei, L., Erinjeri, J. P., Rovainen, C. M. & Woolsey, T. a. Collateral growth and angiogenesis around cortical stroke. *Stroke* **32,** 2179–2184 (2001).

68. Folkman, J. & Shing, Y. Angiogenesis. *Journal of Biological Chemistry* **267,** 10931–10934 (1992).

69. Carmeliet, P. & Jain, R. K. Molecular mechanisms and clinical applications of angiogenesis. *Nature* **473,** 298–307 (2011).

70. Senger, D. R. & Davis, G. E. Angiogenesis. *Cold Spring Harb Perspect Biol* **3,** a005090–a005090 (2011).

71. Risau, W. Mechanisms of angiogenesis. *Nature* **386,** 671–4 (1997).

72. Murohara, T. *et al.* Role of Endothelial Nitric Oxide Synthase in Endothelial Cell Migration. *Arterioscler Thromb Vasc Biol* **19,** 1156–1161 (1999).

73. Auerbach, R., Lewis, R., Shinners, B., Kubai, L. & Akhtar, N. Angiogenesis assays: A critical overview. *Clin Chem* **49,** 32–40 (2003).

74. Navaratna, D., Guo, S., Arai, K. & Lo, E. H. Mechanisms and targets for angiogenic therapy after stroke. 216–223 (2009).

75. Garry, P. S., Ezra, M., Rowland, M. J., Westbrook, J. & Pattinson, K. T. S. The role of the nitric oxide pathway in brain injury and its treatment — From bench to bedside ☆. *Exp Neurol* **263,** 235–243 (2015).

76. Kiechle, F. L. & Malinski, T. Nitric Oxide : Biochemistry , Pathophysiology , and Detection. *Am J Clin Pathol* **32,** 10010 (1994).

77. Zhang, R. *et al.* Nitric oxide enhances angiogenesis via the synthesis of vascular endothelial growth factor and cGMP after stroke in the rat. *Circ Res* **92,** 308–313 (2003).

78. Brenman, J. E. & Bredt, D. S. Synaptic signaling by nitric oxide. *Curr Opin Neurobiol* **7,** 374–378 (1997).

79. Contreras, D. L., Robles, H. V, Romo, E., Rios, A. & Escalante, B. The role of nitric oxide in the post-ischemic revascularization process. *Pharmacol Ther* **112,** 553–563 (2006).

80. Wang, S. *et al.* Endogenous nitric oxide regulates blood vessel growth factors , capillaries in the cortex , and memory retention in Sprague-Dawley

rats. **8,** 5271–5285 (2016).

81. Cooke, J. P. NO and angiogenesis. *Atheroscler Suppl* **4,** 53–60 (2003).

82. Dawson, T. M, and Snyder, S. H., Dawson and Snyder S.H., T. M., Dawson and Snyder, S.H., T. M. & Dawson and Snyder S.H., T. M. Gases as bioilogical messenger: Nitric oxide and carbon monoxide in the brain. *Neuroscience* 5147–5159 (1994).

83. Bredt, D. S. S., Hwang, P. M. M. & Snyder, S. H. H. Localization of nitric oxide synthase indicating a neural role for nitric oxide. *Nature* **347,** 768–770 (1990).

84. Amezcua, J. L., Palmer, R. M., de Souza, B. M. & Moncada, S. Nitric oxide synthesized from L-arginine regulates vascular tone in the coronary circulation of the rabbit. *Br J Pharmacol* **97,** 1119–1124 (1989).

85. Craige, S. M. *et al.* NADPH Oxidase 4 Promotes Endothelial Angiogenesis Through Endothelial Nitric Oxide Synthase Activation. *Circulation* **124,** 731-U193 (2011).

86. Mayer, P. A. and B. Nitric oxide synthases: catalytic function and progress towards selective inhibition. *Naunyn-Schmiedeberg's Arch Pharmacol* **358,** 127–133 (1998).

87. Babu, B. R. & Griffith, O. W. Design of isoform-selective inhibitors of nitric oxide synthase. *Curr Opin Chem Biol* **2,** 491–500 (1998).

88. Knowles, R. G. *et al.* Kinetic characteristics of nitric oxide synthase from rat brain. *Enzyme* **269,** 207–210 (1990).

89. Donnini, S. & Ziche, M. Constitutive and inducible nitric oxide synthase: role in angiogenesis. *Antioxid Redox Signal* **4,** 817–23 (2002).

90. Förstermann, U. & Münzel, T. Endothelial nitric oxide synthase in vascular disease: from marvel to menace. *Circulation* **113,** 1708–14 (2006).

91. Brzozowski, M. J., Alcantara, S. L., Iravani, M. M., Rose, S. & Jenner, P. The effect of nNOS inhibitors on toxin-induced cell death in dopaminergic cell

lines depends on the extent of enzyme expression. *Brain Res* **1404,** 21–30 (2011).

92. Southan, G. J. & Szabó, C. Selective pharmacological inhibition of distinct nitric oxide synthase isoforms. *Biochemical Pharmacology* **51,** 383–394 (1996).

93. Willmot, M., Gibson, C., Gray, L., Murphy, S. & Bath, P. Nitric oxide synthase inhibitors in experimental ischemic stroke and their effects on infarct size and cerebral blood flow: A systematic review. *Free Radic Biol Med* **39,** 412–425 (2005).

94. Rubio-donnadieu, F. Efectos del óxido nítrico en el sistema nervioso central. *Neurochemical* **143,** 409–411 (2007).

95. Mees, B. *et al.* Endothelial nitric oxide synthase activity is essential for vasodilation during blood flow recovery but not for arteriogenesis. *Arterioscler Thromb Vasc Biol* **27,** 1926–1933 (2007).

96. Ziche, M. *et al.* Nitric oxide mediates angiogenesis in vivo and endothelial cell growth and migration in vitro promoted by substance P. *J Clin Invest* **94,** 2036–44 (1994).

97. Godínez-rubí, M., Rojas-mayorquín, A. E. & Ortuño-sahagún, D. Nitric Oxide Donors as Neuroprotective Agents after an Ischemic Stroke-Related Inflammatory Reaction. *Stroke Res Treatmen* **2013,** 16 (2013).

98. Neill, M. J. O. ' *et al.* ARL 17477, a selective nitric oxide synthase inhibitor, with neuroprotective effects in animal models of global and focal cerebral ischaemia. *Brain Res* **871,** 234–244 (2000).

99. Miyauchi, T. *et al.* Waon Therapy Upregulates Hsp90 and Leads to Angiogenesis Through the Akt-Endothelial Nitric Oxide Synthase Pathway in Mouse Hindlimb Ischemia. *Circ J* **76,** 1712–1721 (2012).

100. Fulton, D., Gratton, J. P. & Sessa, W. C. Post-translational control of endothelial nitric oxide synthase: why isn't calcium/calmodulin enough? *J*

Pharmacol Exp Ther **299,** 818–824 (2001).

101. Cheng, G. *et al.* Sinusoidal electromagnetic field stimulates rat osteoblast differentiation and maturation via activation of NO-cGMP-PKG pathway. *Nitric Oxide - Biol Chem* **25,** 316–325 (2011).
102. Ziche, M. & Morbidelli, L. Nitric oxide and angiogenesis. *J Neurooncol* **50,** 139–148 (2000).
103. Isenberg, J. S. Nitric oxide modulation of early angiogenesis. *Microsurgery* **24,** 385–391 (2004).
104. National Institute of Neurological Disorders and Stroke [rt-PA stroke study group]. Tissue plasminogen activator for acute ischemic stroke. *New Engl J Med* **333,** 1581–1587 (1995).
105. Patel, R. A. G. & McMullen, P. W. Neuroprotection in the Treatment of Acute Ischemic Stroke. *Prog Cardiovasc Dis* (2017). doi:10.1016/j.pcad.2017.04.005
106. Sosa-Testé, I. M., García Rodríguez, J. C. & Fernández Limia, O. Estudio del efecto neuroprotector de la eritropoyetina humana recombinante con bajo contenido de ácido siálico aplicada por vía intranasal en biomodelos experimentales de isquemia cerebral. **Doctorado,** (Centro Nacional para la Producción de Animales de Laboratorio, 2007).
107. Goodman, R. & Shirley-Henderson, A. Transcription and translation in cells exposed to extremely low frequency electromagnetic fields. *J Electroanal Chem Interfacial Electrochem* **320,** 335–355 (1991).
108. Danica, B. *et al.* Therapeutic window for multiple drug treament of experimental cerebral ischemia in gerbils. *Neurochemical* **19,** 189–194 (1994).
109. Slevin, M., Kumar, P., Gaffney, J., Kumar, S. & Krupinski, J. Can angiogenesis be exploited to improve stroke outcome ? Mechanisms and therapeutic potential. *Clin Sci* **183,** 171–183 (2006).

110. Rogalewski A Ringelstein EB, Schäbitz WR., S. A. Toward a multimodal neuroprotective treatment of stroke. *Stroke* **37,** 1129–1136 (2006).

111. Ohab, J. J., Fleming, S., Blesch, A. & Carmichael, S. T. A neurovascular niche for neurogenesis after stroke. *J Neurosci* **26,** 13007–13016 (2006).

112. Cao, Z., Balasubramanian, A. & Marrelli, S. P. Pharmacologically induced hypothermia via TRPV1 channel agonism provides neuroprotection following ischemic stroke when initiated 90 min after reperfusion. *AJP Regul Integr Comp Physiol* **306,** R149–R156 (2014).

113. Chamorro, Á., Dirnagl, U., Urra, X. & Planas, A. M. Neuroprotection in acute stroke : targeting excitotoxicity , oxidative and nitrosative stress , and infl ammation. **4422,** (2016).

114. Williams, J. L., Cartland, D., Hussain, A. & Egginton, S. A differential role for nitric oxide in two forms of physiological angiogenesis in mouse. *J Physiol* **570,** 445–54 (2006).

115. Ziche, M. *et al.* Nitric oxide synthase lies downstream from vascular endothelial growth factor-induced but not basic fibroblast growth factor-induced angiogenesis. *J Clin Invest* **99,** 2625–2634 (1997).

116. Delwing, D. *et al.* L-NAME administration prevents the inhibition of nucleotide hydrolysis by rat blood serum subjected to hyperargininemia. *Amino Acids* **29,** 267–272 (2005).

117. Aicher, A. *et al.* Essential role of endothelial nitric oxide synthase for mobilization of stem and progenitor cells. *Nat Med* **9,** 1370–6 (2003).

118. Cartwright, J. E., Johnstone, a P. & Whitley, G. S. Endogenously produced nitric oxide inhibits endothelial cell growth as demonstrated using novel antisense cell lines. *Br J Pharmacol* **131,** 131–7 (2000).

119. Fukumura, D. *et al.* Predominant role of endothelial nitric oxide synthase in vascular endothelial growth factor-induced angiogenesis and vascular permeability. *Proc Natl Acad Sci U S A* **98,** 2604–9 (2001).

120. Giorgi, G. *et al.* Assessing the combined effect of extremely low-frequency magnetic field exposure and oxidative stress on LINE-1 promoter methylation in human neural cells. *Radiat Environ Biophys* 1–8 (2017). doi:10.1007/s00411-017-0683-8

121. Belyaev, I. Exhibit F: An Update on Physical and Biological Variables, Cancer and Safety Standards. *Bioelectromagnetics* **26,** 173–184 (2005).

122. Litvak, E., Foster, K. & Repacholi, M. Health and safety implications of exposure to electromagnetic fields in the frequency range 300 Hz to 10 MHz. *Bioelectromagnetics* **23,** 68–82 (2002).

123. Prato, F. S., Thomas, A. W., Mckay, J. C., Prato, F. S. & Thomas, A. W. A literature review : The effects of magnetic field exposure on blood flow and blood vessels in the microvasculature . **28,** 81–89 (2015).

124. Blank, M. Biological Effects of Electromagnetic-Fields. *Bioelectrochemistry Bioenerg* **32,** 203–210 (1993).

125. Hastings GW, M. F. Electrical effects in bone. *J Biomed Eng* **10,** 515–21 (1988).

126. Otter MW, Palmieri VR, Wu DD, Seiz KG, MacGinitie LA, C. G. A comparative analysis of streaming potentials in vivo and in vitro. *J Orthop Res* **10,** 710–19 (1992).

127. Antonsson, E. & Mann, R. The frequency content of gait. *J Biomech* **18,** 39–47 (1985).

128. Becker, R. *The body electric: electromagnetism and the foundation of life*. (1985).

129. Wachtel, H. Comparison of endogenous currents in and around cells with those induced by exogenous extremely low frequency magnetic fields. *Am Chem Soc* **250,** 99–107. (1995).

130. Bertram R, Sherman A, S. L. Metabolic and electrical oscillations: partners in controlling pulsatile insulin secretion. *Am J Physiol Endocrinol Metab* **293,**

E890–900. (2007).

131. Goyal, S. & Wingreen, N. Growth-induced instability in metabolic networks. *Phys Rev Lett* **98,** 138105 (2007).

132. Kindzelskii, A. L. & Petty, H. R. Extremely low frequency pulsed DC electric fields promote neutrophil extension, metabolic resonance and DNA damage when phase-matched with metabolic oscillators. *Biochim Biophys Acta - Mol Cell Res* **1495,** 90–111 (2000).

133. Bawin, S. M. M., Satmary, W. M. M., Jones, R. A. A., Adey, W. R. R. & Zimmerman, G. Extremely-low-frequency magnetic fields disrupt rhythmic slow activity in rat hippocampal slices. *Bioelectromagnetics* **17,** 388–395 (1996).

134. Pilla AA, M. Bioeffects of weak electromagnetic fields. *Rev Env Heal* **10,** 155–169 (1994).

135. Pilla, A. A. Electromagentic Field instanstaneusly modulate nitric oxide signaling in challenged biological systems. *Biochem Biophys Res Commun* **426,** 330–333 (2013).

136. Tepper, O. M. *et al.* Electromagnetic fields increase in vitro and in vivo angiogenesis through endothelial release of FGF-2. *FASEB J* **18,** 1231–1233 (2004).

137. Yadollahpour, A. & Jalilifar, M. Electromagnetic Fields in the Treatment of Wound : A Review of Current Techniques and Future Perspective. **8,** 2863–2877 (2014).

138. McKay, J. C., Prato, F. S. & Thomas, A. W. *A literature review: The effects of magnetic field exposure on blood flow and blood vessels in the microvasculature*. *Bioelectromagnetics* **28,** 81–98 (Wiley Subscription Services, Inc., A Wiley Company, 2007).

139. Costa, E. V. L., Jimenez, G. C., Barbosa, C. T. F. & Nogueira, R. A. Fractal analysis of extra-embryonic vascularization in Japanese quail embryos

exposed to extremely low frequency magnetic fields. *Bioelectromagnetics* **34,** 114–121 (2013).

140. Morris, C. E. & Skalak, T. C. Chronic static magnetic field exposure alters microvessel enlargement resulting from surgical intervention. *J Appl Physiol* **103,** 629–636 (2007).

141. Delle Monache, S., Alessandro, R., Iorio, R., Gualtieri, G. & Colonna, R. Extremely Low Frequency Electromagnetic Fields (ELF-EMFs) Induce InVitro Angiogenesis Process in Human Endothelial Cells. **5,** 1–9 (2008).

142. Zhou, J. *et al.* Different Electromagnetic Field Waveforms Have Different Effects on Proliferation, Differentiation and Mineralization of Osteoblasts In Vitro. *Bioelectromagnetics* **35,** 30–40 (2014).

143. Willam, C., Schindler, R., Frei, U. & Eckardt, K.-U. Increases in oxygen tension stimulate expression of ICAM-1 and VCAM-1 on human endothelial cells. *Am J Physiol - Hear Circ Physiol* **276,** H2044-51 (1999).

144. Bronckaers, A. *et al.* Angiogenic properties of human dental pulp stem cells. *PLoS One* **8,** e71104 (2013).

145. Giorgi, G. *et al.* An evaluation of genotoxicity in human neuronal-type cells subjected to oxidative stress under an extremely low frequency pulsed magnetic field. *Mutat Res - Genet Toxicol Environ Mutagen* **775–776,** 31–37 (2014).

146. Hilkens, P. *et al.* Pro-angiogenic impact of dental stem cells in vitro and in vivo. *Stem Cell Res* **12,** 778–790 (2014).

147. Rodriguez, L. G., Wu, X. & Guan, J.-L. Wound-healing assay. *Methods Mol Biol* **294,** 23–29 (2005).

148. Chevalier, F., Lavergne, M., Negroni, E., Ferratge, S., Carpentier, G., Gilbert-Sirieix, M., Sineriz, F., Uzan, G., and Albanese, P. Glycosaminoglycan mimetic improves enrichment and cell functions of human endothelial progenitor cell colonies. *Stem Cell Res* 703–715 (2014).

149. Rauš Balind, S. *et al.* Extremely low frequency magnetic field (50 Hz, 0.5 mT) reduces oxidative stress in the brain of gerbils submitted to global cerebral ischemia. *PLoS One* **9,** e88921 (2014).

150. Reif, D. W. & McCreedy, S. A. N-nitro-L-arginine and N-monomethyl-L-arginine exhibit a different pattern of inactivation toward the three nitric oxide synthases. *Arch Biochem Biophys* **320,** 170–6 (1995).

151. Hjorth Lassen, L., Klingenberg Iversen, H. & Olesen, J. A dose-response study of nitric oxide synthase inhibition in different vascular beds in man. *Eur J Clin Pharmacol* **59,** 499–505 (2003).

152. White, R. P., Deane, C., Vallance, P. & Markus, H. S. Nitric oxide synthase inhibition in humans reduces cerebral blood flow but not the hyperemic response to hypercapnia. *Stroke* **29,** 467–472 (1998).

153. Kim, Y. *et al.* Ca2+/calmodulin-dependent protein phosphatase calcineurin mediates the expression of iNOS through IKK and NF-κB activity in LPS-stimulated mouse peritoneal macrophages and RAW 264.7 cells. *Biochem Biophys Res Commun* **314,** 695–703 (2004).

154. Rees, D. D., Palmer, R. M., Schulz, R., Hodson, H. F. & Moncada, S. Characterization of three inhibitors of endothelial nitric oxide synthase in vitro and in vivo. *Br J Pharmacol* **101,** 746–752 (1990).

155. Cechetti, F. *et al.* The modified 2VO ischemia protocol causes cognitive impairment similar to that induced by the standard method, but with a better survival rate. *Brazilian J Med Biol Res* **43,** 1178–1183 (2010).

156. Lawner et al., P. Attenuation of ischemic brain edema by pentobarbital after carotid ligation in the gerbil. *Stroke* **10,** 644–647. (1979).

157. Mosmann, T. Rapid colorimetric assay for cellular growth and survival: application to proliferation and cytotoxicity assays. *J Immunol Methods* **65,** 55–63 (1983).

158. Struys, T. *et al.* Magnetic resonance imaging of human dental pulp stem cells

in vitro and in vivo. *Cell Transplant* **22,** 1813–29 (2012).

159. Salunke, B. P., Umathe, S. N. & Chavan, J. G. Experimental evidence for involvement of nitric oxide in low frequency magnetic field induced obsessive compulsive disorder-like behavior. *Pharmacol Biochem Behav* **122,** 273–278 (2014).
160. Shupak, N. M. Therapeutic Uses of Pulsed Magnetic-Field Exposure: A Review. *Radio Sci Bull* **1,** 9–32 (2003).
161. Pall, M. L. Electromagnetic fields act via activation of voltage-gated calcium channels to produce beneficial or adverse effects Therapeutic bone-growth stimulation via Ca 2 + / nitric oxide / cGMP / protein kinase G Ca 2 + / nitric oxide / peroxynitrite and pathophy. **17,** 958–965 (2013).
162. Lange, K. Microvillar Ion Channels: Cytoskeletal Modulation of Ion Fluxes. *J theor Biolo,* **206,** 561–584 (2000).
163. Díaz-Ruiz C, A. y R. AGENTES Y MECANISMOS NEUROPROTECTORES RELACIONADOS CON EL ESTRÉS OXIDANTE EN EL INFARTO CEREBRAL. *Mensaje Bioquímico* **XXXVI,** 171–199 (2012).
164. George, P. M. & Steinberg, G. K. Novel Stroke Therapeutics: Unraveling Stroke Pathophysiology and Its Impact on Clinical Treatments. *Neuron* **87,** 297–309 (2015).
165. DiCarlo, A. L., Farrell, J. M. & Litovitz, T. A. A simple experiment to study electromagnetic field effects: Protection induced by short-term exposures to 60 Hz magnetic fields . *Bioelectromagnetics* **19,** 498–500 (1998).
166. Tasset, I. *et al.* Neuroprotective effects of extremely low-frequency electromagnetic fields on a Huntington's disease rat model: effects on neurotrophic factors and neuronal density. *Neuroscience* **209,** 54–63 (2012).
167. Gutiérrez-Mercado, Y. K. *et al.* Increased Vascular Permeability in the Circumventricular Organs of Adult Rat Brain Due To Stimulation by Extremely Low Frequency Magnetic Fields. *Bioelectromagnetics* **155,** 145–

155 (2013).

168. Arai, K., Jin, G., Navaratna, D. & Lo, E. H. Brain angiogenesis in developmental and pathological processes: Neurovascular injury and angiogenic recovery after stroke. *FEBS Journal* **276,** 4644–4652 (2009).

169. Ulu, N., Henning, R. H., Goris, M., Schoemaker, R. G. & van Gilst, W. H. Effects of ivabradine and metoprolol on cardiac angiogenesis and endothelial dysfunction in rats with heart failure. *J Cardiovasc* **53,** 9–17 (2009).

170. Patruno, A. *et al.* Extremely low frequency electromagnetic fields modulate expression of inducible nitric oxide synthase , endothelial nitric oxide synthase and cyclooxygenase- 2 in the human keratinocyte cell line HaCat : potential therapeutic effects in wound healing. 258–266 (2010). doi:10.1111/j.1365-2133.2009.09527.x

171. Goodman, R. & Blank, M. Insights into electromagnetic interaction mechanisms. *J Cell Physiol* **192,** 16–22 (2002).

172. Goodman, E. M., Greenebaum, B. & Marron, M. T. Effects of Electromagnetic Fields on Molecules and Cells. *Int Rev Cytol* **158,** 279–338 (1995).

173. Goodman, R. Electromagnetic fields stress living cells. *Pathophysiology* **16,** 71–78 (2009).

174. Naoya Sakamoto Masaaki Sato, T. O. Effect of magnetic field on nitric oxide synthesis of cultured endothelial cells . *J Int J Appl Electromagn Mech* **14,** 317–322

175. Santoro, N. *et al.* Effect of extremely low frequency (ELF) magnetic field exposure on morphological and biophysical properties of human lymphoid cell line (Raji). *Biochim Biophys Acta - Mol Cell Res* **1357,** 281–290 (1997).

176. Golbach, L. A., Philippi, J. G. M., Cuppen, J. J. M., Savelkoul, H. F. J. & Kemenade, B. M. L. V. Calcium signalling in human neutrophil cell lines is not affected by low-frequency electromagnetic fields. *Bioelectromagnetics* **36,**

430–443 (2015).

177. Woldańska-Okońska, M. & Czernicki, J. Effect of low frequency magnetic fields used in magnetotherapy and magnetostimulation on the rehabilitation results of patients after ischemic stroke. *Przegld Lek* **64,** 0–3 (2007).

178. Zheng, T., Yang, W., Song, T. & Huo, X. L. Effects of low frequency pulsed magnetic field on the proliferation and differentiation of HepG2 cells. *Bioelectrochemistry Bioenerg* **21,** 326–328 (2003).

179. Katsir, G. & Parola, A. H. Enhanced Proliferation Caused by a Low Frequency Weak Magnetic Field in Chick Embryo Fibroblasts Is Suppressed by Radical Scavengers. *Biochem Biophys Res Commun* **252,** 753–756 (1988).

180. Robertson, J. A., Thomas, A. W., Bureau, Y. & Prato, F. S. Review The Influence of Extremely Low Frequency Magnetic Fields on Cytoprotection and Repair. *Bioelectromagnetics* **30,** 16–30 (2007).

181. Okano, H., Gmitrov, J. & Ohkubo, C. Biphasic effects of static magnetic fields on cutaneous microcirculation in rabbits. *Bioelectromagnetics* **20(3),** 161–171. (1999).

182. Gutiérrez-Mercado, Y. K. *et al.* Increased vascular permeability in the circumventricular organs of adult rat brain due to stimulation by extremely low frequency magnetic fields. *Bioelectromagnetics* **34,** 145–55 (2013).

183. Chen, J. *et al.* Endothelial Nitric Oxide Synthase Regulates Brain-Derived Neurotrophic Factor Expression and Neurogenesis after Stroke in Mice. **25,** 2366–2375 (2009).

184. Jenrow, K. A., Zhang, X., Renehan, W. E. & Liboff, A. R. Weak ELF magnetic field effects on hippocampal rhythmic slow activity. *Exp Neurol* **153,** 328–34 (1998).

185. Belova, N. A., Acosta-Avalos, D., Belova, N. A. & Acosta-Avalos, D. *The effect of extremely low frequency alternating magnetic field on the behavior of*

animals in the presence of the geomagnetic field. *Journal of Biophysics* **2015,** 1–8 (Hindawi Publishing Corporation, 2015).

186. Sapir, Y., Cohen, S., Friedman, G. & Polyak, B. The promotion of in vitro vessel-like organization of endothelial cells in magnetically responsive alginate scaffolds. *Biomaterials* **33,** 4100–9 (2012).
187. Yang, Y. *et al.* Acute neuroprotective effects of extremely low-frequency electromagnetic fields after traumatic brain injury in rats. *Neurosci Lett* **516,** 15–20 (2012).
188. Church JE, F. D. Differences in eNOS activity because of subcellular localization are dictated by phosphorylation state rather than the local calcium environment. *J Biol Chem* **281,** 1477–1488. (2006).
189. Zhang Q, Church JE, Jagnandan D, Catravas JD, Sessa WC, F. D. Functional relevance of Golgi- and plasma membrane-localized endothelial NO synthase in reconstituted endothelial cells. *Arter Thromb Vasc Biol* **26,** (2006).
190. C.F. Blackman D.E House and W.T. Joines, S. G. B. & C.F. Blackman D.E House and W.T. Joines, S. G. B. Effect of ELF (1-120 Hz) and Modulate (50 HZ) RF Fields on the efflux of Calcium Ions From Brain Tissue in Vitro. *Bioelectromagnetics* **6,** 1–11 (1985).
191. Panagopoulos, D. J., Karabarbounis, A. & Margaritis, L. H. Mechanism for action of electromagnetic fields on cells. *Biochem Biophys Res Commun* **298,** 95–102 (2002).
192. Onose, G., Anghelescu, A. & Muresanu, D. F. A review of published reports on neuroprotection in spinal cord injury. *Spinal Cord* **7,** 125–145 (2009).
193. Adkins, E. *et al.* The evidence of benefits for poor people of increased renewable electricity capacity: Literature review. *Energy Policy* **20,** 1–4 (2012).
194. Farkas E Bari F, L. P. G. & Farkas E Bari F, L. P. G. Permanent, bilateral

common carotid artery occlusion in the rat: a model for chronic ce- rebral hypoperfusion-related neurodegenerative diseases. *Brain Res Rev* 162–180 (2007).

195. Rauš, S. *et al.* Extremely low frequency magnetic field induced changes in motor behaviour of gerbils submitted to global cerebral ischemia. *Behav Brain Res* **228,** 241–246 (2012).
196. Marañón Cardonne M, Sosa Montano AJ, Díaz Rivero BL, Jiménez Jauregui C, Marañón Reyes E, C. R. J. Efecto neuroprotector de los Campos Magnéticos de Frecuencia Extremadamente Baja (CMFEB) en biomodelos de isquemia cerebral. in *Springer* (2012).
197. Bernardini Zannoni, A., Turba, M. E., Bacci, M. L., Forni, M., Mesirca, P.Bersani, F., C. Effects of 50 Hz sinusoidal magnetic fields on Hsp27, Hsp70, Hsp90 expression in porcine aortic endothelial cells (PAEC). *Bioelectromagnetics* **28,** 231–237 (2007).
198. Blackman, C. F., Benane, S. G., Rabinowitz, J. R., House, D. E. & Joines, W. T. A Role for the magnetic field in the radiation-induced efflux of calcium ions from brain tissue in vitro. *Bioelectromagnetics* **6,** 327–337 (1985).
199. Pall, M. L. Electromagnetic fields act via activation of voltage-gated calcium channels to produce beneficial or adverse effects. *J Cell Mol Med* **17,** (2013).
200. Buddensiek, J. *et al.* Cerebrospinal fluid promotes survival and astroglial differentiation of adult human neural progenitor cells but inhibits proliferation and neuronal differentiation. *BMC Neurosci* **11,** 48 (2010).
201. Leventhal C Rafii D, Shahar A, Goldman SA., R. S. Endothelial trophic support of neuronal production and recruitment from the adult mammalian subependyma. *Mol Cell Neurosci* **13,** 450–464 (1999).
202. Yamashita T Hernández-Acosta P, García-Verdugo JM, Sunabori T, Sakaguchi M, et al, N. M. Subventricular zone-derived neuro blasts migrate and differentiate into mature neurons in the post-stroke adult striatum. *J*

Neurosci 6627–6636 (2006).

203. Funk, R. H. W. W., Monsees, T. & Özkucur, N. Electromagnetic effects – From cell biology to medicine. *Prog Histochem Cytochem* **43,** 177–264 (2009).

ANNEXES

Signs	Points	Conditions
Ptosis palpebral	1	Semi-closed left eye
	2	Semi-closed right eye
	3	Completely closed left eye
	4	Completely closed right eye
Bristling	1	Piloerection
Hypotonia	Decreased muscle tone, grip strength and / or motor compromise:	
	1	Left, front or rear leg
	2	Right, front or rear leg
Hyporeflexia	Reduction of the flexor reflex to stretching or pinching of members:	
	1	Left, front or rear leg
	2	Left, front or rear leg
Posture	1	Head tilted to the left, C-shaped body
	2	Head tilted to the right; inverted C-shaped body
March	1	Slow
	2	None
Turns	1	Move up to the left (Contralateral)
	2	A circular motion to the right (Ipsilateral)
	3	Left turns
	4	Right turns

Annex 1: Neurological scale[155]

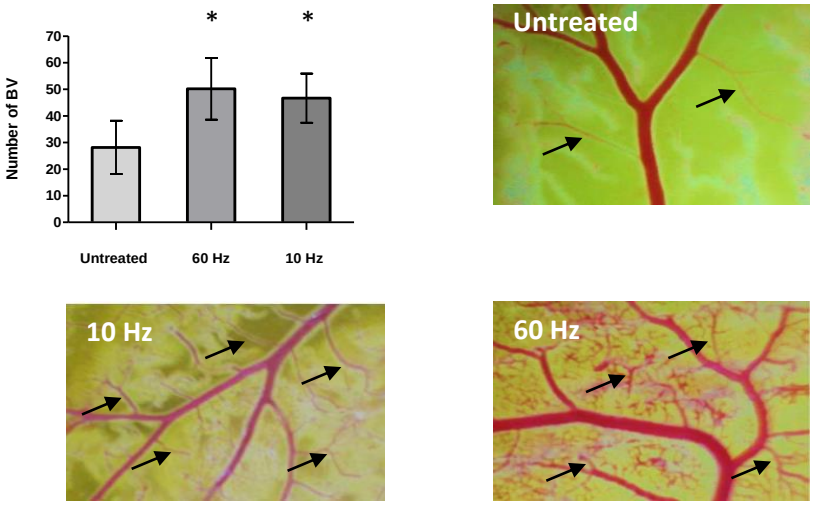

Annex 2: ELFMFs induced angiogenesis in chorio-allantoic membrane assay 'CAM'. At E4 fertilized chicken eggs were subjected to 20 minutes of 13.5 mT NP-SEMF of 10 or 60 Hz for 4 days and at E11 the number of capillary blood vessels was assessed. Pictures show representative photos of the control and treated CAM, the arrows indicate various blood capillaries. (n=6/group).

Trial	Dose of ELFMFs (mT / Hz)	
	13.5 mT / 10Hz	**13.5 mT / 60Hz**
In vitro		
Proliferation	+	-
Migration	+	+
[NO] EC **	-	+
[NO] EC NOS dependent	+	-
[NO] EC eNOS dependent	-	+
NOS dependent migration	NP	++
eNOS dependent migration	NP	+
In vivo		
Survival	+	+
Motor recovery	+	++
Neurological Scale	+	+
Decreased ischemic area	-	+
Formation of BV	-	+
NOS determination *in vivo*		
Survival	NP	+
Ischemic area	NP	+

* Experiments performed with ELFMFs exposure for 20 min. With repeated doses in four sessions, ** Endothelial cells; NO: nitric oxideNOS: nitric oxide; BV: blood vessels; level of significance: significant (+), very significant (++), there are no significant differences (-) ($p \leq 0.05$); NP: not performed.

Annex 3: Results of the in vitro and in vivo tests with their level of significance.

English summary

Cerebral vascular diseases (CVD) are positioned as the third leading cause of death and the leading cause of disability worldwide. They present a complex pathophysiology for which there is only one drug approved in the clinic: tissue plasminogen activator (tPA)[203], which is only available for a small subset of patients. In this context, the search for new therapies is of the highest priority. The objective of the present study was to evaluate the neuroprotective effect of sinusoidal extremely low frequency magnetic field (ELFMFs) application in cerebral ischemia i*n various* animal models, with particular emphasis on the angiogenesis process in vitro and in vivo. In the global ischemia model where occlusion of both carotids was induced in Wistar rats, ELFMFs significantly improved the survival rate and the neurological recovery and also reduced the ischemic lesion at the tested doses (13.5 mT / 10 and 60 Hz). *In vitro*, ELFMFs stimulate the proliferation, migration and tube formation, as well as the production of endothelial nitric oxide syntase (eNOS)-dependent NO, in *in vitro* HMEC-1 endothelial cell cultures. A significant increase in the number of blood vessels in the hippocampus region was observed after treatment with 13.5 mT / 60Hz, suggesting that the neuroprotective effect is mediated by angiogenesis. In addition, when the NOS-inhibitor L-NAME was co-administrated with ELFMF, the survival rate and infarction size was comparable to that of the untreated stroke animals, strongly suggesting that NO is the key signal molecule that mediates in the neuroprotective effect of ELFMF. Overall, the results indicate that ELFMF has a neuroprotective effect at preclinical level, which highlights its therapeutic potential of treatment for acute cerebral ischemia.

Key words: *angiogenesis, ischemic cascade, ELFMF, cerebrovascular diseases, ischemia, stroke, nitric oxide, nitric oxide synthase*.

Publications and presentations

Submitted publications:

• Pérez, L; Marañón, M; González, FG; Brone, B Lambrichts I. 1; Rigo J.M. 1; Bronckaers A, Brône B. Application of magnetic field of extremely low frequency in diseases of the Central Nervous System: Hydrocephalus. Cuban Journal of Biomedical Research. 2017. (Accepted)

• Pérez, L; Marañón, M; González, FG; Brone, B Lambrichts I. 1; Rigo J.M. 1; Bronckaers A; BrôneB.Sinusoidal extremely low frequency magnetic field rescues animals from severe stroke through induction of angiogenesis. Faseb Journal. 2017 (In review)

• Marañón Cardonne M, Pérez Font L, Mancebo Rodríguez A, Gilart González F, Marañón Reyes EJ, García Rodríguez JC. Magnetic field of extremely low frequency: Safety for its application at the level of the central nervous system. Cuban Journal of Biomedical Research. 2017; 2. (Accepted)

Publications:

• Pérez L, Marañón M, Pérez N, Castillo J, Lara A, Nuñez AI, Román A, Morales R. Study of brain bioimpedance in healthy individuals. Preliminary study. Rev. Elect. Medical Portals.com. 5 (20) 10/25/2010. Indexed in: Latindex and DOAJ.

• L. Pérez, M. Marañón, J. Castillo, A. Sosa, A. Lara, A. Nuñez, A. Román, R.Morales, N. Pérez García. Brain Bioimpedance Evaluation in Healthy Individuals. 2013. IFMBE Proceedings Vol. 33. Ed. Springer. ISBN: 978-3-642-21197-3. www.springerlink.com Ed. Folgueras Méndez J, Aznielle Rodríguez TY, Calderón Marín CF, Llanusa Ruiz SB, Castro Medina J, Vega Vázquez H, et al., Ed. V Lat. Am. Congr. Biomed. Eng. CLAIB 2011 May 16-21, 2011, Havana, Cuba Sustain. Technol. Heal. All, Berlin, Heidelberg: Springer Berlin Heidelberg. doi: 10.1007 / 978-3-642-21198-0_6. (Book Chapter)

• Marañón, M; Pérez, L; Garcia, A; Garcia JC; Gilart, F; Marañón, EJ. Therapy and Diagnosis Device for Neuroprotection in Cerebrovascular Disease. Patent Application No .: 2016-0136, Presentation Date: 09/19/2016.

• Marañón, M; Pérez, L; Mancebo, A; Gilart, F; Marañón, EJ; Garcia JC. Extremely low frequency magnetic field of: Safety of its application at the level of the central nervous system. Cuban Journal of Biomedical Research. Accepted for publication in No. 2. 2017 (Indexed in: Scopus, Scielo)

• Marañón, M; Pérez, L; Font, O; Moya, A. Models and trials for the study of angiogenesis. MEDISAN 20 (1): 102-110. 2016 (Indexed in: Scielo)

• Marañón, M, Pérez, L, Moya, A. Neuroprotection in cerebral ischemia: potentials of the magnetic field Research and Knowledge. III (1): 1-14. 2014 (Indexed in DOAJ).

• Marañón, M; Sosa, A J; Díaz, B L; Jiménez, C; Marañón, E; Rodríguez, JC; Pérez, L; Pérez, N; Gilart, F. Neuroprotective Effect of Magnetic Fields of Extremely Low Frequency in Biomodels of Cerebral Ischemia. In: IFMBE Proceedings Vol. 33. Ed. Springer. ISBN: 978-3-642-21197-3. www.springerlink.com Ed. Folgueras Méndez J, Aznielle Rodríguez TY, Calderón Marín CF, Llanusa Ruiz SB, Castro Medina J, Vega Vázquez H, et al., Ed. V Lat. Am. Congr. Biomed. Eng. CLAIB 2011 May 16-21, 2011, Havana, Cuba Sustain. Technol. Heal. All, Berlin, Heidelberg: Springer Berlin Heidelberg, p. 21-4. 2013. (Book chapter)

Monographs:

• Monograph Bioelectrical impedance. ISBN: 959-207-087-3. 2011

Oral presentations:

• Pérez, L; Marañón, M; Pérez, N; Azanza, G; Castillo, J.Evaluation of the magnetic field application in hydrocephalus biomodels. V Conference on Applied

Electromagnetism, April 9 to 12, 2013. Santiago de Cuba, Cuba. ISBN: 978-959-207-479-8.

• L. Pérez, M. Marañón, F. Gilart, D. Romero. Magnetic field of extremely low frequency as a treatment of Hydrocephalus. Preliminary study. 2014. International Convention of Technical Sciences. FIE 2014, Santiago de Cuba, Cuba. Published in Memories CD: ISBN: 978-959-207-529-0.

• Pérez, L; Marañón, M; González, FG; Brone, B Lambrichts I. 1; Rigo J.M. 1; Bronckaers A; Brône B. Extremely Low Frequency Magnetic Field (13.5 mT / 60 Hz) induces migration in HMEC-1 cells Ca^{2+} dependent NOS pathway. Fourth international Neuroimmunology meeting. CUBANNI 2017

• Marañón, M; Pérez, L; Gilart, F; Moya A; Garcia, JC; Marañón, EJ; Brone, B Neuroprotective Treatment with Sinusoidal Extremely Low Frequency Magnetic Field: Experimental Evidences. Fourth international Neuroimmunology meeting. CUBANNI 2017

• Marañón, M; Pérez, L; García, J.C; Gilart, F; Marañón E.J; Torres, Y. Neuroprotective Effect of Magnetic Fields of Extremely Low Frequency in Biomodels of Cerebral Ischemia. 2013. V Applied Electromagnetism Conference, April 9 to 12, 2013. Santiago de Cuba, Cuba. ISBN: 978-959-207-479-8. .

• Marañón, M, L. Pérez, F. Gilart, J. C. Garcia, E. J. Marañón, A. Moya. The Magnetic Field of Frequency Extremely low as a neuroprotector in Biomodels of Cerebral Ischemia. 2014. International Technical Science Convention. FIE 2014, Santiago de Cuba, Cuba. Published in Memories CD: ISBN: 978-959-207-529-0.

Main awards and recognitions obtained in the period related to the investigation:

1. Provincial Award for Technological Innovation from the Academy of Sciences of Cuba: Introduction of the NaK Magnetic Stimulator in the Health System. 2010.

(Coauthor).

2. Annual Provincial Health Prize: Introduction of the local NaK Magnetic Stimulator in the Health System. 2011. (Coauthor).

Acknowledgments

I want to start by thanking Miriam Marañón Cardonne who, besides being my friend, trusted me to carry out such a beautiful research, always praising my work ....and encouraging me!

I also want to thank the opportunity given to me a few years ago by Dr. Jean Michel Rigo, Dr. Bert Brone and Dr. Annelies Bronckaers, when they confirmed that I could start this project in their laboratory that ends here today. It has been a pleasure to work with you. I have no words to express gratitude for all that I have been taught, both professionally and personally.

To Liliana Gómez Luna who with her great command of the writing and above all of the research has taken care of every detail so that this work will come to an end.

To Fidel Guilart Gonzales who, with his clarifications, allowed me to understand a little the physical part of the ELFMFs.

I want to especially thank three people who behaved unconditionally with me during the time I was away from my country to complete the experimental part, making my days in the lab more bearable, they are Petra (my Petra, for me you are special), Annelies (there is no doubt that without her I would not have been able to reach the goal) and Sophi.

To the people of the physiology group: Dorien, Jirka, Maxim, Elke, Quirine, Silke, Lize, Jens, Sophie (Smolder and Kesels)..., Petra (of the morphology group), in short

to all those who helped me during my stay in Biomed. To Neldris for your technical support in the CNEA lab. To my colleagues from CNEA, to Melek, Elizabeth, Camue, Clarita, Yilan, Albis, Ramón, Kenya, Leine, Yudeisi .... A special thanks to Pascual, Joaquín, Iván, Castillo, Javier, Oraima, Angel, Mesa ...

To Tony who is always looking out for me, thanks to him we have a equipment of ELFMFs in Hasselt, you are the best!

To my colleagues that we share stay in Belgium: Harold, Yander, Monica, Douglas, Yisel and Alexander.

To Stijn, Lia and Marijke whom I consider my friends and who made my days in Genk and Diepenbeek more bearable, I will miss them....

To Gonzalo for giving me encouragement, you are the best ...

To Drs. Gisella, Luis, Nivaldo, Cachita, Jose, Maria, Yohani, Gustavo, Riverón ... to all of the National Commission of Health Sciences for reading critically and providing me with comments necessary for the culmination of this thesis.

Of course, to my family. To my parents, my aunts, niece, cousins. To my mother-in-law who is like a mother, to Loren and my dear Chicho. Especially my grandmothers, thank you because they are my support at all times, they are my role model and, one day, I hope to be able to become half of what they are. To my sisters. I love all of you so much!

To my husband, thank you for your patience and for waiting for me, nothing is left ... Thank you for putting everything so easy, well, sometimes, and for making me so happy ...

To my beautiful daughter Angela, everything is for you ...

To my laptop, to endure until the last moment ;). And of course, all the mice and rats that unwittingly gave their lives for this work. And I stop because this stage has been so beautiful and so spectacular that if I continue writing I will left escape tears for the memory and emotion ....